Spring 5-1-2019

IN-SITU FIELD MONITORING OF A UHPC AND HPC BRIDGE SUPERSTRUCTURE UNDER DIAGNOSTIC LOAD TESTING USING DIGITAL IMAGE CORRELATION

Prajwol Sharma

IN-SITU FIELD MONITORING OF A UHPC AND HPC BRIDGE SUPERSTRUCTURE UNDER DIAGNOSTIC LOAD TESTING USING DIGITAL IMAGE CORRELATION

by

PRAJWOL SHARMA

A thesis submitted in partial fulfillment
of the requirements for the degree of
Master of Science in Civil Engineering
Department of Civil Engineering

Michael Gangone, Ph.D., Committee Chair

College of Engineering

The University of Texas at Tyler
May 2019

The University of Texas at Tyler
Tyler, Texas

This is to certify that the Master's Thesis of

PRAJWOL SHARMA

has been approved for the thesis requirement on
April 2, 2019
for the Master of Science of Civil Engineering degree

Approvals:

Thesis Chair: Michael Gangone, Ph.D.

Member: Michael McGinnis, Ph.D., P.E.

Member: Gokhan Saygili, Ph.D., P.E.

Chair, Department of Civil Engineering

FOR JK

Dean, College of Engineering

Dedication

This thesis is dedicated to my grandmother Dila Kumari Sharma, my mother Kalpana Sharma, my father Laxmi Raj Sharma, my sister Anushka Sharma, my uncle Avishek Joshi and ballu for their support and love throughout the time. I would also like to dedicate it to Ashmita Wasti as in her smile I see something more beautiful than the stars.

Acknowledgements

This thesis would not have been possible without the support and love of many people. I'm especially grateful to my adviser Dr. Michael Gangone and Dr. Michael McGinnis and Dr. Gokhan Saygili for the continuous support and advice throughout the project. Thanks to Department of Civil Engineering for the continuous financial support. Also, I want to thank Dr. Torey Nalbone, and Dr. Mena Souliman for their support. And, finally I want to thank my parents, my friends and everyone who gave me love and support throughout this process.

Table of Contents

List of Tables

List of Figures

Abstract

IN-SITU FIELD MONITORING OF A UHPC AND HPC BRIDGE SUPERSTRUCTURE UNDER DIAGNOSTIC LOAD TESTING USING DIGITAL IMAGE CORRELATION

Prajwol Sharma

Thesis Chair: Michael Gangone, Ph.D.

The University of Texas at Tyler
May 2019

New innovative methods of bridge design are being sought to increase the service life of these structure. High Performance Concrete (HPC) and Ultra-High-Performance Concrete (UHPC) utilizes a mix of high strength concrete with steel fibers to create a strong and ductile reinforced concrete mix. While not new to civil engineering construction, this material still has some uncertainty of its performance both long and short term. As a result, in-situ experimental monitoring is important to verify methods of design and the suitability of the materials. A two-span pre-stressed UHPC and HPC reinforced concrete bridge superstructure was designed at New Mexico State University (NMSU) and constructed outside of Las Cruses, New Mexico in 2017. Monitoring of the superstructure took place in January 2018 and February 2019 where multiple sensor systems were deployed to capture the behavior under controlled loading conditions. A team from the University of Texas at Tyler (UT Tyler) deployed multiple 3-D and 2-D Digital Image Correlation (DIC) sensor systems to monitor deflections and strain at various location of the girder. To the knowledge of the research team both tests are the largest simultaneous deployment of DIC systems for experimental load testing of a

bridge. In DIC, the measured object is photographed with either a pair of digital cameras (for 3-D DIC) or a single digital camera (for 2-D DIC) before, during and after a load event, and a stochastic pattern marked on the object is tracked from one set of images to the next such that a full field of displacements is derived. The DIC system was successful in capturing displacements but strains were too low and not within the resolutions of the system. The testing serves as an early in-service response of the structure that can be used in comparing long-term performance of the superstructure. The results from testing indicate DIC is a powerful non-contact measurement approach to capturing in-situ displacement of highway bridges.

Chapter One

Introduction

Constant monitoring and testing of any standing structure are equally important as construction of the structure. Due to a level of uncertainty, some structures do not reach the design life. Deformation, deterioration and entropy are constant and impact the service life of the structure. The use of sensors like a potentiometer requires to be attached to a base which needs to be solid. This is impossible in large bridges unless scaffolding is used. Digital Image Correlation (DIC) can be used for measurements of material properties as well as surface strain and displacement to better monitor a structure. The span of the bridge also experiences sagging which can be easily quantified using DIC. One of the most important aspect of DIC is that it can be used to measure distress over a large field of view which is beneficial due to size of bridge elements. Whenever a loading is on the bridge minor deformations occur which might be unnoticed when measured by conventional techniques which measure response on a local scale. Another area is when a bridge is experiencing minor cracks which remain undetected to the naked eyes. The crack width can be quantified easily and efficiently by the use of DIC. Every structure is designed for a certain design life and most of the finite element programs are not able to characterize the structure based on the current condition of the structure. Lots of data inputs are required and intense modelling of the structure should be done to characterize the present condition. DIC has an advantage with this situation because the images which are captured portrays the live condition of the structure and is comprehensive in showing actual deformation present in the structure. This trait is one of

the most crucial in structural health monitoring. The repetitiveness of monitoring or the frequency of monitoring will be more accurate in determining the condition of the structure. The use of DIC also has its drawbacks which includes needs for appropriate lighting conditions and a rigid mounting base for the camera system to ensure it will not move throughout the testing period. The two main deformation (displacement and strain) are measured in this study and are comprehensively explained below.

1.1 Displacement measurement of a bridge superstructure

Displacement is one of the parameters considered during monitoring of a bridge superstructure. To meet serviceability requirements of any structure the design must limit the maximum displacement per code requirement. For bridges, the displacement is typically limited to L/800 inches per American Association for State Highway Transportation Officials (AASTHO) requirements. Displacement measurements are gathered at the mid span of a beam element as this is the location to experience maximum displacement at the most critical flexural loading case. In this study, the section represents the beam as a whole and deflection value obtained by averaging the displacement over the section is considered as displacement of the beam. The displacement is calculated for both UHPC and HPC beams for single, back-to-back and triple truck loading. Displacement values are also categorized as positive and negative where positive represents uplifting of the bridge and negative representing sag. The maximum value of deflection can be compared with the allowable displacement value to monitor the sagging characteristics of the bridge. The value of displacement can be used

to predict the effect of fatigue and other limit state of serviceability. This can be later used to forecast the evolution of a bridge's health.

1.2 Strain measurement of a bridge superstructure

Strain measurement of a structure relates directly to the stiffness and ductility of a material. A non-contacting method for measurement of strain in a bridge is DIC. The loading conditions change the strain produced in the span of a bridge. Strain fields are created directly by DIC using displacement values. The strain value measured by DIC has greater accuracy for large strain values compared to low micro-strains. The strain maps are also a good way of detecting cracks present in the beam or identifying the crack width. If the strain gauges are placed between two cracks in a span it gives relatively high values of strain because of noise. Strain directly correlates to the performance and helps in monitoring of bridge effectively. DIC helps in constant monitoring of strain values non-destructively.

1.3 Comparison with conventional methods of deflection analysis

The deformation of structures is measured by reliable and accurate contact-based methods (e.g. LVDT, string potentiometer). The measurements are often used as benchmarks for other methods to compare the measurements. Strain gauges and displacement transducers are used to compute the strain and displacement values respectively with high reliability. Conventional methods require extensive setup of equipment if the monitoring is to be done on higher elevation structures that are difficult to access. Setup with DIC can be easier as it requires less equipment and is not in contact

with the structure. The effectiveness of DIC is compared with measurement obtained from conventional wired sensors to validate its effectiveness on in-service bridges.

1.4 Objectives

The objectives of this study were:

a) To understand the behavior of the bridge using DIC.
b) To determine the feasibility of using DIC to measure in-situ strain.
c) To determine the feasibility of using DIC to measure 2D/3D displacement.
d) To determine displacement of from 2D DIC with bridge mounted camera.

Chapter Two

Literature Review

Load testing is a vigorous technique to understand the distribution of load on a structure. Data obtained from strain gauges provide an assessment of how load is being distributed on the bridge. While load is encompassing in practice the use of strain gauges and deflection sensors are very important to characterizing bridge performance. Numerous techniques including Digital Image Correlation (DIC), an optical non-contact method of monitoring is emerging as a new way of field testing or even field monitoring. The method used for DIC are: 2-D in-plane measurement only and 3-D which includes in-plane and out-of-plane also. A 3-D system consists of a two-camera system which uses images from both cameras are used to calculate out-of-plane movements of the monitored surface.

2.1 Structural health monitoring using Digital image correlation

Long-term monitoring is different from periodic testing as it can last for a period of days, weeks even months. Visual inspection has many limitations that can lead to challenges in obtaining accurate assessment. Spalling, cracks, bulging and sagging even if noticed are difficult to quantify just by visual measures. Structure health can be monitored using DIC by analyzing the strain and/or displacement measurement for different loading conditions.

2.1.1 Laboratory tests of DIC for damage detection capabilities

Nonis (2013) conducted a study to detect damage in a concrete beam which was setup in a laboratory. Three tests were performed on three separate beams which were similar in geometry and composition. Beams were loaded incrementally until failure was observed. Strain data obtained from DIC showed non-visible cracks appearing based on strain amplification even before a person could identify that there were changes in the structure. Even the use of a magnifying glass at different testing loads the cracks and changes could not be identified.

2.1.2 Digital image correlation application to bridge inspections

Previously visual inspection relied upon the use of basic non-advanced tools (e.g. tape measures, plum-bob) in determining health of a structure. The introduction of strain gauges, LVDT (linear Variable Displacement Transformers) and accelerometer have enhanced the field of monitoring. Digital Image Correlation is being introduced as a new method for Structural Health Monitoring.

Brogan (2010) also conducted a study using (3D- DIC) on a bridge in Massachusetts where a single 3D camera system was used. The results from the camera was processed by Vic-Snap. The data obtained from DIC was compared with the modelled data from SAP (Structural Analysis Program). The bridge deflected upward at start and then dropped downwards as the front axle of the truck reached the mid span of the bridge. The bridge reached to critical state when the truck was at the middle of the test and then dropped down as the rear axle of the truck reached the mid span of the

bridge. The data for some of the tests were noisy because of bad patterns and also because the calibration file was corrupted in the middle of the test.

2.1.3 Analysis of crack behavior in a reinforced concrete beam during a load test

Crack behavior can also be predicted studying the fatigue behavior of reinforced concrete structures. Kuntz et al. (2011) conducted a study to address potential concerns for serviceability of the Saint-Marcel bridge built in 1944. Crack width was measured, and shear cracks were noticed on the bridge and using DIC the crack was easily quantified. Along with the crack sagging was also detected. The crack width obtained from the DIC test results were compared with the crack width recorded by the potentiometer and similar results were obtained. DIC proved to be an important tool to understand crack kinematics and distribution of loads on the girders of the bridge.

2.1.4 Photographic strain monitoring during full-scale failure testing of Ornskoldsvik bridge

In some case use of photographic strain monitoring techniques prove better than monitoring strain gauges using electrical strain gauges for of two reasons: a) strain gauges give strain data only for a smaller surface area local measurement b) photographic strain monitoring provides better insights on structure's failure mode as it allows graphical visualization of strain fields.

Sas et al. (2012) conducted a full-scale test on a bride in Ornskoldsvik. The bridge had to be removed to build a new railway line and a full test was conducted during its demolition. Along with DIC more than 100 electrical strain monitoring gauges were used to measure the strain across the bridge. Load was generated by using two 1000-ton

hydraulic jacks that were placed on top of the loading beams. Loads vs Displacement were measured for east and west beam and small difference in displacement was obtained. DIC proved to be an important method for this particular scenario. As the strain gauges had to be placed at the area where cracks had already appeared, they gave unreasonably high values of strain and when the gauges were placed between two cracks the strain values that were observed were particularly low. The ability for photographic strain measurement can also be used to study strain in very small areas particularly changes that occur during slip and peeling strength along the length of bond.
The strain and displacement measurement obtained from Digital Image technology is compared with one reliable and conventional method of testing. The method of testing usually used are use of strain gauges or finite element modelling of the structure to study the behavior under different loadings.

Malesa et al. (2010) conducted a test on Nieporet Poland. The camera system that was used for the study was one three-dimensional camera system. The displacement result that were obtained from DIC testing were compared with the result from FEM model and satisfactory results were obtained. Although the results that are obtained from the FEM do not account for any damaged or deterioration that is present in the structure. Gencturk et. al. (2014) conducted a test on a full scale prestressed concrete structure. Ultimate load tests were conducted on a full scale prestressed I beam, and displacement was measured. The test was also conducted using conventional method and displacement transducers were used. The results from the test compared well with the results obtained from the displacement transducers. Although, lighting and pattern on the structure was an

issue the test was able to produce data with reasonable accuracy. The problem with the test was the crack width was difficult to measure after the spalling of concrete occurred. Loss of data points occurred after the specimen cracked which created hinderance to measure the crack width. The use of DIC gave detailed result which included in-plane and out-of-plane strain values.

2.1.5 Bridge deflection measurement using Digital Image Correlation

Yoneyama (2011) conducted a test on a 20 meters long bridge and deflection under usual traffic load was measured. The study primarily focused on the correction required because of camera movement during the test. The test measuring deflection of the bridge's fascia girder was carried out in the open. Wind was an inevitable issue which compromised the position of the camera. Due to slight movement of DIC cameras the change in the measurement is observed. The displacement values were normally distributed and correction for the movement of the camera was obtained. After the correction were made on the displacement data, the displacement values were similar to the one's measured by the displacement transducers. Although, DIC has many limitations the studies are conducted to provide corrections on the shortcomings of measurement using DIC.

2.1.6 Digital Image Correlation (DIC): An advanced nondestructive testing method for life extension of nuclear power plants

Hohmann (2012) conducted a study to measure shape deformation, strain and displacement on nuclear power plants. The study was conducted on the R.E. Ginna plant which has been in commercial operation since 1970. The objective of the test was to

study the behavior of concrete when pressurized. A principle strain map was generated from the test and high strain values indicated the cracks occurring during the test which lasted for 38 hours. The displacement data were also used to conclude cracks were present in the structure. Out-of-plane displacement were also measured to monitor the behavior of concrete during high pressure. Strain vs time plots were obtained to understand the crack propagation during various stages of the test. The results from the tests were kept as a baseline for the test which will be taken after 10 years. The results obtained from DIC was kept as a baseline for further tests and measurements.

2.1.7 Digital Image Analysis in geotechnical engineering education

Digital Image Analysis was used in two projects by Ayidlek (2007). Project 1 pore structure evaluation of geosynthetic fibers. Due to the two-dimensional structure of woven geotextiles and the presence of relatively large pore openings, a direct method such as digital image analysis was very appropriate for this purpose. The three-dimensional structure of nonwoven geotextiles required capturing pore structures from two-dimensional images. Planar and cross-sectional thin sections of these geotextiles were necessary to provide detailed information.

Project 2 was conducted to determine the strain produced on the geosynthetic during tension testing. Strain fields were evaluated after the images were processed. Strain gauges were also placed on the geosynthetic specimen to determine the localized strain during tensile testing. Comparison were made between the strain taken manually and strain obtained from processed images.

2.2 Aramis as an image processing software

Aramis is a non-contact measuring system that is based on DIC. It is an image processing software that is developed by GOM^{TM}. The system provides high precision measurement data regardless of specimen geometry and temperature. The marks made on the structure is well read and processed by ARAMIS. The computation speed is also quick and dynamic work interface ensures protection of calibration file as well as the project. It is a massive improvement over other image processing software as the user interface is simple and easier to use. The export feature allows to share data to other working environment for further processing. There is no need for a time-consuming and expensive preparation. For statically or dynamically loaded specimens and components. The measurements provided by ARAMIS are:

3D coordinates, 3D displacements, velocities, accelerations, Surface strain, Material properties for simulation (Young's modulus etc.), Evaluations of 6 degrees of freedom (6DoF) Aramis (2019).

2.2.1 Input data for ARAMIS

ARAMIS can provide information by processing a large number of images. Inputs such as calibration file, image files (Left and Right) and information regarding environmental conditions are required for the analysis of structures. Information regarding the input parameters are explained as:

a) Calibration

The start of the test always marks with the development of calibration file which is the most crucial part of the experiment. The camera required for the tests are arbitrarily placed and for proper measurement of distances over the field of study calibration is necessary. A calibration board with sizable dots is used for smaller field of view whereas a large calibration cross is used for larger field of view. The ARAMIS is able to create the calibration file after a series of images are fed to it.

b) Image files

The camera system includes two cameras left and right. The images captured from both cameras are used simultaneously to calculate 3D displacements. The calibration file together with two sets of images numbered sequentially processed and measurements like displacement and surface strains are calculated. The three-dimensional camera system used both (left and right) set of images to calculate displacements whereas two-dimensional camera system used only one set of images. The image file should be sequentially numbered for ARAMIS to recognize the sequence of image as it was taken during the test.

c) Environmental conditions

The effect of lighting condition has direct relation on clarity of images taken by the camera. Therefore, lighting condition should be adequate during test period. The shutter speed for the camera can be adjusted according to light available but good lighting conditions are preferred. The temperature of air also plays a vital role. The air temperature can cause changes in the specimen behavior and geometry. The difference in

temperature between laboratory conditions and field conditions can make a substantial difference when the measurement is extremely small (micro-strains).

Field testing helps us to understand the behavior of structures. BDI sensors, LDVT, Strain gauges and Potentiometer are extensively used for Structural Health Monitoring. The conventional techniques provide good accurate data, but the setup can be difficult in most scenarios. Equipment setup and monitoring over a long period of time can be expensive which can be replaced by DIC technique which is a non-contact test provided that it measures strains and displacement with reasonable accuracy.

Chapter 3

Experimental Test Setup

3.1 Bridge superstructure

The bridge consists of a two span multi-girder/stringer bridge superstructure located just outside of Las Cruces, New Mexico. The bridge was designed by New Mexico State University and constructed in 2017. Each span is approximately 6.9 m (22.5 ft.) in length and 9.8 m (32 ft.) wide with 9-precast girders at a center-to-center spacing of 1.2 m (4 ft.). One span of the bridge is constructed of High-Performance Concrete (HPC) and the other span of Ultra High-Performance Concrete (UHPC). The slab is cast in place with reinforcement extending out of the girder to create composite action. An elevation view of the bridge is seen in Figure 1.

Figure 1. Bridge test structure

3.2 Load testing protocol

The bridge superstructure was divided into multiple test lanes and subjected to prescribed vehicle load patterns that were applied by fully loaded H-Trucks with known axle weights. One, two, three or four H-Trucks were simultaneously positioned at different locations of the bridge to maximize the flexural and shear response of each span. Figure 5a shows a single truck in path 1 of the bridge whereas figure 5b shows double truck back-to-back in path 7 and figure 5c in triple truck loading in path 10. Figure 3 shows examples of truck positioning for one, three and four trucks. The orange chalk lines (visible in Figure 5a) were used on the surface to position the vehicles. In each load test, the truck started on the UHPC bridge span then moved across the bridge to the HPC span before exiting. Figure 2-4 illustrates 10 load paths used in the testing.

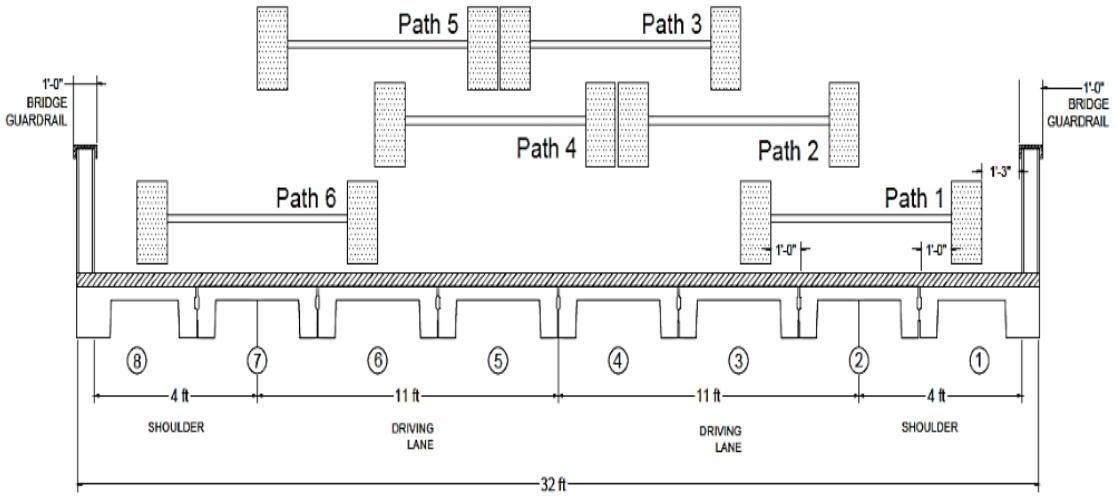

Figure 2. Transverse load paths for a test vehicle (NOTE: 1 ft. = 0.3 m)

DOUBLE TRANSVERSE LOAD PATHS
Centered exterior truck axle on girder center line.

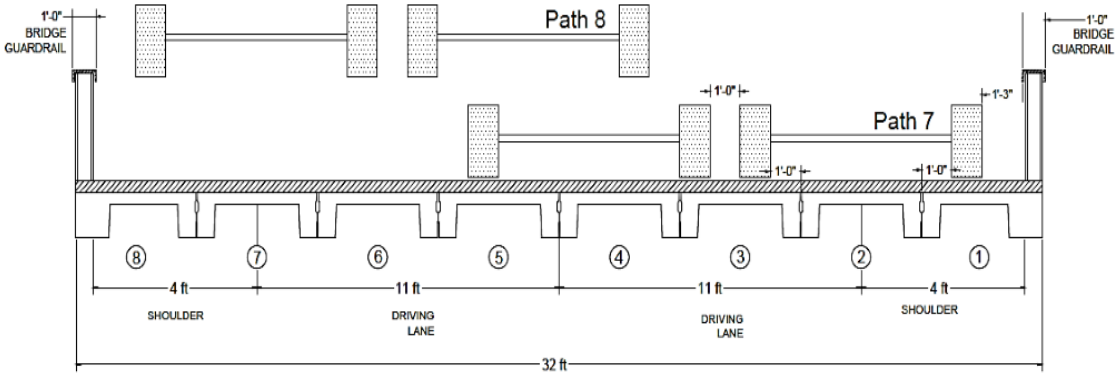

Figure 3. Transverse load paths for a test vehicle (NOTE: 1 ft. = 0.3 m)

TRIPLE TRANSVERSE LOAD PATH
Centered exterior truck tire on girder center line.

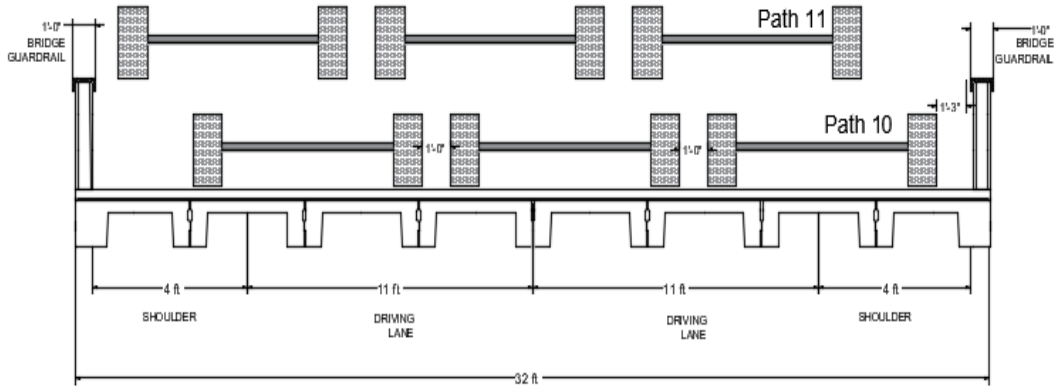

Figure 4. Transverse load paths for a test vehicle (NOTE: 1 ft. = 0.3 m)

(a)

(b)

(c)

Figure 5. Example of truck positioning with (a) one truck, (b) four trucks back-to-back, (c) three trucks side by side

3.3 DIC Sensor Deployment

The test on the bridge was conducted twice. The first test was done in January 2018 and the second test was done in February 2019. The two tests had different setups, but the load tests remained same. A more comprehensive monitoring approach was taken on the second test setup and the number of camera system was also increased. A detailed explanation of both test setups follows this section.

3.3.1 Test 1 setup

The bridge superstructure was instrumented with a series of Bridge Diagnostic Incorporated (BDI), strain transducers, as well as vibrating wire and fiber optic sensors (FOS) to capture strain measurements at critical locations for shear and moment demand. The data gathered from these sensors were processed by researchers at New Mexico State University (NMSU) and not presented in this report. A total of eight Digital Image Correlation (DIC) sensor systems were deployed at various locations of the bridge. Four 3D and four 2D DIC systems were positioned at the mid-span of both fascia girders and one of the interior girders for each span. For this testing, the DIC sensors were used to measure surface strains and displacements. A pattern used to capture these measurements was drawn on the surface of the girder using chalk. The surface strains captured will be compared to measurements obtained from BDI strain transducers placed at the same location. This comparison will be discussed in chapter five. A limitation of most experimental load testing is the ability to capture in-situ displacement measurements due to the limitations in mounting the sensors directly to the bridge element. Traditional displacement sensors like Linear Variable Displacement Transducers (LVDTs) and String Potentiometers (String Pots) only allow for displacements to be measured at a single point. The DIC system allows for the cameras to be positioned away from the element which allows for a full field view of displacement readings and is not limited to a single point measurement.

As mentioned previously, multiple DIC systems were deployed. The camera systems used for this testing included: The FASTEC IL5 and FASTEC HiSpec1 high

speed digital cameras, a 2M ARAMIS system, DMK monochrome industrial cameras from The Imaging Source, 2 GoPro Hero + cameras and 2 GoPro Hero 3 cameras. Table 1 outlines the camera systems used on the two different spans, their location, their normal (perpendicular) distance to the bridge girder surface and whether the system was used as a 2D or 3D system. Each of the testing systems that were deployed are shown in Figures 6-11.

Table 1. Camera systems used for DIC monitoring

	Camera System	***2D/3D DIC***	***Sensor Location***	***Normal Distance from camera to beam surface***
HPC	Hi-spec 1	3D	Exterior Girder	2.82 m (9.25 ft.)
	Go Pro Hero +	2D	Exterior Girder	Approximately 3 m (9.84 ft)
	Go Pro Hero +	2D	Exterior Girder	Approximately 3 m (9.84 ft)
	DMK	2D	Interior Girder	1.32 m (4.33 ft.)
UHPC	IL5	3D	Exterior Girder	3.02 m (9.92 ft.)
	Go Pro Hero 3	2D	Exterior Girder	Approximately 3 m (9.84 ft)
	Go Pro Hero 3	2D	Exterior Girder	Approximately 3 m (9.84 ft)
	2M	2D	Interior Girder	1.04 m (3.42 ft.)

Figure 6. FASTEC IL5 System for monitoring exterior girder of UHPC span

Figure 7. FASTEC HiSpec1 System for monitoring exterior girder of HPC span

(a)

(b)

Figure 8. GoPro Hero + System for monitoring exterior girder of HPC span (a) view from behind cameras, (b) view from in front of cameras

(a)

(b)

Figure 9. GoPro Hero 3 System for monitoring exterior girder of UHPC span (a) view from behind cameras, (b) view from in front of cameras

Figure 10. 2M System for monitoring an interior girder of UHPC span

Figure 11. 2M System for monitoring an interior girder of UHPC span

The sensors monitoring the fascia girders were mounted on custom designed frames made from L2x2x1/4" angle iron and quick grips to create a frame that would not

only support the weight of the camera system but was also rigid enough to keep the cameras from swaying as a result of any wind. Example of this frame system are seen in Figures 6-11. Figures 12 and 13 show the location of the four 3D DIC systems as well as the command station where the camera systems were controlled. Figures 8a and 9a show very clearly example of the chalk patterning used for DIC. Figure 14 illustrates the location of each DIC system using a plan view of the bridge.

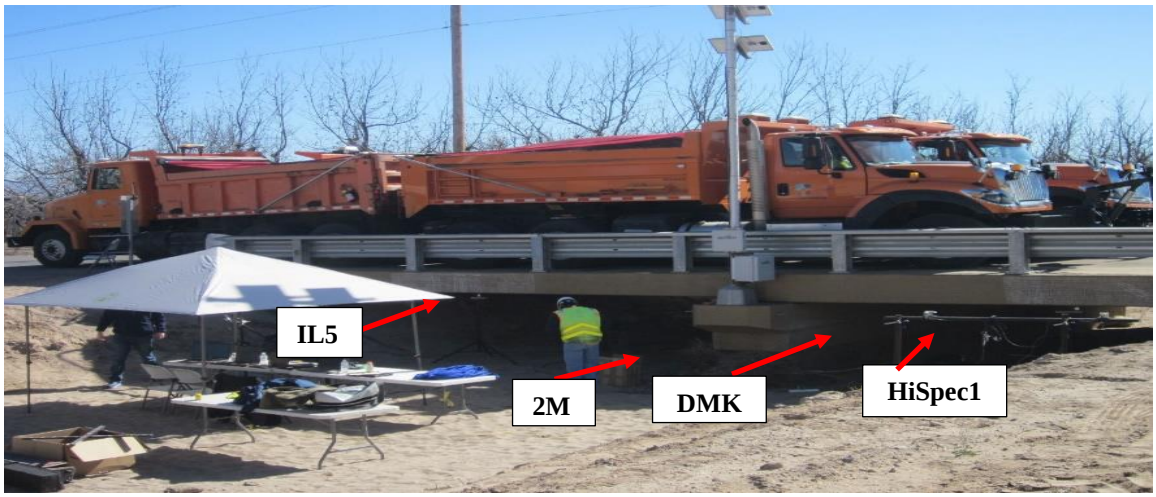

Figure 12. Side view of the bridge showing 4 DIC systems

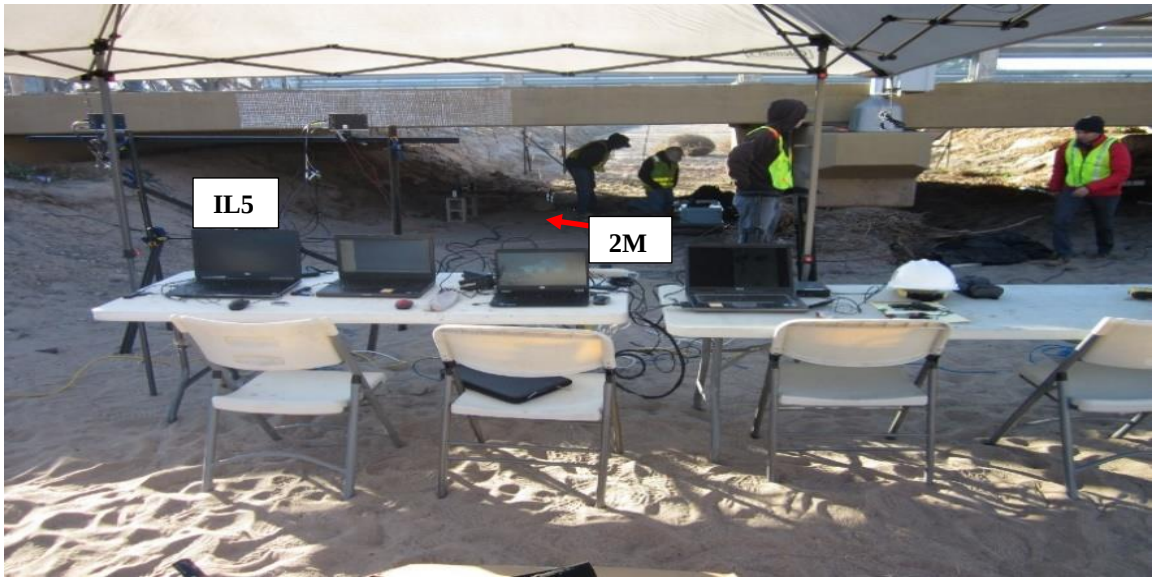

Figure 13. Command station with computer systems running DIC cameras

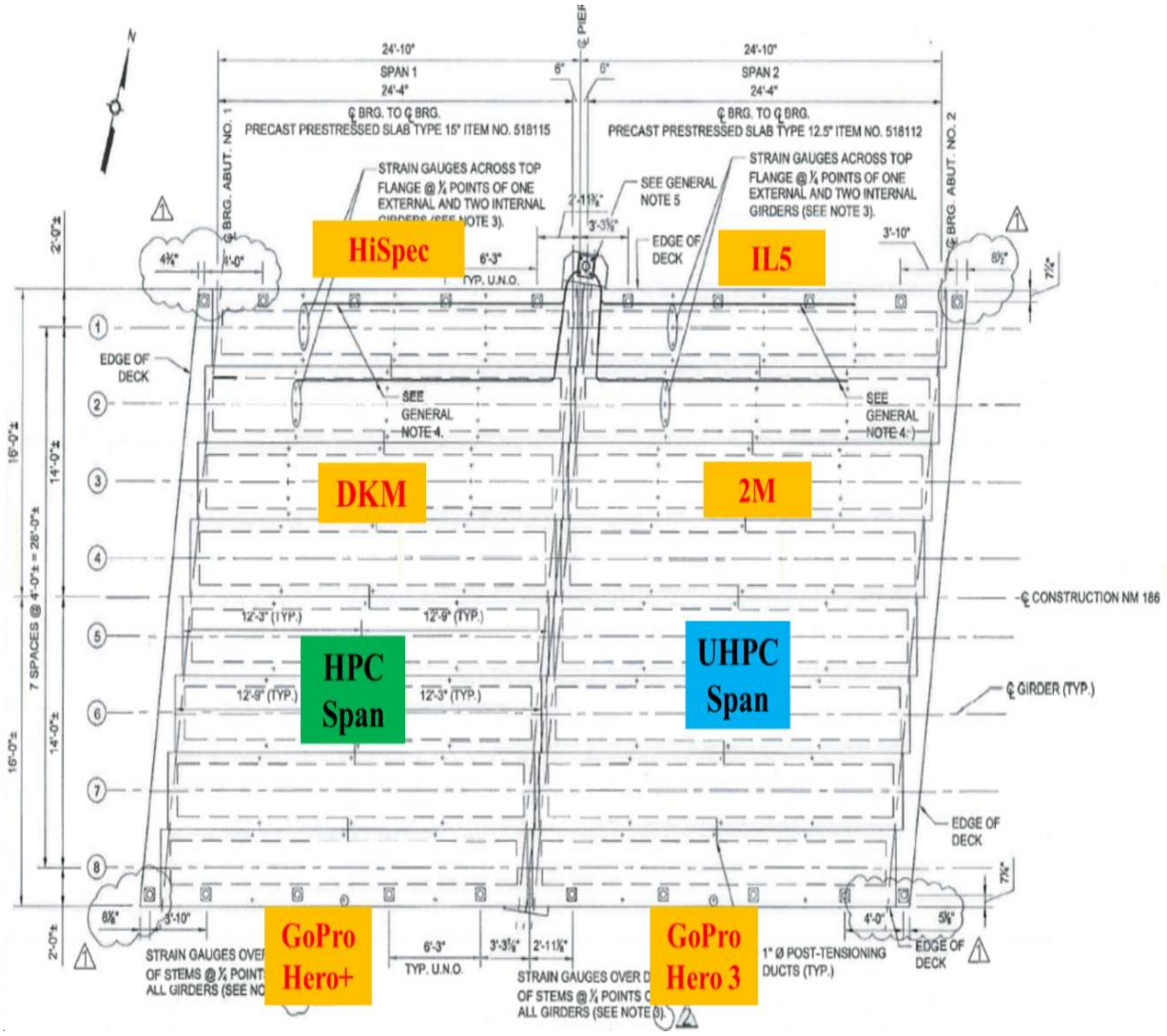

Figure 14. Location of each DIC camera system for Test setup 1

3.3.2 Test 2 Setup

The bridge superstructure was monitored for a second time with multiple DIC sensor systems. A total of 11 DIC sensor systems were deployed at various locations of the bridge. Eight 2D and three 3D DIC systems were installed for detailed monitoring of both internal and fascia girders. The 2D systems were positioned on the center pier facing

outward to capture displacements of the interior girder near midspan. The 3D systems were positioned to monitor the center pier and to capture displacements of the north stem of girder 1 on both spans. For this testing, the DIC sensors were used to measure displacements only. A pattern used to capture the measurements of the fascia girder as drawn on the surface of the girder using chalk. For the interior girders, a steel plate was bent at 90 degrees and attached with epoxy to the bottom of girder stem. A pattern drawn on the plate was taped to the plate.

As mentioned previously, multiple DIC systems were deployed. The camera systems used for this testing included: The FASTEC IL5 and FASTEC HiSpec1 high speed digital cameras, a 2M ARAMIS system, DMK monochrome industrial cameras from The Imaging Source, 2 GoPro Hero + cameras, 2 GoPro Hero 3 cameras and 2 Amp scope Cameras. Every camera system was in pair. The cameras in pair were labelled as left and right or camera 1 and camera 2 according to the model used. The naming was used to keep track of the images. Table 2 outlines the camera systems used on the different spans, their location, and whether the system was used as a 2D or 3D system. Figure 15 shows a pictorial representation about the position of every DIC camera system. The 2D system were installed underneath the bridge whereas the 3D system monitored the fascia girders of the bridge. One of the 3D systems also monitored the pier of the bridge for out of plane displacements which was also installed underneath the bridge on the HPC side looking below girder 3 and 4. Figures 16-21 show various picture of the setup under the bridge. Figure 18 in particular shows a string pot and dial gauge positioned just behind a patterned section for measurement verification.

Table 2. Camera systems used for DIC monitoring for test 2

	Camera System	***2D/3D DIC***	***Sensor Location***
HPC	Hi-spec 1	3D	Exterior Girder
	Go Pro Hero Plus L	2D	Interior Girder
	Go Pro Hero 3 1	2D	Interior Girder
	Amp Scope 2	2D	Interior Girder
	DMK 1	2D	Interior Girder
UHPC	IL5	3D	Exterior Girder
	Go Pro Hero Plus R	2D	Interior Girder
	Go Pro Hero 3 2	2D	Interior Girder
	Amp Scope 1	2D	Interior Girder
	DMK 0	2D	Interior Girder

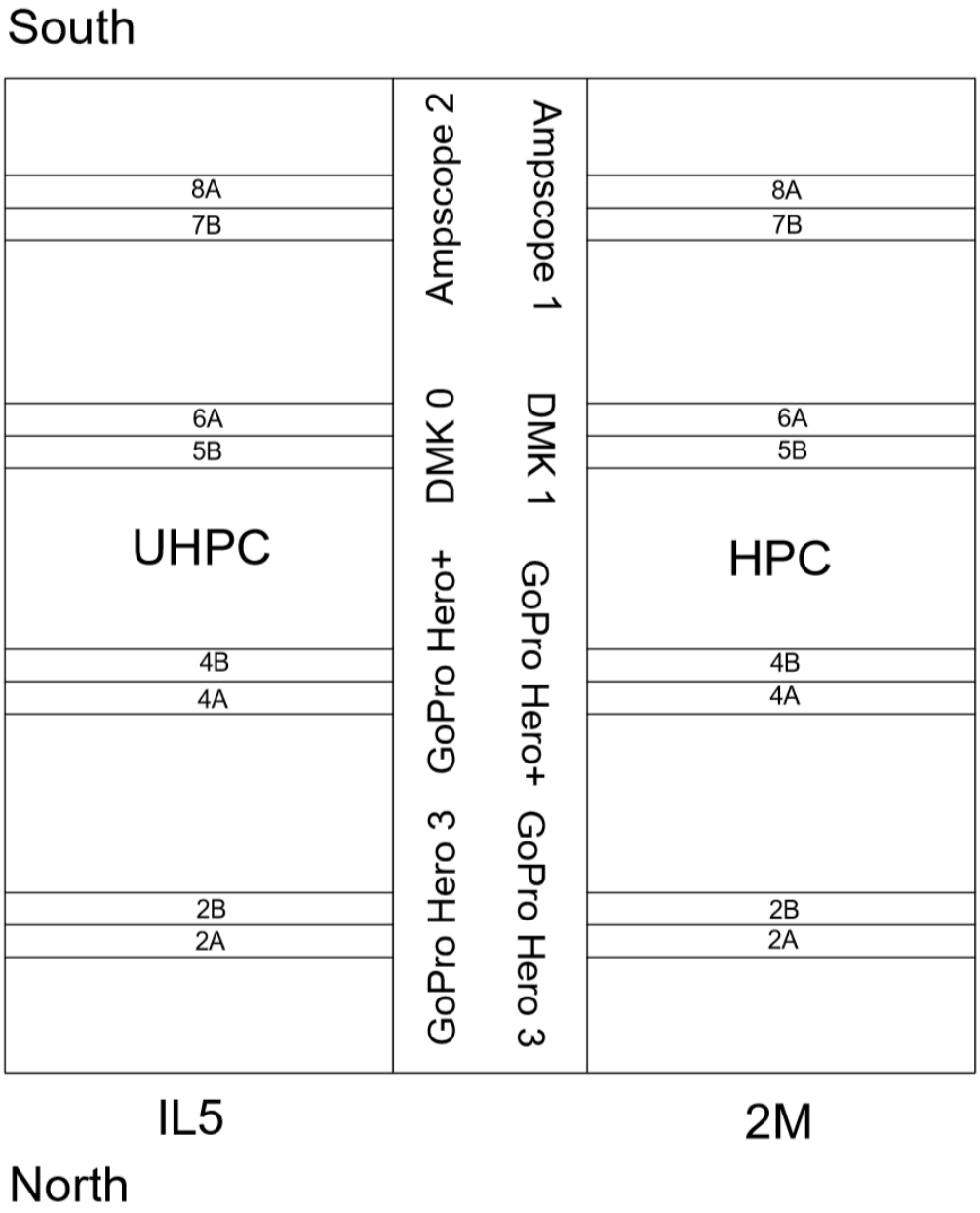

Figure 15. Location of each DIC camera system for test setup 2 and stem of the monitored girder.

Figure 16. Internal girders

Figure 17. Internal girders with attached targets for displacement measurement

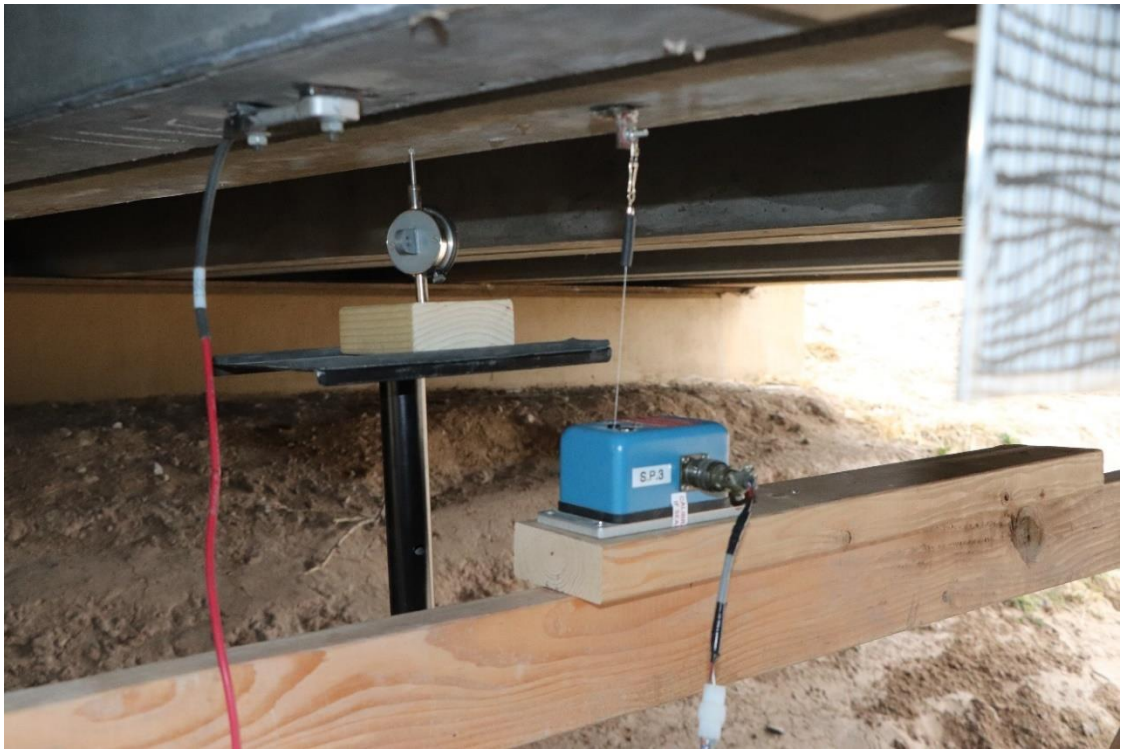

Figure 18. Dial gauge placed on an internal girder

Figure 19. Amp Scope camera

Figure 20. Go Pro Camera

Figure 21. Hi-spec camera system for measurement of out-of-plane displacement of the bridge pier

3.4 Image Organization

The images from the test were extracted and an index was created to track every image. An index was essential to separate images according to the loading conditions. The images were sorted by load position and kept track using excel. The organization was helpful in processing the data. The image organization was done similarly for both tests (2018 and 2019). A spreadsheet was created, and color coding was used to identify the images.

3.4.1 Test 1 organization

The images were extracted from six camera systems. The images were collected and organized using a spreadsheet. A total of 1598 images were captured during the processing and all were synchronized and arranged to properly locate the image according to time and loading stage. At each loading stage there were six different images from six camera system. All of the images were sequenced for further processing. The spreadsheet was used as a reference when ARAMIS was used for processing of the images. The images were sequentially numbered and were matched exactly with other camera systems. Table 3 is an example of a single load test with data of each camera system present. Every testing had an average of 10 images and the images corresponded to the span of the bridge which was marked at an interval of 5 feet. A time was also recorded to double check the sequence of the image. The labeling of the image number was done according to the default number present on the camera system during testing period. Later the numbering was done sequentially to process the images in ARAMIS and obtain the deformation data.

Table 3. Image organization for all six-camera system taken at same time

TIME		HERO+		HERO 3		STAGE	DMK	IL5	HiSPEC1
		LEFT	RIGHT	LEFT	RIGHT				
	INITIAL	55	2607	1519	30			30	
	0	56	2606	1518	31	STAGE 0			1:05
1:07	5'	57	2609	1521	32	STAGE 1		32	
				1523	34				
				1524	35				
	10'	58	2610	1525	36	STAGE 2	42	57	1:16
	15'	59	2611	1526	37	STAGE 3	43	58	1:22
	20'	60	2612	1527	38	STAGE 4	44	59	1:25
	25'	61	2613	1528	39	STAGE 5	45	60	1:37
	30'	62	2614	1529	40	STAGE 6	46	61	1:39
	35'	63	2615	1530	41	STAGE 7	47	62	1:40
	40'	64	2616	1531	42	STAGE 8	48	63	1:44
	45'	66	2618	1532	43	STAGE 9	49	64	1:46

Along with the set of images the type of loading was also mentioned to determine the type of test. For a test with one truck loading on path 1 the Hi-spec had nine images similar to that of IL5 which also had nine images. Every image was named as a particular stage number and a time reference is also provided in the second column for further aid to identify the right image. All the camera systems had their own number system except the Hi-spec camera system which had time reference to identify the sequence of the image. The Go-Pro camera system had a left, and right image stored separately in two different folders where as IL5 and Hi-spec had left, and right image stored in the same folder which later were sorted as left and right respectively. The index was checked twice after processing the images to make certain that no stage was replaced or missing, ensuring accuracy in the data. For the GoPro camera, the number on the front of each camera and a time were recorded for every stop on a load test.

3.4.2 Test 2 organization

Test 2 had similar organization, but folders were created directly under a file name according to the type of loading condition. The images were tracked according to the notes made in the field during the time of testing. The organization was easier as every picture obtained from the camera had the same label as was marked on the notes. A baseline was recorded for each test, in part, minimize to track any misplaced image. After the images were organized inside their respective folder, it was sequentially numbered and was then used for processing.

Chapter 4

Calibration

Calibration

Calibration for DIC is one of the most important steps for the test. Before the test begins, the calibration of the instrument should be done, and calibration file should be created. There are several panel sizes from which to choose. The ideal panel size is the one that occupies the field-of-view of the cameras fully. If the panel size is smaller than the field-of-view, the parameters need to be adjusted during the calibration process.
In the first step of calibration process, the calibration panel was placed near the site where the specimen is to be tested. The line of sight of camera should be focused on the calibration panel. The cameras are locked after the focus is sharpened and both cameras are looking at the same image. The cameras are locked throughout the test and should not be moved with respect to one another. Twelve pairs of images were taken from two cameras and then are used to create calibration file. ARAMIS gives two option for the calibration process. The first option is creating the calibration file using the instruction given by ARAMIS regarding the orientation of the calibration object. The second option is not using the instructions, but the number of images taken, and orientation should be similar.

4.1 Calibration file generation

The calibration for a test can be performed at any time but the cameras should not be moved at any time during the test. The focus of the camera should also be kept constant. The focus for the camera can be manually changed by rotating the lens or by the

software. The ARAMIS software can run on both Linux, Windows XP. The software was used for both operating systems during the test. The calibration process remained the same for both operating systems as the user interface was same for both. The calibration images used for two systems were different as the Hi-spec was controlled by the computer to snap the pictures and later imported to ARAMIS for processing whereas for the 2M system the images were directly taken through ARAMIS and then processed for the calibration file. Figure 22 shows the setup screen for calibration in ARAMIS.

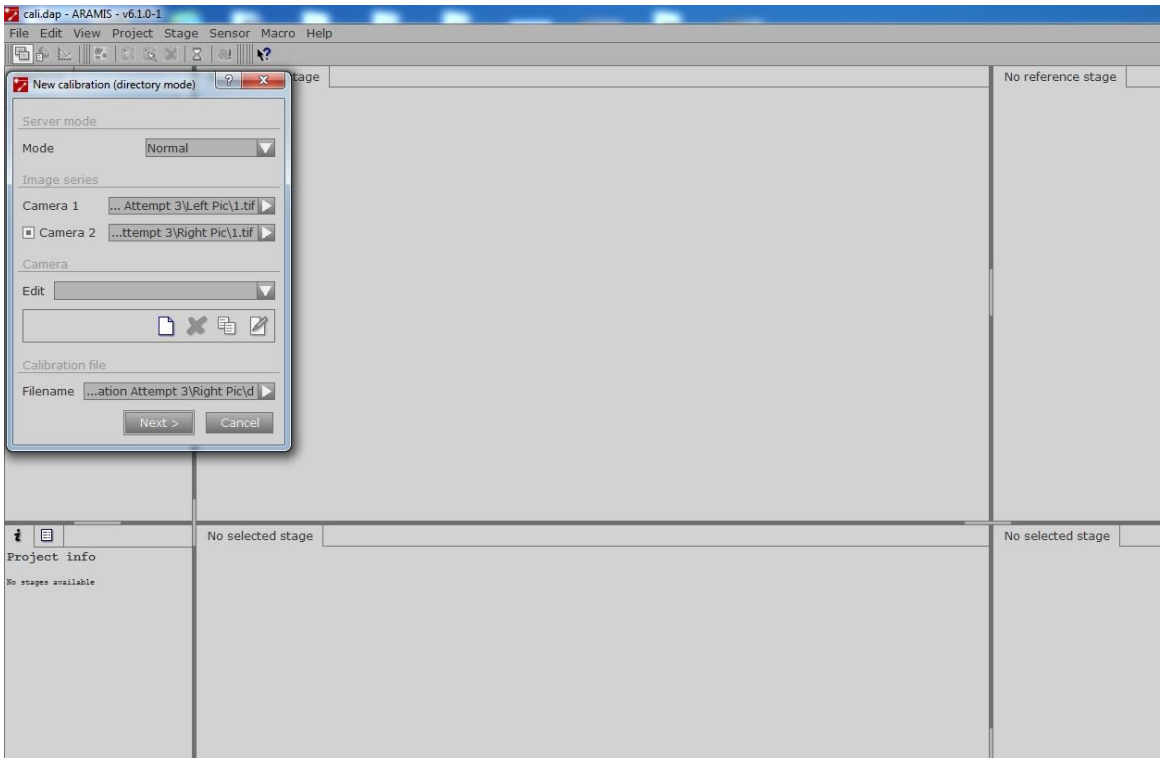

Figure 22. Image of calibration screen display

The following user interface appears after ARAMIS is opened and the option "Sensor">> "Calibration from image series" is selected. Then the camera is selected according to the model of the camera. The camera for the test were the HI-spec 1 and Fastec 1280x1024 500fps. Then, according to the comfort of the user orientation of the

board can be changed. The images during the process are taken. The image is shown on the window on the right and left sides immediately. The calibration board shows a green light if the points on the board are identified. The image should be re-taken, or the board should be placed again if the green points do not flash. Figure 23 shows an example of a calibration being done using a calibration panel.

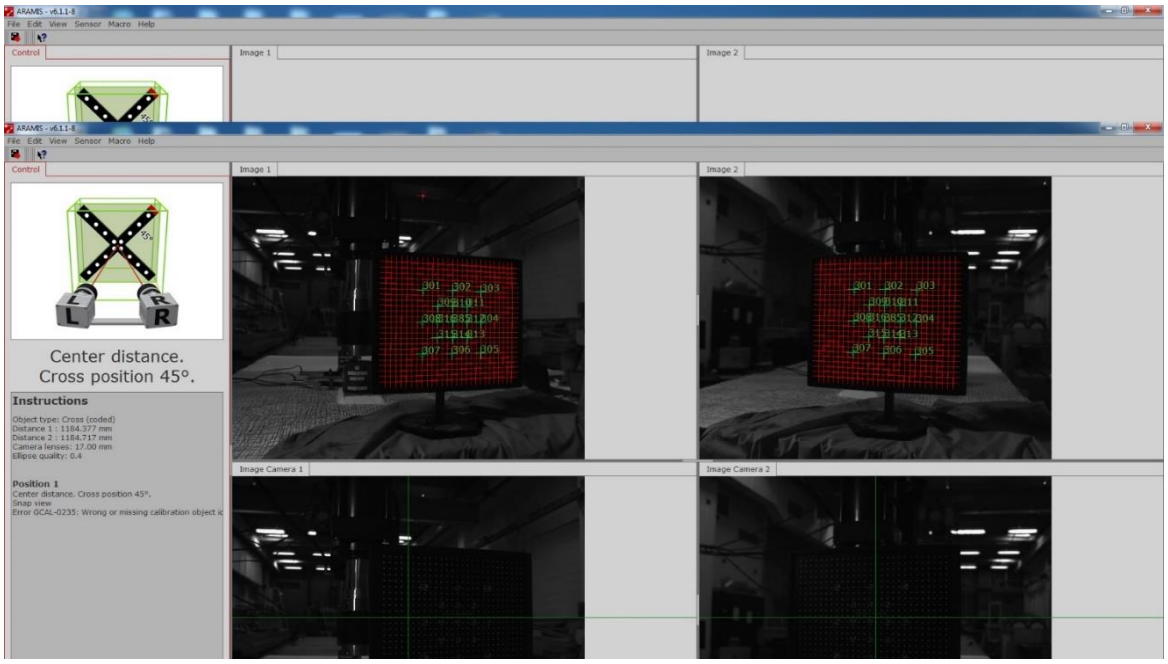

Figure 23. Image of Calibration screen display with calibration panel

The showing of the green points indicates that the points on the calibration panel are picked by the camera and then recognized by ARAMIS. In case, the points do not get identified, the image should be snapped again, the focus of the camera should be checked, or placement of the calibration board must be changed. The green points should be identified in both cameras and only then the calibration work would go further. After snapping all 12 pairs of images, ARAMIS compiles and using the method of least squares calculates the distance from each point. The calculated distance from two cameras to the points present in the calibration board depth can also be calculated. A three-dimensional

field is created by the method of least squares and any deformation within the field of view can be easily calculated using ARAMIS. Figure 24 is a screenshot of the calibration process in ARAMIS.

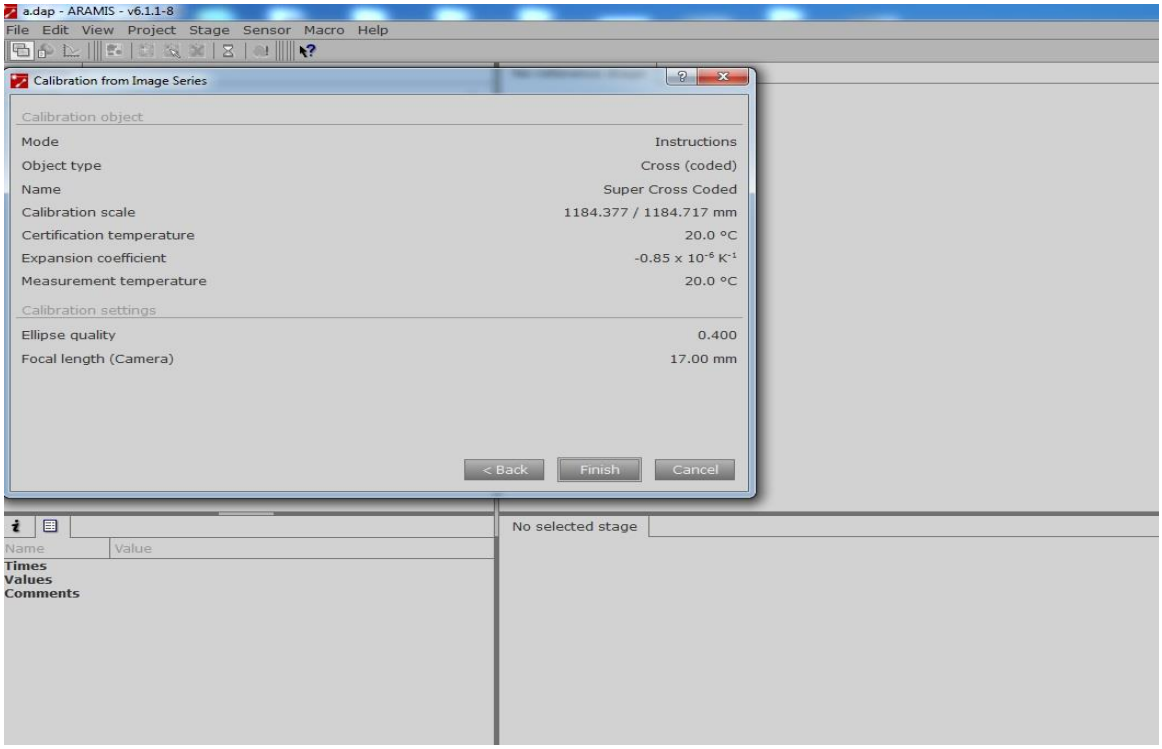

Figure 24. Image of calibration summary for environmental condition and material properties

The set of images are then processed by ARAMIS and calibration file is obtained. The calibrated file will also have the details regarding “calibration scale”, “cert. temp” and “Exp Coeff” which is kept constant. After the calibration, a summary of the calibration file is shown. The effect of temperature has a vital role to play during testing. Since the calibration is done at 20.0 C, the temperature effect during testing conditions might affect the material that is to be tested. If the structure is made up of steel or aluminum the temperature can affect the expansion or contraction of the metal. The focal length of the camera is changed according to the presence of light during testing. After

the generation of calibration file, the camera is not moved from its position throughout the test and is kept fixed. Any change made with the position of the camera might affect the measurement and ruin the whole test.

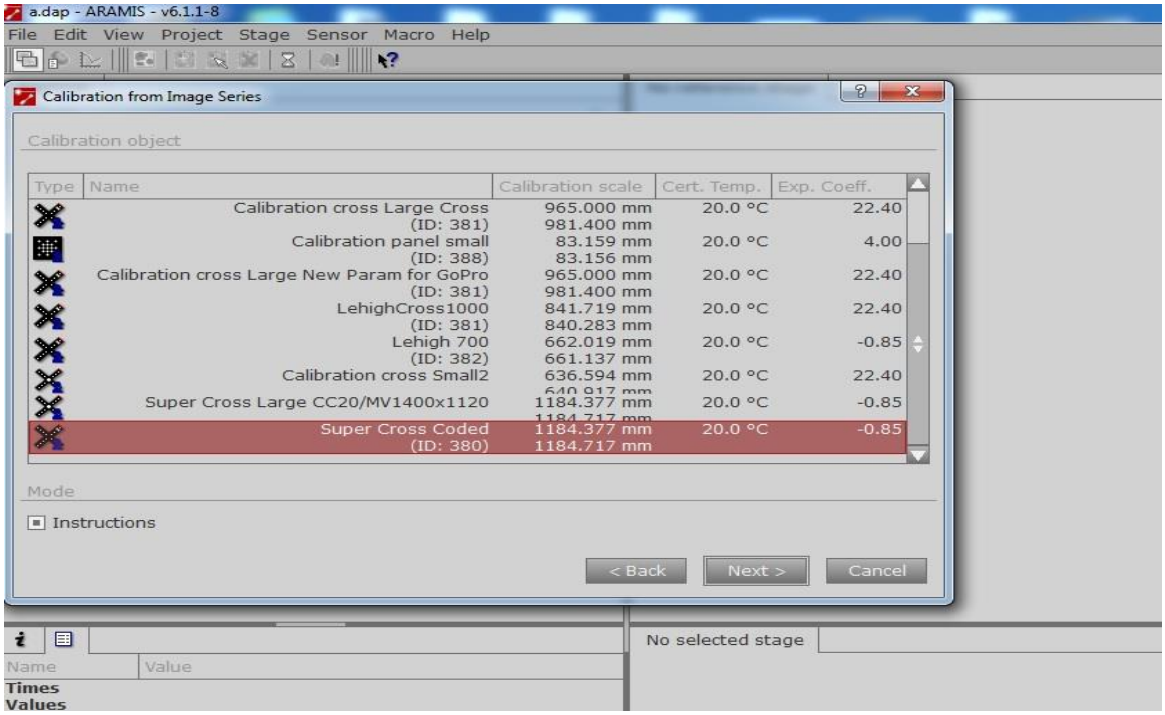

Figure 25. Image display for types of calibration panels

As mentioned previously, the calibration object is important when building a calibration file. Figure 25 show stored parameters of different calibration objects. The calibration result needs to be checked for validity. The calibration deviation indicates calibration accuracy and should be less than 0.04. The camera angle is the actual angle between the cameras. The camera variance should be around ±40°. The height variance value must be less than any of the three values listed for the measuring volume. If any of above parameters are not within the acceptable range, the calibration file is not acceptable. The only way to solve this problem is to redo the image calibration procedure (Bryne, 2017).

4.2 Pattern (specimen preparation)

The camera picks up the patterns which are laid out on the specimen. During the calibration the camera picks up the dots present in the calibrating board whereas during the test the beams where marked in a graphical pattern for the camera to recognize. It can be done by chalk, spray paint, or marker. The paint can be of any color however the color should be in contrast with the target surface.

For the HPC and UHPC beams chalk was used to create a graphical pattern. Figure 26 shows the pattern drawn with chalk on one span. The use of a different color is vital because the processed image would be able to give more clear representation of the beam and can be used to cover the area of study as a whole beam rather than in parts. The patterns were recognized by the camera and ARAMIS was able to process the virtual image of the beam. The processed image of the beam was then used for analysis of strain and displacement measurement. The distance between two points while creating a pattern also remains a sizable component in pattern development. Therefore, pattern development on the specimen becomes a vital aspect of the whole test.

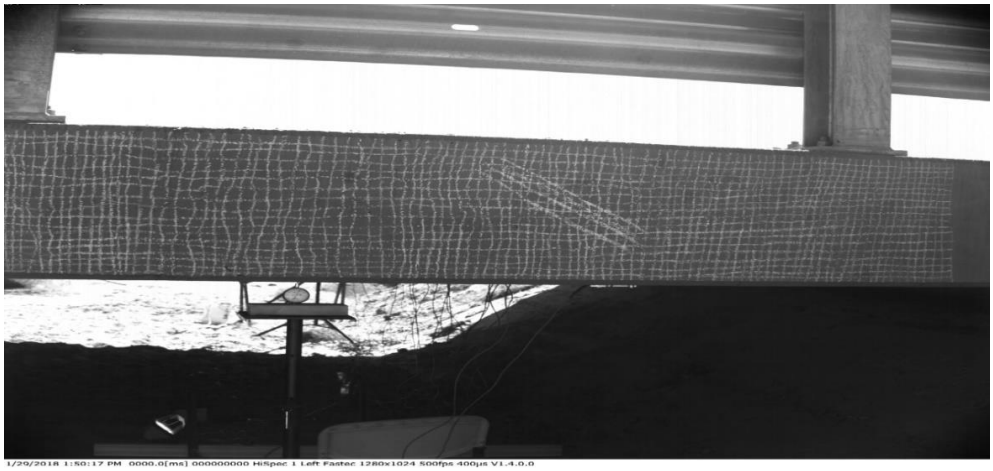

Figure 26. Pattern drawn on HPC beam (fascia girder) picture taken from left camera

The following image is taken from the left Hi-spec camera. The pattern is drawn with a chalk on the HPC beam. It is made in a grid like pattern to depict proper points for the camera to identify. The pattern should be in contrast with the specimen color to be picked by the camera.

Figure 27. Pattern drawn on UHPC beam (fascia girder) picture taken from right camera

Similarly, Figure 27 is taken by the right Hi-spec camera. The cameras are focused to the same object just like the human eye. This helps to create a three-dimensional field of view and helps to calculate the depth in the field as well as out of plane displacement and strain.

Figure 28. Pattern with high contrast attached to the internal girder

Figure 28 shows a pattern used to measure the vertical displacement from a 2D system during the 2019 testing. The pattern was created and attached to the internal girders. The two points on the pattern represent the edge of diagonal which is used to scale the image later when it is processed. The pattern was made on a piece of sheet metal and was attached with epoxy to the bottom of the girder stem.

4.3 Sequence of images

During the calibration process the image file should be numbered sequentially. The numbering also helps to identify the order of the photograph taken. The sequencing of the image file should be done for both calibration and during analysis. The image number can start from any number but has to be serially without any gap in between. The

image files are generated by two cameras left and right. The image from the left should be numbered the same way to the image from the right and should be kept in different folders. During the calibration or analysis, the input dialogue box will ask for two separate image files from two cameras.

4.4 Facets

Pixels and facets are similar yet different. The pixel of an image is the smallest cell which collectively become a photograph. The facet is a group of pixels which the ARAMIS uses to calculate relative displacements. Each facet becomes a data point and then relative displacement in the facet is calculated. The default size of a facet is 15x15 pixels (Bryne, 2017). The size of the facet is directly proportional to the measurement accuracy. If the size of facet is increased, then the accuracy is increased because a greater number of pixels is accountable for the measurement of displacement and strain. However, the increase in facet size will compromise the local deformation within the facet. A small facet size captures the localized effects better. This was enough to compute the profile of the beam completely. The images obtained were sharp and good enough to compute the analysis further. However, precaution should be taken while increase the facet size in an attempt to project the image completely. The increase in facet size would project the image of the beam fully whereas the local deformation within the facet might be neglected which can cause an issue with strain or displacement measurements. Therefore, a proper balance should be found while the facet size is chosen.

4.5 Stage parameter setting

One of values which should be taken into consideration is the stage deviation number which starts from zero. The intersection deviation value can be set to 0.3 pixels or higher, which is a criterion to accept or reject a computed facet point depending on the deviation between measurements from the two cameras (Bryne, 2017). The increase in value for stage deviation might result in error in measurements.

4.6 Challenges faced with calibration

Bridge testing has a lot of added challenges during the testing procedure such as environmental effects. A significant increase in temperature, glare and wind are main causes the alteration focusses of the camera. The solar glare could cause a disturbance in the camera lenses. Appropriate lighting condition is an absolute requirement for quality images. Images taken too early or too late during the day can have a problem when processed with ARAMIS. Another important aspect to be considered during testing is the base where the tripod of the camera stands. The surface should be solid and should not sink or move further during the duration of the test. Any movement might be a cause of hinderance to obtain quality data. The use of many camera system is a good way to capture the deformation of the structure all together, lots of confusion can also occur during the execution of the camera system. All the camera systems should be able to capture the deformation of the bridge at a similar loading stage to compare the results from all camera systems. Proper signaling should be given to respective team members operating the camera systems. Another challenge which should be dealt with is the advancement of equipment and the durability of the computer as well as camera systems.

The testing period can last an entire day and problems regarding wiring, batteries and computer can occur. Every problem should be addressed and noted down. During the test some of the camera systems were down for few tests and some systems where not in synchronization with each other. Adjustment were made during the processing of the images. A spreadsheet file was created to keep track of all the images. Every image file was tracked and kept in order for processing. The images were also synchronized using the time data on the picture and also with the aid of numbering done on each photo file.

Chapter 5

Deformation Analysis for Test 1

Introduction

The movement from its initial position after the application of load is the displacement of a bridge. The deflection profile of the beam is plotted by calculating the displacement of individual facet over the length of the bridge span. The load applied to the span is through the axle loading of trucks. The use of truck loading over the span of bridge deflects the beam. The Image which are taken during different stages of loading are analyzed using ARAMIS to calculate the displacement values. The displacement values are plotted against the position of rear axle load. The deflection profile was plotted using displacement data obtained from four camera systems (Hi-spec, IL5, Go Pro Hero +, Go Pro Hero 6). The maximum displacement value is compared with the value set by the American Association of State Highway Transportation Officials (AASHTO) Bridge Design Specification.

To start the displacement analysis in ARAMIS, the first step is to arrange the images from the camera in two different folders. Since two cameras are used the folders can be named as LEFT and RIGHT. The images are then numbered sequentially from zero to identify the images chronologically.

5.1 Analysis of displacements using ARAMIS

The ARAMIS software program, a DIC platform from GOM, was used in processing the images from the camera systems to obtain the displacements at the locations monitored. For each test, an image was taken prior to loading on the bridge to

obtain a reference, or baseline measurement. An image, or stage, was also taken each time the truck stopped on the bridge. The images from the test were then input into ARAMIS and processed to obtain a full field of displacements over the patterned area. A line segment through the center of the measurement field was established and the vertical displacements across that line for a particular stage were output from the ARAMIS program similar to what is shown in Figure 29. The displacement readings across that line segment were then averaged to obtain a single vertical displacement value at the monitored location. This approach was completed for all displacement readings that follow in the next sections of the report.

In ARAMIS under File>>New Project, name the project and select 3D analysis and then facet size and facet step are selected 21 and 15 respectively. The standard deviation is selected between 0.3 to 0.9. The images were extracted from their respective folders and then the calibration file was pulled out. After processing the images, the mapped version of span of beam appears on the interface. The mapped version of the beam has strain profile already attached to it. The scale on the right-hand side of the screen depicts strain levels which is in various scales. The images are referred to as stages and displacement is measured comparatively to the displacement with previous stages. The computation time for every analysis was under a minute and there was a total of 800 images that was analyzed. Not all beams were mapped because of facet size and deviation were small. The deviation was increased for this problem which resulted in good mapping of the beams. However, the increase in deviation compromised the local deformation within the facet but it resulted in proper mapping which was crucial.

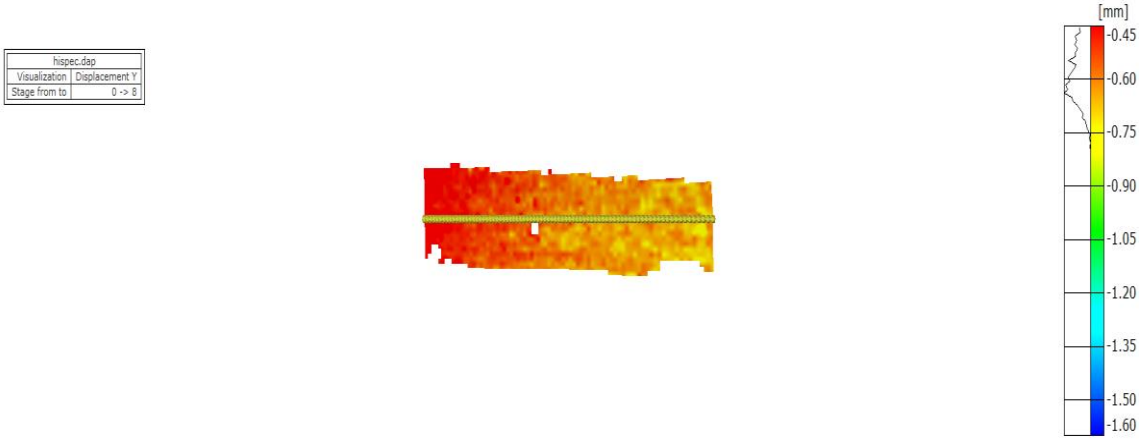

Figure 29. Y Displacement of an UHPC beam obtained from ARAMIS

After the images were mapped, a section along the middle section of the beam was created. The section was parallel to the X-axis. Every point along the section represented a data point which had a value for displacement (see figure 30). Every stage had its own displacement value. For every stage the displacement along the section was averaged and a single displacement value for each stage was obtained. The displacement value was then plotted against the span length along the bridge and then deflection profile of the beam was obtained. The process was done for all six camera systems.

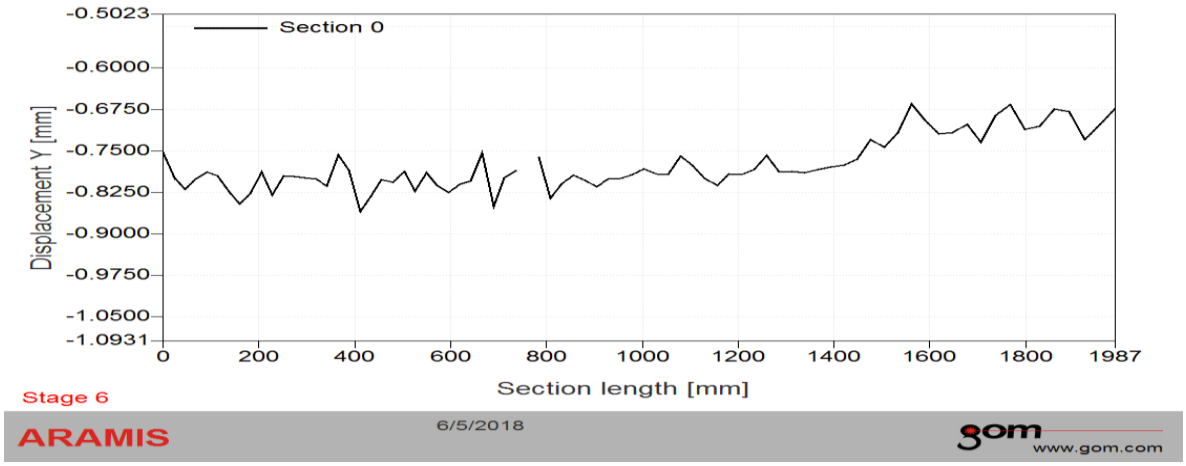

Figure 30. Vertical displacement value of a UHPC beam under single truck loading on path along a line segments (NOTE: 1 in. = 25.4 mm)

The UHPC beam was monitored by IL5 and Go Pro Hero 3 camera system along the span and monitored by 2M system from beneath. The HPC beam was monitored by Hi-spec 1 system, Go Pro Hero + camera system along the span and was monitored by DMK system from underneath.

5.2 Experimental testing results for vertical displacement

The vertical displacements were measured by taking a section along the span of the bridge. The displacement values were averaged over a sectional length and average value of displacement was obtained for a particular stage. The displacement value was plotted against span length of the bridge to develop displacement profile.

5.2.1 Performance of the HPC span

The HPC span was monitored using the HiSpec1, and GoPro Hero + systems at the mid-span of the fascia girders and the DMK system at the mid-span of an interior girder. Upon completion of testing it was determined that none of the images from the DMK system were not able to be used successfully in determining displacements. Therefore, no data from the DMK system will be presented in this report. Additionally, it should be noted that some stages were not captured and as a result some displacement values are missing from the influence line plots of vertical displacement. A negative displacement indicates downward deflection while a positive displacement would mean the element moved upward. The rear axle placement is in relation to the start of the UHPC span.

The HiSpec1 camera system monitored the behavior of an exterior girder on the HPC span of the bridge. The influence line plots for vertical displacement of a single H-

Truck on the bridge for paths 1-6 shown in Figure 2 are presented in Figure 31 with the corresponding numerical values in Table 4. It is noted that path 1 is closest to the HiSpec1 system while path 6 is farthest away. As expected, the greatest response is when the truck is moving along path 1 and the rear axle is directly over the location of the measured field. The peak vertical displacement for this test run is 1.2 mm (0.05 in.). It is interesting to note that when the truck is running along path 3 there appears to be some twisting in the bridge with the exterior girder moving slightly upward 0.47 mm (0.02 in.). This upward motion is present but faint for paths 5 and 6. The data from path 2 seems to suggest some continuity between the two spans as there is a slight downward movement on the HPC side when the truck is on the UHPC span.

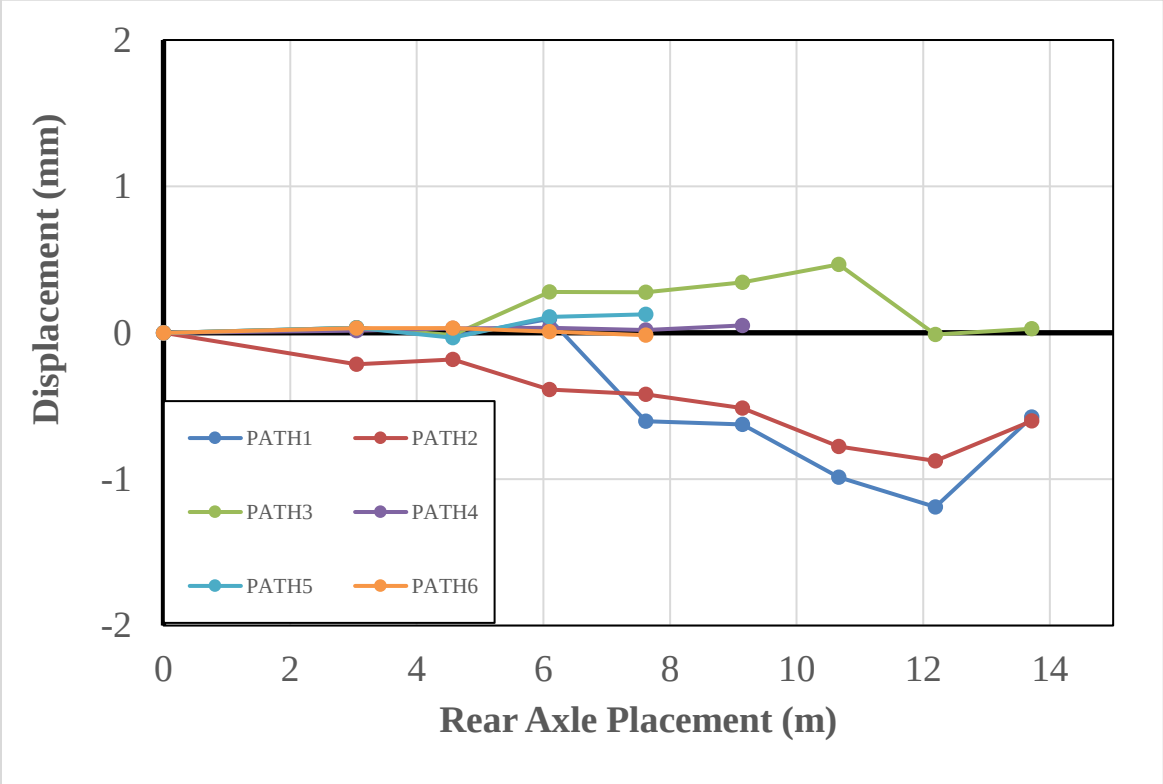

Figure 31. Displacement vs rear axle placement for an exterior HPC beams for single truck loading measured by the HiSpec1 system

Table 4. Numerical values for the vertical displacements corresponding to Figure 31

Rear Axle Location (m)	***PATH 1 (mm)***	***PATH 2 (mm)***	***PATH 3 (mm)***	***PATH 4 (mm)***	***PATH 5 (mm)***	***PATH 6 (mm)***
0	0	0	0	0	0	0
3.048	0.0339	-0.216	0.034	0.0151	0.0338	0.0315
4.572	-0.0234	-0.183	-0.0153	0.0288	-0.034	0.0311
6.096	0.0949	-0.388	0.278	0.0334	0.109	0.00885
7.62	-0.604	-0.421	0.276	0.0198	0.126	-0.0165
9.144	-0.627	-0.514	0.345	0.0503		
10.668	-0.986	-0.776	0.467			
12.192	-1.19	-0.875	-0.0109			
13.716	-0.576	-0.603	0.0272			

Data for vertical displacements captured from the HiSpec1 system due to the back-to-back truck configuration is shown for paths 2, 3, 5 and 6 in Figure 32. Data was only captured for this system when the centerline of the two rear truck axles were on the UHPC span. For each path, there appears to be a minimal downward displacement at the mid-span of the HPC exterior girder when the vehicles are on the UHPC span. However, when the centerline of the two axles are positioned on the HPC span there is more vertical displacement, up to 1.35 mm (0.053 in.) and the displacement is greatest when the trucks are closest to the sensor.

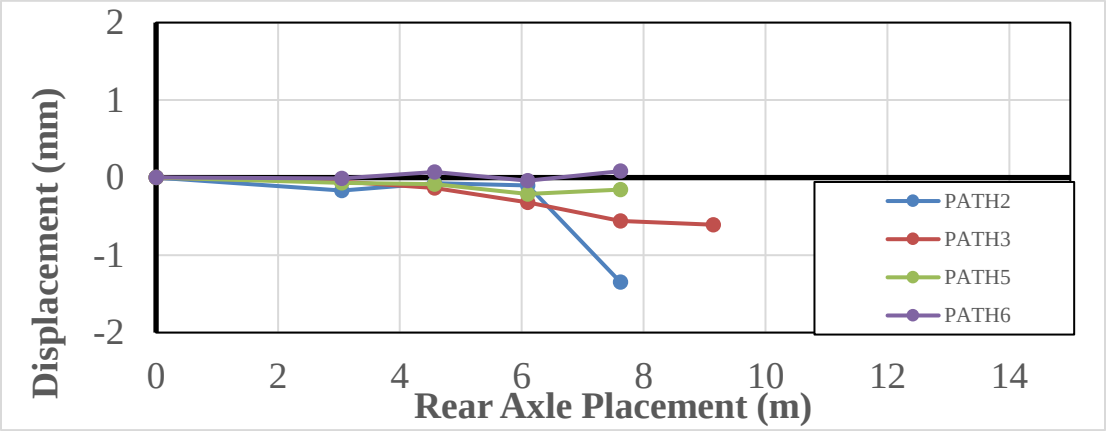

Figure 32. Displacement vs centerline location of rear axle placement for an exterior HPC beams for back-to-back truck loading measured by the HiSpec1 system

Table 5. Numerical values for the vertical displacements corresponding to Figure 32

Center Location of Rear Axles (m)	***PATH 2 (mm)***	***PATH 3 (mm)***	***PATH 5 (mm)***	***PATH 6 (mm)***
0	0	0	0	0
3.048	-0.169	-0.051	-0.0682	-0.0112
4.572	-0.0741	-0.135	-0.0847	0.0742
6.096	-0.103	-0.319	-0.211	-0.0399
7.62	-1.35	-0.56	-0.156	0.0828
9.144		-0.608		

Three trucks were positioned side-by-side-by-side to maximize the transverse load across the bridge spans. Displacements were computed from the images gathered with the HiSpec1 system and reported in Figure 33 and Table 6. The data shows that as the trucks are on the UHPC span there is some slight upward displacement on the UHPC side. When the trucks transition to the UHPC span the displacements are downward with

a maximum of 0.65 mm (0.026 in.) when the axles are near the mid-span. This again suggests some continuity between the UPHC and HPC spans.

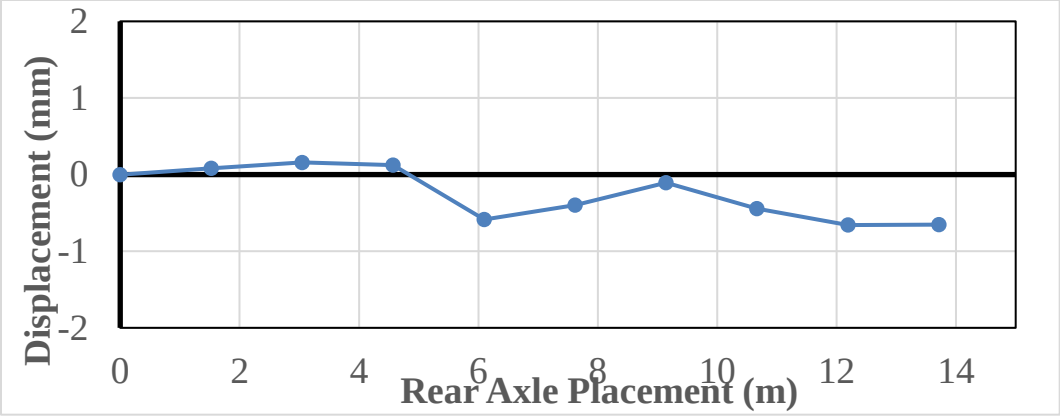

Figure 33. Displacement vs centerline location of rear axle placement for an exterior HPC beams for three side by side trucks measured by the HiSpec1 system

Table 6. Numerical values for the vertical displacements corresponding to Figure 33

Center Location of Rear Axles (m)	***Vertical Displacement (mm)***
0	0
1.524	0.080180332
3.048	0.16
4.572	0.124996108
6.096	-0.584978157
7.62	-0.396649023
9.144	-0.106802757
10.668	-0.443748364
12.192	-0.65889513
13.716	-0.653352452

The GoPro Hero+ was used as two separate cameras capturing the same field of view on the exterior girder opposite of the HiSpec1 cameras. Since the cameras were run separately, the images were processed using 2D DIC analysis. The Hi-spec camera system was monitoring the girder where load path 1 and 2 were closest to the girder where the Hero+ camera system was closest to the load path 5 and 6 of the camera system. Figure 34 shows the data gathered from the GoPro Hero+ system. The path is compared in a such a way that both loading path are similar for both camera system. The deflection starts immediately for both system as the truck loading also began from the UHPC side of the bridge. The deflection for the Go Pro is higher in magnitude compared to the displacement observed by the Hi-spec camera system.

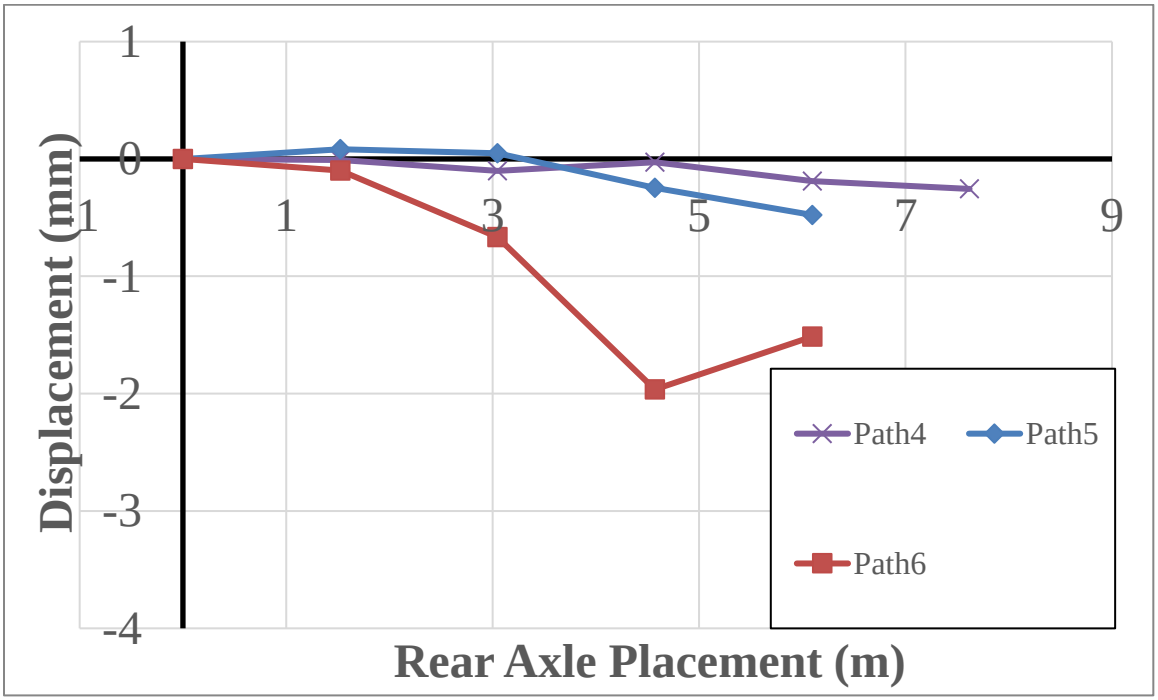

Figure 34. Displacement vs rear axle placement for an exterior HPC beams for single truck loading along path 4,5,6 measured by the GoPro Hero+ system

Table 7. Numerical values for the vertical displacements corresponding to Figure 34

Span(m)	***Path4 (mm)***	***Path5 (mm)***	***Path6 (mm)***
0	0	0	0
1.524	-0.008335298	0.082656	-0.09783
3.048	-0.100663181	0.049693	-0.66534
4.572	-0.02785	-0.24501	-1.96393
6.096	-0.188083266	-0.47734	-1.51371
7.62	-0.255292257		

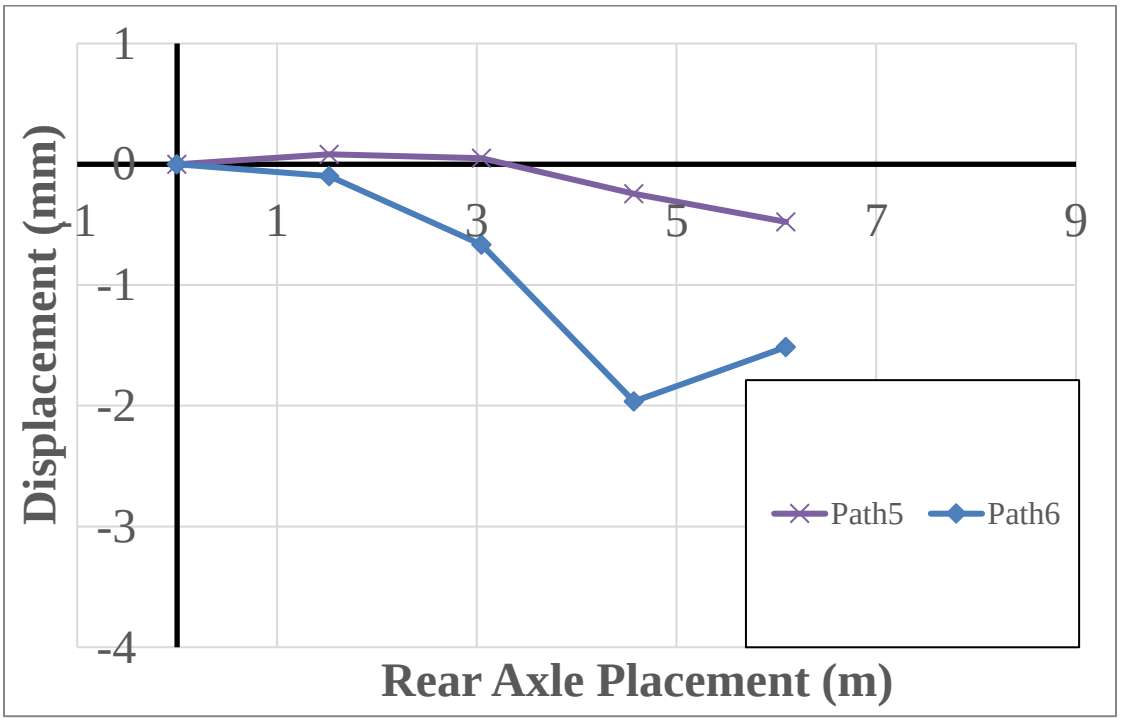

(a)

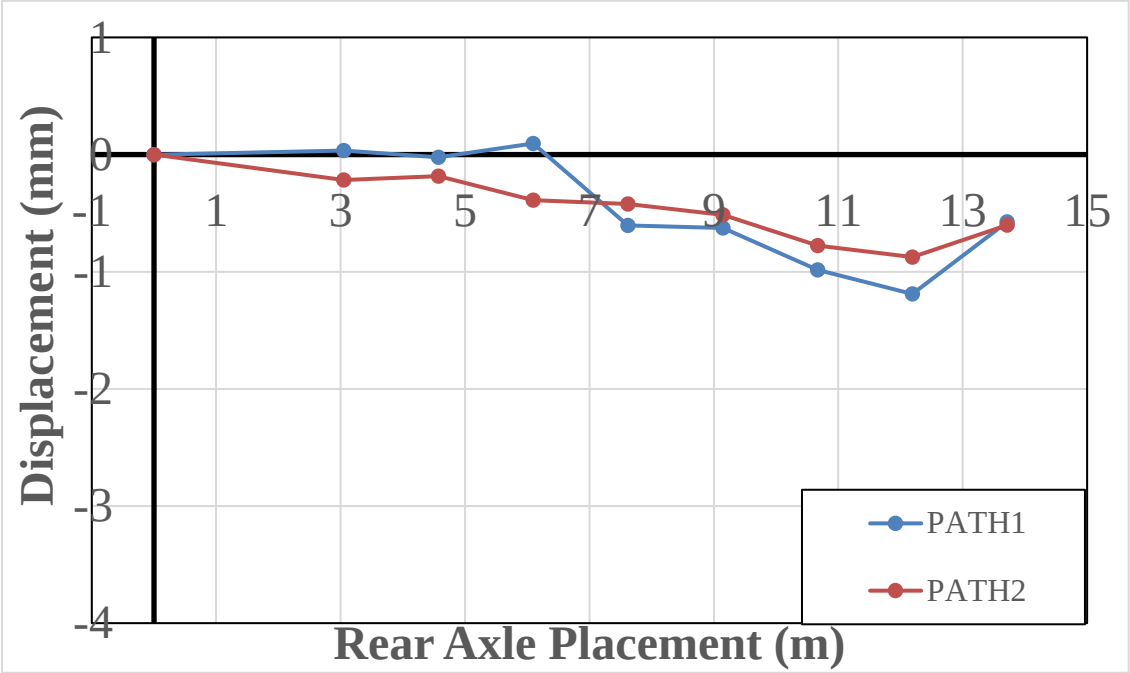

(b)

Figure 35. Comparison of vertical displacement vs rear axle placement for the exterior HPC beams for single truck loading along path 1 and 2 (b) with 5 and 6 (a).

5.2.2 Performance of UHPC span

The UHPC span was monitored using the IL5, and GoPro Hero 3 systems at the mid-span of the fascia girders and the 2M system at the mid-span of an interior girder. It should be noted that some stages were not captured and as a result some displacement values are missing from the influence line plots of vertical displacement. A negative displacement indicates downward deflection while a positive displacement would mean the element moved upward. The rear axle placement is in relation to the start of the UHPC span.

The IL5 camera system monitored the behavior of an exterior girder on the UHPC span of the bridge. The influence line plots for vertical displacement of a single H-Truck

on the bridge for paths 1-6 shown in Figure 2 are presented in Figure 3b and Table 10. It is noted that path 1 is closest to the IL5 system while path 3 is closer to the centerline of the bridge. For paths 1 and 2 as the truck enters on the bridge the displacements at the mid-span begin to increase. As expected, the greatest response is when the truck is moving along path 1 and smallest for paths 3, 5 and 6. The peak vertical displacement for this test run is approximately 1 mm (0.04 in.). When the truck is running along paths 3-6 there appears to be some twisting in the bridge with the exterior girder moving very slight upward with a maximum displacement of 0.43 mm (0.017 in.). This is slightly lower than what was seen for the HPC span. The data from path 1 seems to suggest some continuity between the two spans as there is a slight upward movement on the UHPC side when the truck is on the HPC span.

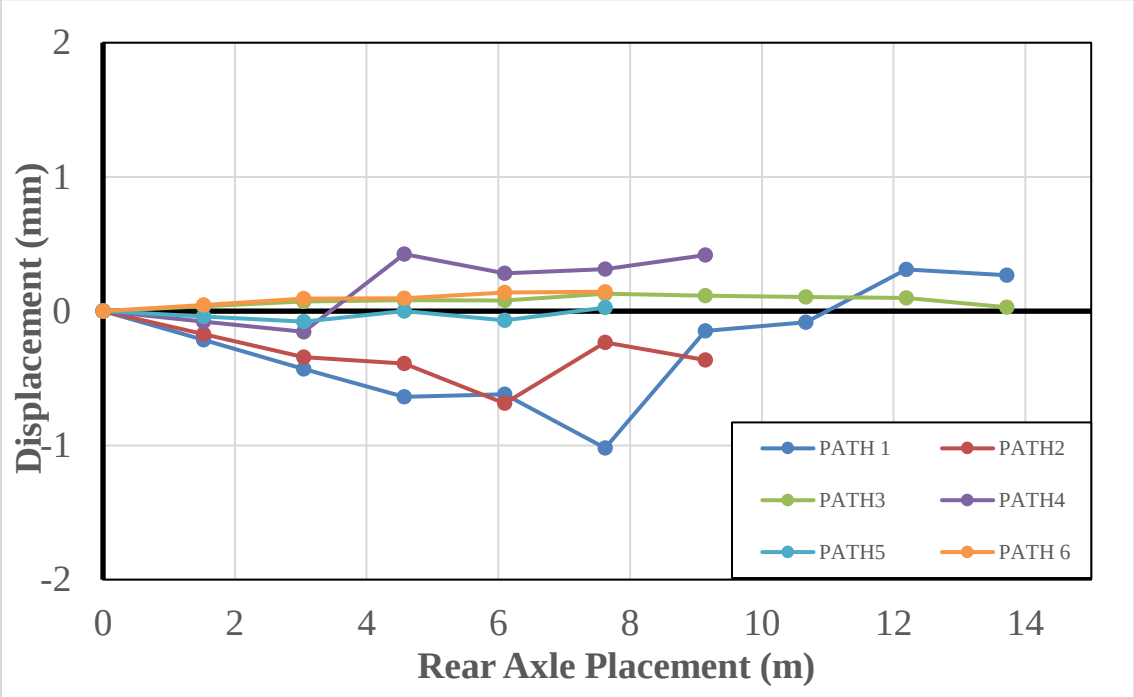

Figure 36. Displacement vs rear axle placement for an exterior UHPC beams for single truck loading measured by the IL5 system

Table 8. Numerical values for the vertical displacements corresponding to Figure 36

Rear Axle						
Location (m)	***PATH 1 (mm)***	***PATH 2 (mm)***	***PATH3 (mm)***	***PATH 4 (mm)***	***PATH 5 (mm)***	***PATH 6 (mm)***
0	0	0	0	0	0	0
1.524	-0.215	-0.1715	0.0361	-0.0769	-0.03916	0.0463835
3.048	-0.43	-0.343	0.0722	-0.15381	-0.07832	0.092767
4.572	-0.638	-0.39	0.0817	0.425234	0.001695	0.0949137
6.096	-0.62	-0.687	0.0787	0.282311	-0.06844	0.1377856
7.62	-1.02	-0.233	0.13	0.312833	0.026139	0.1447496
9.144	-0.147	-0.363	0.114	0.418648		
10.668	-0.0824		0.105			
12.192	0.311		0.0995			
13.716	0.267		0.0293			

The GoPro Hero 3 was used as was used as two separate cameras capturing the same field of view on the exterior girder opposite of the IL5 cameras. Since the cameras were run separately, the images were processed using 2D DIC analysis. To verify both sets of images were capturing the same, or nearly the same, displacements, the results were compared then averaged. The results are shown in Table 9 and Figure 37.

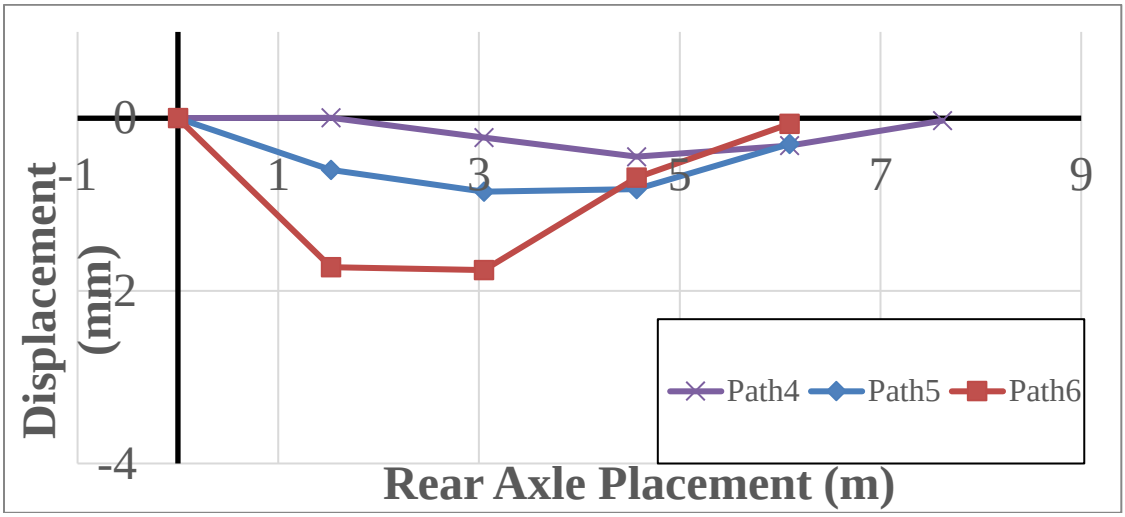

Figure 37. Displacement vs rear axle placement for an exterior UHPC beams for single truck loading along path 4,5,6 measured by the GoPro Hero3 system

Table 9. Numerical values for the vertical displacements corresponding to Figure 37

Span(m)	***Path4(mm)***	***Path5(mm)***	***Path6(mm)***
0	0	0	0
1.524	0.004945633	-0.600313392	-1.725673444
3.048	-0.223681951	-0.85098924	-1.759114343
4.572	-0.445042929	-0.822700476	-0.68743
6.096	-0.31608275	-0.299346143	-0.065599409
7.62	-0.02904814		

The UHPC side of the bridge was monitored by GoPro Hero 3 and IL5 camera system. The IL5 camera system was monitoring the girder where load path 1 and 2 were closest to the girder where the Hero3 camera system was closest to the load path 5 and 6 of the camera system. The path is compared in a such a way that both loading path are similar for both camera system. The deflection starts immediately for both system as the truck loading also began from the UHPC side of the bridge. The deflection for the Go pro is

higher in magnitude compared to the displacement observed by the Hi-spec camera system.

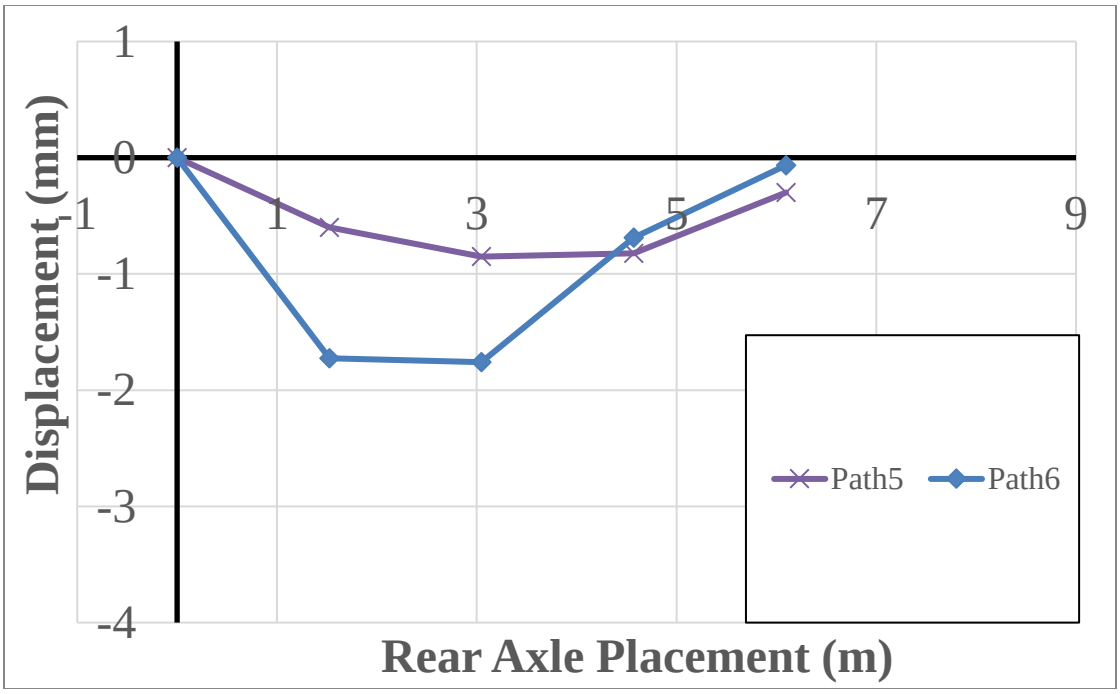

(a)

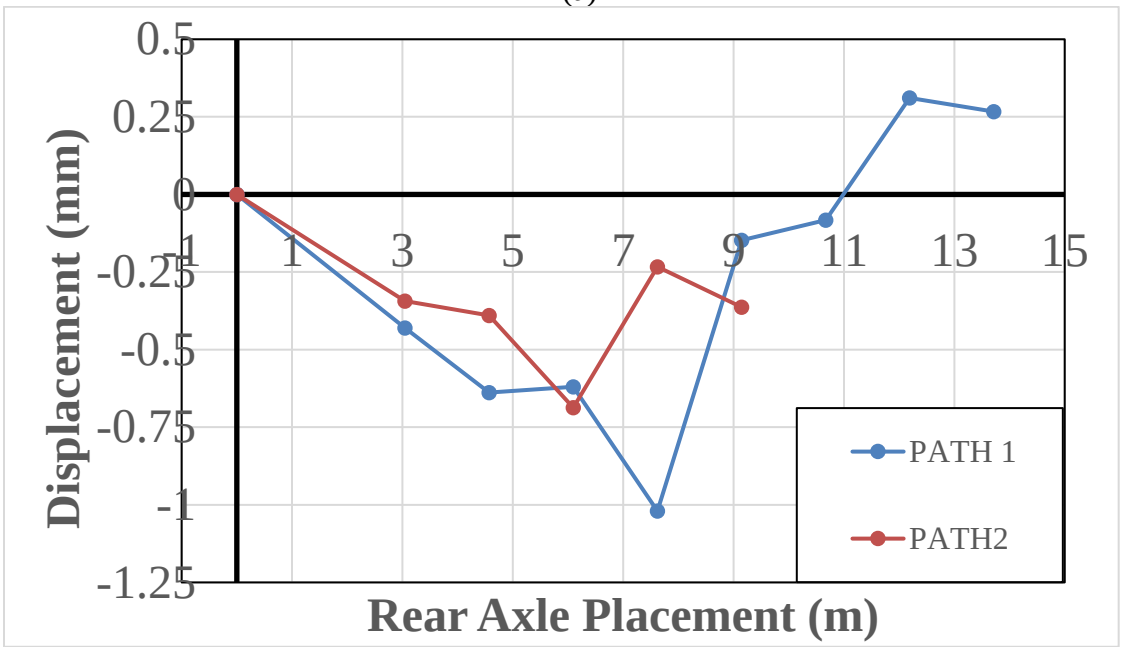

(b)

Figure 38. Comparison of vertical displacement vs rear axle placement for the exterior UHPC beams for single truck loading along path 1 and 2 (b) with 5 and 6 (a).

A comparison of vertical displacement was completed at the mid-span of the exterior girders monitored by the IL5 and HiSpec1 systems for a single vehicle on paths 1-3. The results for this are shown in Figure 39 with the corresponding numerical values in Table 15. The dashed and solid lines correspond to the IL5 and HiSpec1 systems respectively. For both beams the maximum downward vertical displacements occur when the truck is along path 1. This maximum value is 1.02 mm (0.04 in.) and 1.19 mm (0.047 in.) for the UHPC and HPC spans respectively. Path 3 produces an upward movement of the exterior girder for both spans with the larger result on the HPC span. While comparing the values for displacement for UHPC and HPC beams at similar stages and under similar loading stages, the displacement value of HPC beam are comparatively higher than the UHPC beam.

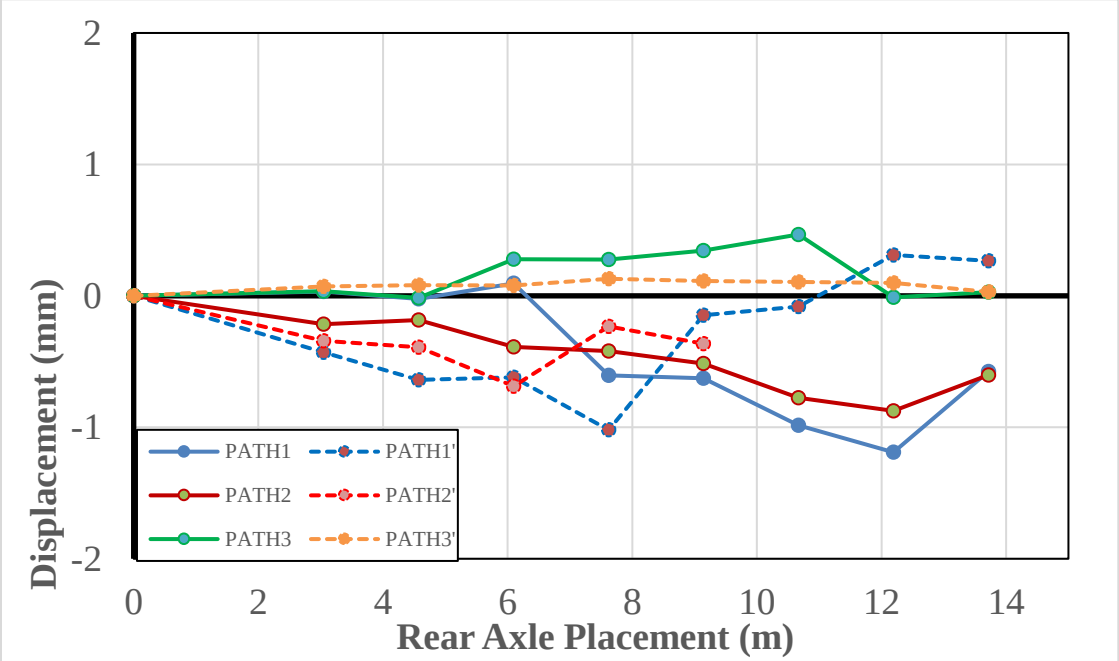

Figure 39. Comparison of displacement vs rear axle placement for the exterior beams from IL5 (dashed lines) and HiSpec1 (solid lines) under single truck loading

Table 10. Numerical data for vertical displacements corresponding to Figure 39

Center Location of Rear Axles (m)	***PATH 1 HiSpec1 Vertical Displacement (mm)***	***PATH 1' IL5 Vertical Displacement (mm)***	***PATH 2 HiSpec1 Vertical Displacement (mm)***	***PATH 2' IL5 Vertical Displacement (mm)***	***PATH 3 HiSpec1 Vertical Displacement (mm)***	***PATH 3' IL5 Vertical Displacement (mm)***
0	0	0	0	0	0	0
3.048	0.0339	-0.43	-0.216	-0.343	0.034	0.0722
4.572	-0.0234	-0.638	-0.183	-0.39	-0.0153	0.0817
6.096	0.0949	-0.62	-0.388	-0.687	0.278	0.0787
7.62	-0.604	-1.02	-0.421	-0.233	0.276	0.13
9.144	-0.627	-0.147	-0.514	-0.363	0.345	0.114
10.668	-0.986	-0.0824	-0.776		0.467	0.105
12.192	-1.19	0.311	-0.875		-0.0109	0.0995
13.716	-0.576	0.267	-0.603		0.0272	0.0293

The 2M system was near the mid-span of an interior girder on the UHPC span of the bridge. Figure 40 and Table 11 depict the vertical displacements as a single truck passes over paths 1-6. For each influence line the vertical displacement is in the downward direction as expected. The largest displacement occurs for paths 1 and 2 with a maximum displacement of 1.7 mm (0.07 in.). The displacements are smallest for paths 5 and 6 which are farthest from the monitored location. Very small amounts of displacement are seen at this location when the vehicle is positioned on the HPC span of

the bridge. While they are small, there does appear to be some interaction between the two spans.

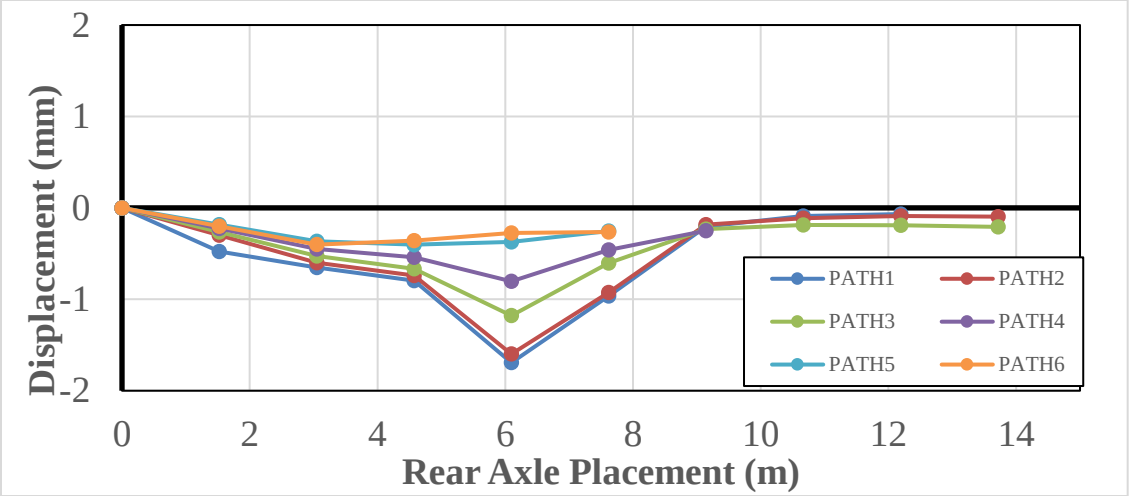

Figure 40. Displacement vs rear axle placement for an interior UHPC beams for single truck loading along paths 1-6 measured by the 2M system

Table 11. Numerical values for the vertical displacements corresponding to Figure 40

Rear Axles (m)	***PATH 1 (mm)***	***PATH 2 (mm)***	***PATH 3 (mm)***	***PATH 4 (mm)***	***PATH 5 (mm)***	***PATH 6 (mm)***
0	0	0	0	0	0	0
1.524	-0.47611	-0.29954	-0.26366	-0.224	-0.18207	-0.201
3.048	-0.65278	-0.59908	-0.52732	-0.44799	-0.36414	-0.402
4.572	-0.79429	-0.74122	-0.66743	-0.54134	-0.4022	-0.35892
6.096	-1.69298	-1.59879	-1.17877	-0.80367	-0.37115	-0.27376
7.62	-0.96249	-0.9267	-0.60335	-0.45845	-0.25334	-0.2643
9.144	-0.2051	-0.18447	-0.23237	-0.25041		
10.668	-0.08933	-0.11286	-0.18711			
12.192	-0.06834	-0.09031	-0.19044			
13.716		-0.09513	-0.20781			

The IL5 and 2M systems were compared for testing in paths 1-3 for a single truck loading and shown in Figure 41 and Table 12. The data indicates higher vertical displacement measured by the 2M system towards the center of the bridge compared to that measured by the IL5 on the exterior. It was expected that the exterior girder should have higher displacements than an interior girder because the loading is near the exterior. Path 2 on the other hand is more directly over the location of the 2M system so that should have higher displacement. A possible reason for the lower displacements on the exterior girder is the result from a stiffer cross-section compared to an interior beam. More investigation into this finding needs to be completed before any conclusions can be drawn.

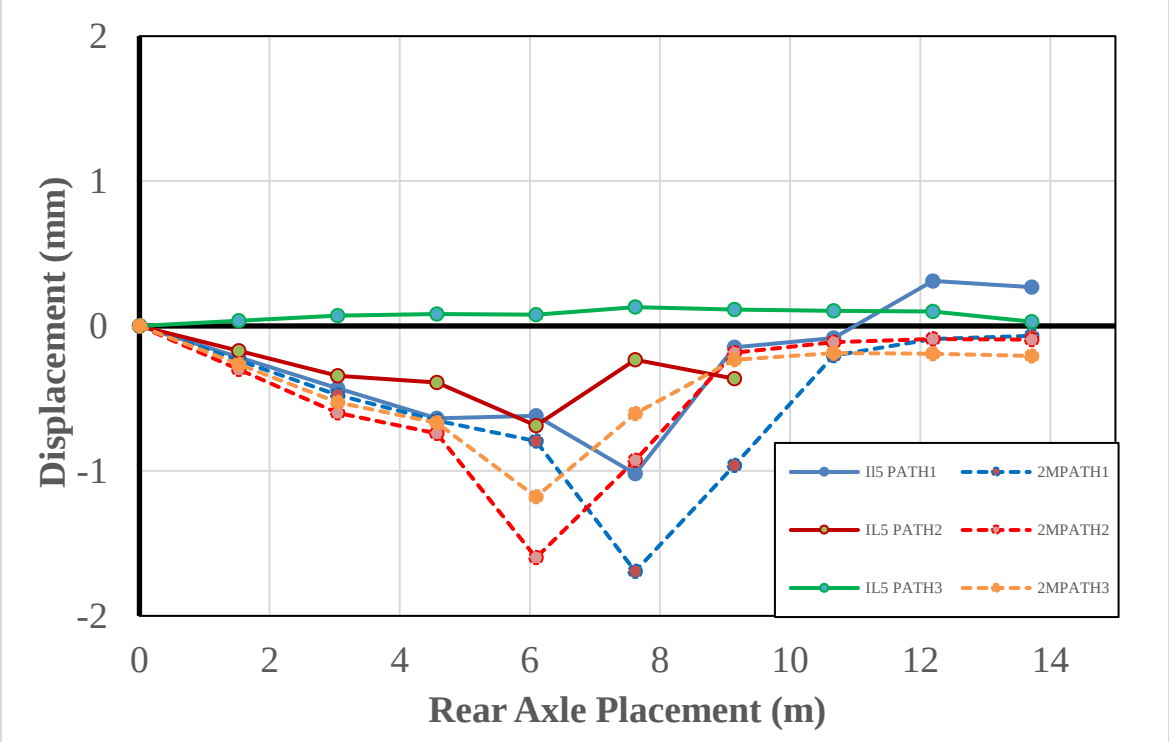

Figure 41. Comparison of vertical displacement vs rear axle placement for beams from IL5 (solid lines) and 2M (dashed lines) systems under single truck loading

Table 12. Numerical values for the vertical displacements corresponding to Figure 41

Rear Axles (m)	***IL5 PATH 1 Displacement (mm)***	***2M PATH 1 Displacement (mm)***	***IL5 PATH 2 Displacement (mm)***	***2M PATH 2 Displacement (mm)***	***IL5 PATH 3 Displacement (mm)***	***2M PATH 3 Displacement (mm)***
0	0	0	0	0	0	0
1.524	-0.215	-0.238057	-0.1715	-0.29953955	0.0361	-0.2636576
3.048	-0.43	-0.4761139	-0.343	-0.59907909	0.0722	-0.5273152
4.572	-0.638	-0.6527754	-0.39	-0.74121914	0.0817	-0.6674349
6.096	-0.62	-0.7942945	-0.687	-1.59879403	0.0787	-1.1787692
7.62	-1.02	-1.6929848	-0.233	-0.92669697	0.13	-0.6033512
9.144	-0.147	-0.9624898	-0.363	-0.18447343	0.114	-0.2323686
10.668	-0.0824	-0.2050996		-0.11286294	0.105	-0.1871089
12.192	0.311	-0.089333		-0.09031235	0.0995	-0.1904354
13.716	0.267	-0.068345		-0.09513039	0.0293	-0.2078125

Load testing of a 2 span multi-girder/stringer pre-stressed concrete bridge was undertaken in New Mexico. One span of the structure was constructed using UHPC and the other HPC. During this testing four 3D and four 2D DIC systems were deployed to monitor displacements at various locations of the structure under controlled prescribed loading. The loading was selected as to generate maximum flexural and shear responses within both spans. Images were captured at each static positioning of the loading on the bridge. These images were processed using the ARAMIS GOM DIC software package to generate displacement measurements. The results appear to indicate that the UHPC span is stiffer than the HPC span. This can be seen from the smaller displacements of the

exterior fascia girders monitored by the HiSpec1 and IL5 systems under identical loading conditions. It was noted in some tests that there was very small upward displacement of an exterior girder which suggests the possibility of the bridge twisting slightly. In any case, all displacement measurements were well below the maximum allowed by AASHTO Bridge Design Specifications (Bell et al., 2010).

The test was carried out for single truck loading and displacement were calculated. However, double truck loading and triple truck loading were also used for the testing. The test had two trucks placed back to back and also three trucks side by side which also marked the highest loading for the test. The observation for the test with loading more than a single truck are shown and discussed below.

The displacement calculated using DIC has advantages over many techniques used today. Finite Element Analysis can also be used to calculate deformation on a structure but DIC is able to capture the current condition of the structure as well. FEA analysis such as SAP2000 can calculate deformation but conditions like age of the structure, deterioration cannot be accurately defined. The use of image helps to capture the condition of the structure as it is in the current situation and will be able to give data accurately with less assumptions. This is a crucial aspect of DIC in cases where micro measurements are considered. The deviation in accuracy of data can be minimized using DIC. Although, FEA analysis is obligatory during deformation analysis, DIC can paint an accurate view of how a structure behaves in present conditions. The advantage of DIC for structural health monitoring is vital as it can depict present condition of structure with reasonable accuracy and relatively easily compared to other methods.

The loading greater than a single truck loading were conducted to calculate maximum displacement in both UHPC and HPC beam. The deflection of two beams are calculated separately to measure the performance of both beams.

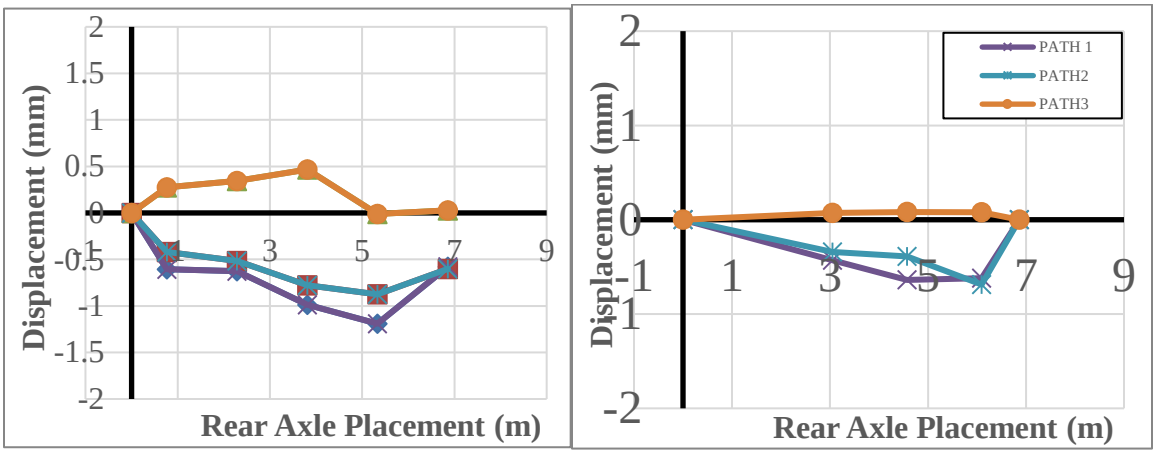

(a) *(b)*

Figure 42. Comparison of displacement of HPC (left) (a) and UHPC (right) (b) under single truck loading

The comparison between displacement value captured by Hi-spec and IL5 can be studied side by side. The displacement value obtained from Hi-spec camera showed larger displacement values than the IL5. This UHPC beam gave less deflection value than the HPC beam under similar loading condition. For test done under similar path with different truck loadings the displacement obtained from UHPC beam was less than the displacement obtained from the HPC beams. The deflection values for similar loading in same path was compared side by side for both UHPC and HPC beams. The downward displacement was lesser compared to the HPC beams which implies the beam deflected lesser than the HPC beam. The positive displacement (upward displacement) is also lesser in UHPC beam compared to the HPC beam concluding that the UHPC beams are

stiffer than the HPC beams. The comparison for two beams for different loading is shown from Figure 43-45.

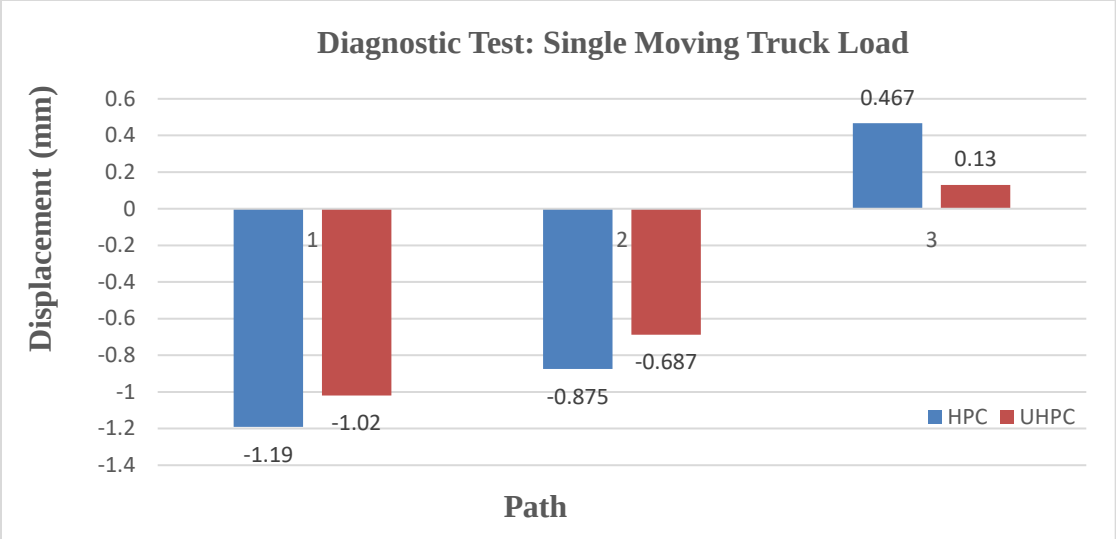

Figure 43. Comparison of HPC and UHPC under similar loading condition on same path

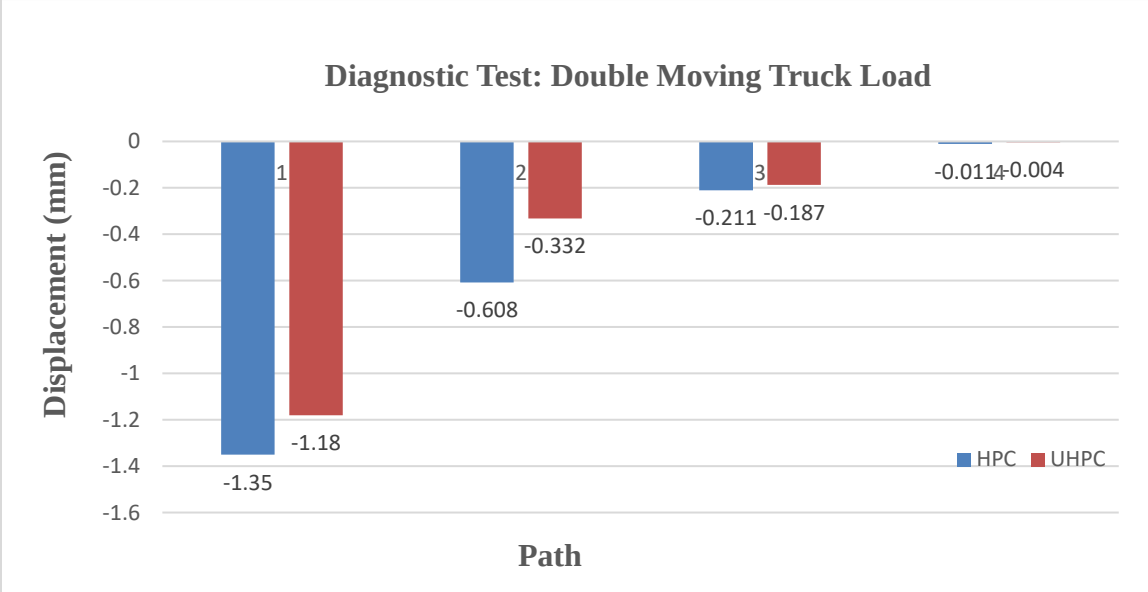

Figure 44. Comparison of HPC and UHPC under similar loading condition on same path

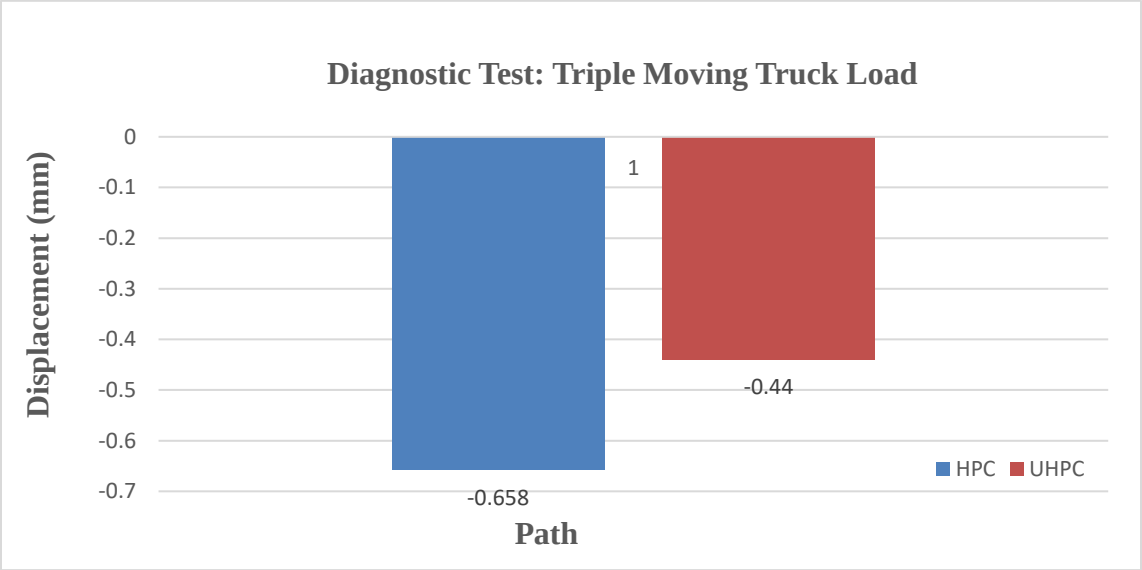

Figure 45. Comparison of HPC and UHPC under similar loading condition on same path

5.3. Strain analysis

This technique works by applying a pattern to the surface of a test specimen, capturing a series of images of the specimen during a test, and then analyzing the images with an algorithm that determines first the displacement field and then the strain field for each image. The first image which is processed has no strain associated with it. The image is then split into small subsets and the patterns within each subset of subsequent images are compared to the reference image and displacements are calculated. From these displacements, a strain map is calculated. The strain maps of all the strain components (axial, transverse, shear strain), along with maximum and minimum normal strains, can be determined. Compared to traditional methods of local strain (e.g. strain gauges) or average strain over a large gauge length (e.g. extensometers) measurement, full-field strain measurement yields an enormous amount of additional information that

can help engineers and scientists better understand the behavior of materials and structures.

ARAMIS has built in algorithm to compute strain fields. The in-plane stress along X axis and Y axis are computed from displacement fields. However, the out- of plane stresses are calculated by plane stress or plane strain model. There are two ways to compute the strain from the data points: linear strain computation and spline strain computation. The linear strain computation uses displacement data points (facets points) to calculate the strain, whereas the spline strain computation interpolates the displacement data points to create additional points first and then uses both the interpolated and original data points to calculate the strain. The default linear strain computation size is three, which means a total of nine neighboring facet points, including the center facet, are used to compute the strain at the center facet. A large computation size reduces the noise, but it also may reduce the total number of strain computation points. A validity quote of 100% means 100% of the neighboring facets points must be present in order to compute the strain. This value is usually not set to 100%. Instead, it is set to 55% in order to compute the strain near the edges or cracks on the target. The spline strain computation is able to compute the strain in a location where there is a small radius of curvature. The spline strain can calculate the strain on the surface or in the middle of the target. There are also two ways to present the computed strain results: the total strain method and the step-by-step method. The first method uses the first stage as the reference stage, whereas the latter method always uses the previous to current stages. To compute the stress on the target, the material properties, such as the Young's

modulus, are required. The plane stress model is appropriate for thin materials, whereas the plane strain model is suitable for thick material.

The strain computation method used for the test was linear strain computation method. The first step is similar to the one used to calculate displacement. After mapping of the HPC and UHPC beam a section along the beam is created. Unlike during the calculation of displacement. The section is created 1inch from the bottom of the beam. Strain gauges were used at the bottom of every fascia girders and the section was created 1" above the area where the strain gauges were placed. The reason for selecting 1inch from the bottom was to avoid potential noise which is obtained at the edges of the mapped object. The other reason being the mapped surface might not have the edge of the beam mapped completely which brings inconsistency in the data. After the section is created, linear computation of strain is chosen. Since every point along the section has its own strain value, the average value along the section of the beam is taken. The strain value for every stage is calculated. The strain value for every stage represents the strain produced during each stage of loading.

The calculated value of strain is then plotted against the distance along the span of the beam. The change in strain at different level of loading during the test can also be represented by color code which is incorporated with ARAMIS. The change in strain can also be monitored as the loading on the bridge changes. Along with the color code the strain values are displayed on a scale. The strain gauges were deployed in every girder to calculate the strain measurements. The strain values obtained from DIC was also compared with the strain values obtained from the strain gauges to validate the strain

measuring method using DIC. Similar to the displacement analysis, the strain values are measured for single truck loading, double truck loading and triple truck loading.

When looking at very small strains, high noise levels may make it difficult to get good results. As with all measuring techniques, noise is not avoidable in DIC, but steps can be taken to minimize it.

In most of the cases while measuring strain values of a bridge the measured value of strain is very small and high noise level makes it very difficult to get good results. There are various methods to reduce noise levels during a test. Necessary steps can be taken to reduce the level of noise during a test.

One of the reasons is the speckle pattern created on the specimen before the testing. A good pattern will allow the correlation to be made with high confidence and produce low noise. The pattern should meet requirements to produce good results. The color used to create speckle should be high in contrast, the speckle pattern should be consistent in size. The speckle size should be adequate because if the size of the speckle is too small the resolution of the camera might not be able to pick it up. If the size is too big the speckle might cover a large area and the small displacement cannot be observed. Inconsistent size and repetitive pattern can be a potential cause to create a high noise band for the test. The original displacement fields calculated at discrete locations using DIC are unavoidably contaminated by noises. If the strain fields are directly computed by differentiating the original displacement fields, the noises will be amplified even at a higher level, and the resulting strain fields are untrustworthy. The criteria which required the pattern to be in contrast was satisfied for the test AASTHO (2010).

Noise is unavoidable during testing of DIC but can be minimized by taking the necessary precautions. Pattern being one of the most important elements to minimize the noise level. There are other components which can be considered: a) focus b) contrast c) lighting d) glare e) F-stop.

Sharp focus on the pattern can detect it more accurately than otherwise. Hard and sharp edges would help to keep the facet size to a minimum and still produce good mapping of the specimen.

The contrast of the marker used also determines the effectiveness of mapping and noise reduction. Hard edges, constant speckle size and less bright areas gives good mapping. The aperture of lens also has a vital role in determining the appropriate amount of light going inside the camera.

5.3 Experimental Testing Results for Strain Measurement

The strain measurement was calculated over a section on a beam. The section was selected at a distance of one inch from the bottom of the span. The strain value was averaged along the section created. The strain value was obtained for every loading stage.

5.3.1 Performance of HPC span

The HPC span of the bridge was monitored by the Hi-spec camera system and Go Pro Hero + on the fascia girders and the interior girders were monitored by DMK camera system. The span monitored by the Hi-spec 1 is closer to path 1 whereas path 6 was closer to Go Pro Hero + camera system. The strain values were also measured using strain gauges for fascia girders and also for internal girders. The strain values obtained from the strain gauges are shown in Table 13.

Table13. Strain Values measurement of bridge girders for HPC beams measured by strain gauges

Diagnostic Test: HPC Single Moving Truck Load

Strain (με)

Gauge Location	***Path 1***	***Path 2***	***Path 3***	***Path 4***	***Path 5***	***Path 6***
HPC NBG1	73.7	37.5	11.8	5.9	1.8	2.36
HPC SBG1	76.0	50.3	19.2	13.5	5.7	5.69
HPC NBG2	78.0	60.1	27.7	17.3	6.5	7.18
HPC SBG2	69.8	72.3	44.8	29.4	14.7	14.72
HPC NBG3	66.8	68.1	44.2	30.4	15.7	12.86
HPC SBG3	56.0	60.8	62.7	49.9	29.9	24.49
HPC NBG4	55.9	61.0	65.1	54.7	34.6	26.08
HPC SBG4	49.3	52.7	74.9	73.0	59.9	53.67
HPC SBG5	24.6	29.5	57.2	71.5	74.3	72.74
HPC SBG6	9.4	11.5	27.5	42.7	69.9	77.35
HPC SBG7	2.3	5.2	13.1	22.0	42.6	77.76
HPC SBG8	-1.8	2.7	7.2	10.3	24.7	77.98

For every girder in the bridge one strain gauge was deployed named as north bound gauge and other as south bound gauge. For eight girders a total of 12 strain gauges were used. The data obtained from DIC was compared with the data obtained from the strain gauges in Table 14.

Table14. Strain values comparison of bridge girders for HPC beams measured by strain gauges and DIC

Path	***Strain Gauge (με)***	***Digital Image correlation (με)***
1	76.03	130.62
2	69.76	69.16
3	55.98	-6.57
4	49.3	-9.56
5	-1.79	-2.06

The strain gauges measured strain for the fascia girder for loading on all load paths. The strain values also decreased gradually as the truck moved further from the outer girder. The maximum value of strain obtained from DIC was 130.62 με whereas the strain gauge measured a value of 76.03 με. The minimum value measured by DIC was -9.568 με whereas the minimum value measured by the strain gauge was -1.79 με. For strain measurement on HPC beam DIC did not show good accuracy based on the results. The noise band can be considered as one of the reasons to affect the accuracy of DIC while measuring micro-strain values. The value measured for strain on the fascia girder of the HPC beam is tabulated in Table 15.

Table 15. Strain values for HPC beam on single truck loading

SPAN	PATH1	PATH2	PATH3	PATH4	PATH5
0	0	0	0	0	0
1.524	-6.1896281	-73.39129	-55.2512	-30.10881	-2.34252127
3.048	-25.028789	-57.54847	-75.43354	-55.98545	-4.73808453
4.572	26.5990212	-35.11456	-58.74307	-26.37857	-2.06622648
6.096	-86.72323	31.037274	-6.572099	-9.568169	-4.50330627
7.62	38.2373913	-9.632036	-16.56176		
9.144	84.43159	49.152845	-26.56315		
10.668	130.625787	69.164651	-43.01237		
12.192	-20.7522379	20.980115	-8.695627		

5.3.2 Performance of UHPC span

The UHPC span of the bridge was monitored by the IL5 camera system and Go Pro Hero plus on the fascia girders and the interior girders were monitored by 2M camera system. The span monitored by the IL5 is closer to path 1 whereas path 6 was closer to Go Pro Hero plus camera system. The strain values were also measured using strain gauges for fascia girders and also for internal girders. Unlike the DMK camera system the 2M system was able to give decent displacement data and therefore it was also used to process the strain data. The strain values obtained from the strain gauges are shown in Table 16.

Table 16. Strain values measurement of bridge girders for UHPC beams measured by strain gauges

Diagnostic Test: UHPC Single Moving Truck Load						
Strain (με)						
Gauge Location	***Path 1***	***Path 2***	***Path 3***	***Path 4***	***Path 5***	***Path 6***
UHPC NBG1	80.7	47.4	19.2	8.4	4.2	3.28
UHPC SBG1	87.9	61.8	27.9	16.9	9.2	6.87
UHPC NBG2	81.0	61.3	29.0	19.2	7.0	5.62
UHPC SBG2	67.0	63.2	41.5	28.9	12.5	10.13
UHPC NBG3	66.1	64.7	48.0	32.1	14.9	13.51
UHPC SBG3	60.5	65.5	64.0	51.1	27.8	25.78
UHPC NBG4	54.2	54.7	60.0	54.2	31.7	24.47
UHPC SBG4	45.2	47.5	66.0	69.2	55.8	47.54
UHPC SBG5	21.4	22.8	47.0	62.9	60.1	62.38
UHPC SBG6	12.5	11.6	28.2	44.4	64.2	71.16
UHPC SBG7	4.7	4.7	13.7	25.0	45.8	86.42
UHPC SBG8	1.9	1.5	5.3	17.8	31.8	85.34

For every girder in the bridge one strain gauge was deployed named as North bound gauge and other as south bound gauge. For eight girders a total of 12 strain gauges were used. The data obtained from DIC was compared with the data obtained from the strain gauges in Table 17.

Table 17. Strain values measurement of bridge girders for UHPC beams measured by strain gauges and DIC (mention girder)

Path	***Strain Guage (με)***	***Digital Image correlation (με)***
1	87.88	81.29
2	67.04	72.04
3	60.49	17.45
4	45.23	47.70
5	4.72	97.45
6	1.93	33.5

The strain gauges measured strain for the fascia girder for loading on all load paths. The strain values also decreased gradually as the truck moved further from the outer girder. The maximum value of strain obtained from DIC was 97.45 με whereas the strain gauge measured a value of 87.88 με. The minimum value measured by DIC was 17.458 με whereas the minimum value measured by the strain gauge was 1.93 με. For strain measurement on HPC beam DIC did not show good accuracy based on the results. The strain value measured from two different method were not found to be similar. The strain value from DIC had more errors and accuracy was very less. Similar reasons regarding noise bands ranging between -100 micro-strain to 100 micro-strain, the other reason being the bridge girder was directly monitored only on the fascia girder and not on the internal girders. The strain measurement from IL5 measured strain only for the outer girder and the measurement of strain gauges were more comprehensive as it covered most part of the bridge. The DIC gave values for changes in strain only for the outer girder. Further studies can be implemented by using camera system on the internal girder

and comparison must be done with the strain values obtained from it. The value measured for strain on the fascia girder of the UHPC beam is tabulated in Table 18.

Table 18. Strain value for UHPC beam on single truck loading

SPAN(m)	PATH1(με)	PATH2(με)	PATH3(με)	PATH4(με)	PATH5(με)	PATH6(με)
0	0	0	0	0	0	0
1.524	78.9202272	-86.46709	-73.4959	-19.76298	27.36017466	-3.74064
3.048	9.55724956	-65.86747	-182.984	-57.12862	97.45725766	26.94795
4.572	81.2994149	72.043668	-25.31237	37.54688	74.04209235	33.5
6.096	-16.2302353	62.151391	-44.23032	47.709794	86.48795207	29.75576
7.62	31.8431635	108.1673	-184.0114	-24.7848		
9.144	-101.685347		-21.5419			
10.668	53.9294455		-58.27356			
12.192	-21.0629254		17.458725			

5.3.3 Performance of UHPC span from 2M system

The 2M camera system measured the bridge directly from underneath the UHPC bridge. The camera system was located around the mid-span of the bridge. The 2M system measured strain for loading along the bridge and since the displacement values were along Z direction, out-of-plane displacement was measured. The strain values measured from the 2M camera system are summarized in Table 19.

Table 19. Strain values measurement of bridge girders for UHPC beams measured by 2M system

SPAN (m)	***PATH1 (με)***	***PATH2 (με)***	***PATH3 (με)***
0	0	0	0
1.524	186.2	23.2	15.4
3.048	192.1	145.2	121.2
4.572	212.2	188.2	175.3
6.096	228.6	198.3	192.3
7.62	198.2	156.2	165.8
9.144	263.4	144.2	172.5
10.668	176.5	112.7	92
12.192	117.2	109.2	56.2
13.716	56.2	72.3	82.8

The strain values were measured for loading on path 1,2 and 3 for single truck loading. Again, the strain value measured from DIC was not accurate for the 2M system. The value ranged for a highest value of 263.4 με to a lowest of 15.4 με. The DIC system was unable to represent strain value for the bridge. The strain modelling to obtain a single value of strain as obtained by the bridge should be checked for further tests. The camera system should capture the portion of the bridge where the strain gauges are precisely located. This would involve more camera system to be deployed. The strain value should then be calculated by choosing a section that would pass through the point where the strain gauges are measuring strain values. Correction factors are developed from data analysis to improve the accuracy of DIC data for strain measurement.

5.4 Comparison of strain value from 2M system with strain gauges for north bound girder 3 (NG3)

The 2M system was a 3D system monitoring two internal girders. The 2M system was measuring 2 stems of the internal girder. The strain gauges were placed on the south bound girder and a north bound of girder 2 and 3 respectively. The strain value was measured from DIC for single truck loading on path 1,2 and 3. The value was compared with the north bound strain gauge monitoring of girder 3. A comparison is made for the strain measured from the 2M system with the BDI strain gauges in Table 20.

Table 20. Strain Values measurement of bridge girders for UHPC beams measured by strain gauges and DIC (NG3)

Path	***Strain Gauge (με)***	***Digital Image correlation (με)***
1	54.2	228.6
2	54.7	198.3
3	60	192.3

5.4 Comparison of strain value from strain gauges to measure performance of UHPC and HPC beam

According to the strain measurement from strain gauges, the UHPC beams experience more strain than the HPC beams on the fascia girders whereas for the internal girders the strain values for UHPC beams were obtained more than the HPC beam. The strain values were recorded when the loading was a single moving truck load. The UHPC beam measured a highest value of 87.88 με whereas the HPC beam measures a highest value of 78.0 με under single truck loading on various load path 1. The strain values for other paths are summarized in Table 21.

Table 21. Strain values measurement of bridge girders for UHPC and HPC from strain gauges

Diagnostic Test: Single Moving Truck Load		
Strain (με)	***HPC***	***UHPC***
Path 1	78	87.88
Path 2	72.32	65.45
Path 3	74.88	66
Path 4	73.01	69.23
Path 5	74.29	64.23
Path 6	77.98	86.42

According to the measurement from strain gauges, the UHPC beams experience more strain on the fascia girders than the internal girders. The strain values for HPC beams were obtained more than the UHPC beam when the loading was increased from single truck to double truck. The UHPC beam measured a highest value of 113.5 με whereas the HPC beam measures a highest value of 125.6 με under double truck loading. The strain values for other paths are summarized in Table 22.

Table 22. Strain Values measurement of bridge girders for UHPC and HPC from strain gauges

Diagnostic Test: Double Moving Truck Load		
	HPC(με)	***UHPC(με)***
Path 1	110.7	113.5
Path 2	125.6	110
Path 3	121.1	113.1

According to the measurement from strain gauges, the UHPC beams and HPC beam experience the same trend when the loading is changed from double truck loading to triple truck loading. The UHPC beam measured a highest value of 127.5 με whereas the HPC beam measures a highest value of 127.3 με under triple truck loading. The strain values for other paths are summarized in Table 23.

Table 23. Strain values measurement of bridge girders for UHPC and HPC from strain gauges

Diagnostic Test: Triple Moving Truck Load

Strain	***HPC(με)***	***UHPC(με)***
Path 1	127.3	127.5
Path 2	121.5	121.4

5.5 Conclusion

The strain value obtained from DIC were not as accurate as the data measured from the strain gauges. The reasons can be because of the incapability of DIC to measure micro-strain especially in the region of -100 to +100 με. Another reason can be the section taken for consideration for strain measurement. The section taken for strain measurement was 1 inch from the bottom of the fascia girder. This was done to find the strain value closest to the strain gauges. The strain values obtained from the strain gauges were used to characterize the performance of UHPC and HPC beam. The data obtained from DIC was discarded as the values were inconsistent. Although, the magnitude of strain values also increased with the increase in loading conditions there was big fluctuations which can be caused because of the noise band. The use of DIC for micro-

strain measurement was poor compared to the strain gauges. Therefore, strain values for DIC were not taken for study.

Chapter 6

Deformation Analysis for Test 2

Introduction

The second test used eight 2-D and three 3-D systems. The 2-D systems were used to monitor the displacement of internal girders. There was no strain measurement done for the second test. Displacement was calculated using ARAMIS and plotted to get the displacement profile at a point as the truck moves along the bridge. The loading protocol used was similar to the first test which was single truck loading, double truck loading and triple truck loadings. The second test had a different processing approach compared to the first one. The second process involved calculation of displacement using single point instead of a section. The first test used a section to calculate the displacement whereas point displacement on the center of the target was used to calculate the displacement for the 2-D system. The displacement was calculated for eight camera systems. New Mexico State University also measured displacement for the same testing conditions using dial gauges, LVDTs and string pots. The data obtained from the dial gauges and transducers were compared with the displacement obtained from DIC.

6.1 Analysis of displacement using ARAMIS

The ARAMIS software program, a DIC platform from GOM, was used in processing the images from the camera systems to obtain the displacements at the locations monitored. For each test, an image was taken prior to loading on the bridge to obtain a reference, or baseline measurement. An image, or stage, was also taken each time the truck stopped on the bridge. The images from the test were then input into

ARAMIS and processed to obtain a full field of displacements over the patterned area. Because the displacements are computed for the entire field of the pattern there is a lot of flexibility in where to take the displacement measurement. A point on the center of the pattern as shown in figure 47 was chosen to calculate displacement values. This approach was completed for all displacement readings that follow in the next sections of the report.

In ARAMIS under File>>New Project, name the project and select 3D analysis and then facet size and facet step are selected 15 and 13 respectively. The standard deviation is selected between 0.3 to 0.7. The images were extracted from their respective folders and then the calibration file is was pulled out. After processing the images, the mapped version of span of beam appears on the interface. The images are referred to as stages and displacement is measured comparatively to the displacement with previous stages. The computation time for every analysis was under a minute and there was a total of 1122 images that was analyzed.

The displacement for the second test was plotted against stops where every stopped represented the placement of the axle loading of the truck used. The two beams were divided quarterly and were named as Q1, M and Q2 for first quarter, mid-span and second-quarter respectively. The truck axles are represented in figure 46 where a double back-to-back loading is on the bridge. The front axle of the truck on the UHPC beam was marked as the first 3 stops, the front axle of the truck on the HPC beam was marked as the next 3 stops and the rear axle of the truck on the HPC beam was considered as the last three stops. Therefore, the testing had a distinct 9 stops depending on the position of the axle of the truck.

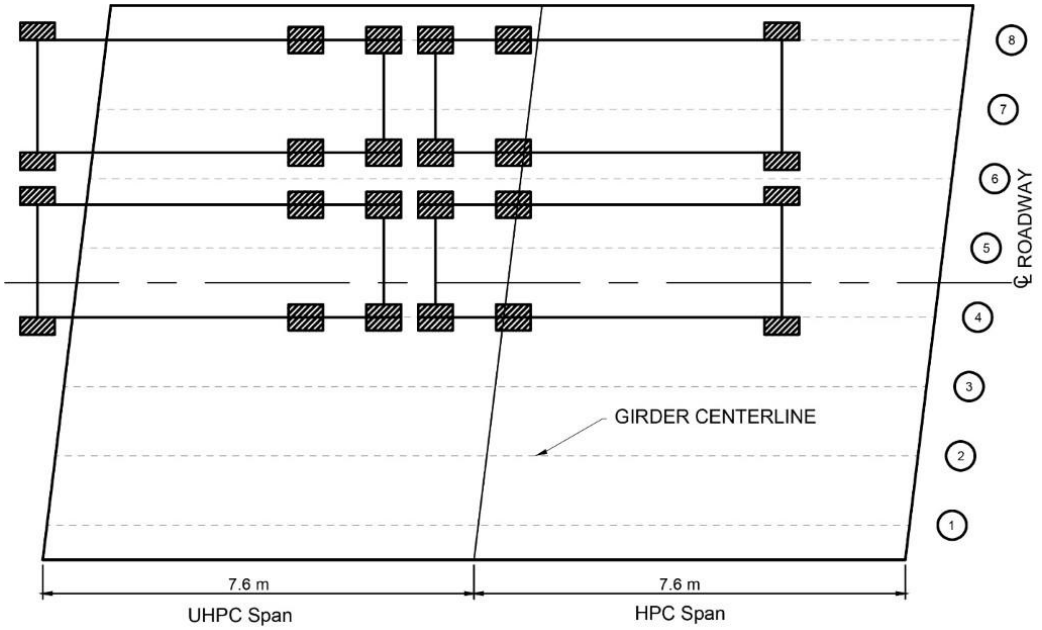

Figure 46. Axle load representation on bridge

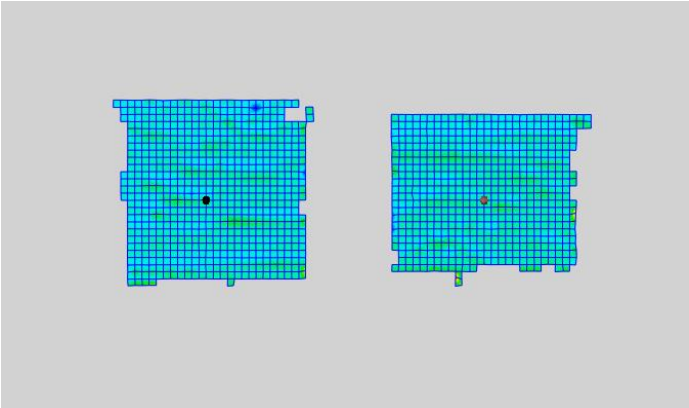

Figure 47. Y Displacement of an internal girder on UHPC beam obtained from ARAMIS

After the images were mapped, a point on the mid-section of the pattern was created. Since it was a point displacement, there was a single value for displacement which was used in the displacement profile. The displacement value was then plotted against the stop along the bridge and then deflection profile of the beam was obtained. The process was done for all eight camera systems. Figure 49 is an example of the displacement for two stages along a line segment.

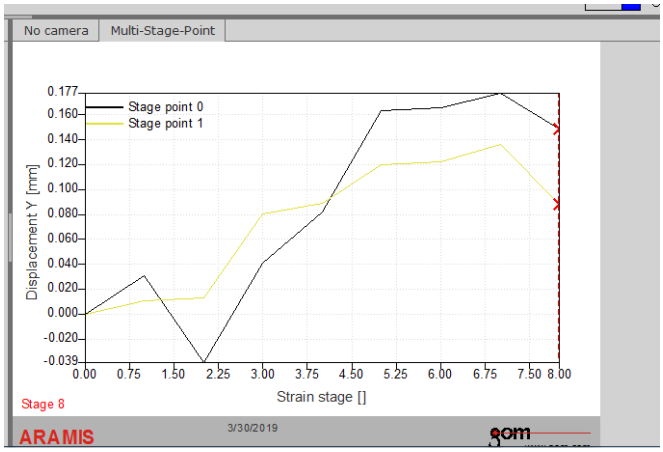

Figure 48. Vertical displacement value of a UHPC beam under single truck loading on path along a line segment

6.2 Experimental testing results for vertical displacements

The internal girder of HPC side was monitored using Ampscope 1, DMK 1, Go Pro Hero + Right and Go Pro Hero3 1. The eight internal girders were marked as A and B for north and south side respectively. Two girders were monitored by a single camera and displacement profile was plotted for different loading conditions. Similarly, the internal girder of UHPC side was monitored using Ampscope 2, DMK 0, Go Pro Hero + Left and Go Pro Hero3 2. The vertical displacement was plotted against the stop and displacement profile was obtained.

a) Go Pro Hero3 1

The Go Pro Hero 3 1 was monitoring internal girder 2A and 2B. A negative displacement indicates downward deflection while a positive displacement would mean the element moved upward. The loading started from the UHPC span from stop 0 to stop 8.

6.2.1 Displacement of internal girder under single truck loading from path 1-6

Figure 49 shows the displacement near mid span of girder 2 on the HPC beam When the front axle is on path 1 of the UHPC span the HPC span moved upwards from stop 0 to 3 but when the truck moved towards the HPC span the deflection of the beam started to go downwards. The girders 2A and 2B are closest to path1. The girder stem 2A comes down the most with the maximum displacement value of 1.7049mm. The beam 2B comes down with a displacement value of -1.0034mm. The displacement decreases gradually when the single truck loading moves away from girder 2A and 2B. Minimum positive displacement is noticed when loading is on path6. The minimum value was 0.0154mm as shown in Figure 49 and represented in Table 24. The upward movement of the girder suggests that there was continuity.

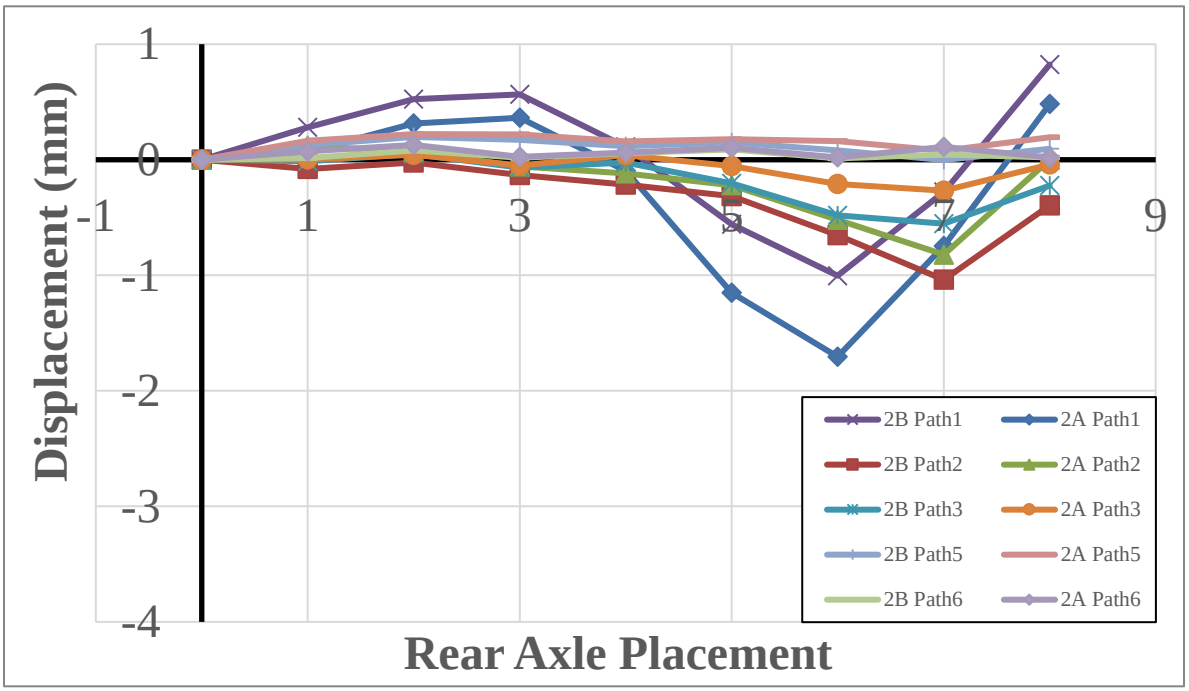

Figure 49. Displacement data for single truck loading on path1 to path6 for HPC beam for stem 2A and 2B

Table 24. Numerical value of displacement data for single truck loading from path 1 to 6 in figure 50 (mm).

Stage (Stop)	***2B Path1***	***2A Path1***	***2B Path2***	***2A Path2***	***2B Path3***	***2A Path3***	***2B Path5***	***2A Path5***	***2B Path6***	***2A Path6***
0	0	0	0	0	0	0	0	0	0	0
1	0.2791	0.0695	-0.0789	0.1184	-0.0134	0.0029	0.1262	0.1642	0.0154	0.0721
2	0.5233	0.3146	-0.0233	0.0694	0.0503	0.0428	0.1976	0.2221	0.0797	0.1286
3	0.5653	0.3633	-0.1327	-0.0573	-0.0685	-0.0499	0.1724	0.2186	0.0186	0.0269
4	0.1126	-0.0966	-0.2145	-0.1194	-0.0237	0.0391	0.1165	0.1585	0.0551	0.0623
5	-0.5602	-1.1524	-0.3151	-0.2205	-0.2039	-0.0558	0.1511	0.1766	0.0897	0.1025
6	-1.0034	-1.7049	-0.6518	-0.5187	-0.4811	-0.2090	0.0803	0.1610	0.0119	0.0188
7	-0.2804	-0.7479	-1.0381	-0.8208	-0.5534	-0.2678	-0.0024	0.0780	0.0462	0.1122
8	0.8239	0.4813	-0.3951	0.0000	-0.2225	-0.0404	0.0949	0.1959	0.0195	0.0208

6.2.2 Displacement of internal girder under double trucks back-to-back loading

For double back-to-back truck loading there were only 5 stops. The maximum displacement occurs when the two axles reach the mid-span of the HPC beam. This the maximum loading condition as the girders 2A and 2B are closest to path 1. The girder 2A has the maximum displacement value of 2.609mm. The girder adjacent to 2A comes down. The displacement value decreases when the loading moves further away from girder 2A and 2B. Loading on Path 6 had the least displacement value on girder 2A and 2B. The least value of displacement was 0.00044mm when the truck was moving on path 6. The numeric displacement value is summarized in the table below.

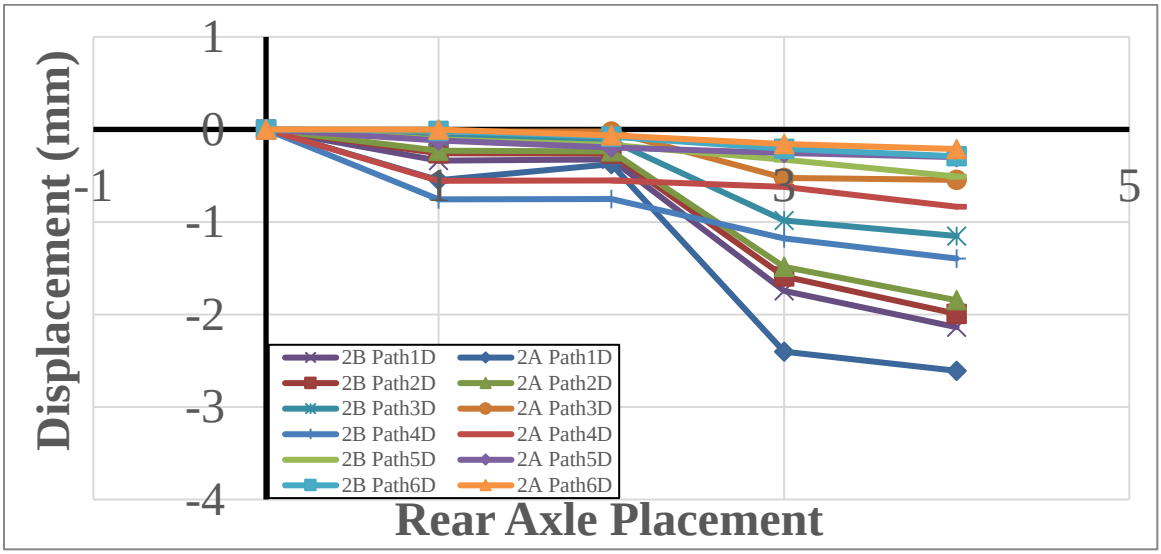

Figure 50. Displacement data for back-to-back loading from path1 to 6 of HPC span

Table 25. Numerical value of displacement data for double truck loading from path 1D to 3D in Figure 50 (mm)

Stage (Stop)	***2B Path1D***	***2A Path1D***	***2B Path2D***	***2A Path2D***	***2B Path3D***	***2A Path3D***
0	0	0	0	0	0	0
1	-0.339	-0.548	-0.257	-0.231	-0.082	-0.023
2	-0.322	-0.375	-0.259	-0.237	-0.118	-0.022
3	-1.746	-2.4	-1.588	-1.487	-0.985	-0.525
4	-2.138	-2.609	-1.993	-1.846	-1.152	-0.545

Table 26. Numerical value of displacement data for double truck loading from path 4D to 6D in Figure 50 (mm)

Stage (Stop)	***2B Path4D***	***2A Path4D***	***2B Path5D***	***2A Path5D***	***2B Path6D***	***2A Path6D***
0	0	0	0	0	0	0
1	-0.75546	-0.55513	-0.10748	-0.11993	-0.01557	-0.00044
2	-0.75289	-0.55033	-0.16813	-0.19473	-0.07772	-0.06394
3	-1.17724	-0.62147	-0.32636	-0.2539	-0.20913	-0.15822
4	-1.39556	-0.8355	-0.50871	-0.29901	-0.29042	-0.21182

6.2.3 Displacement of internal girder under two double truck loading

The displacement on stage 1 was not calculated as the image for the loading was not obtained. The two trucks were placed back-to-back and there was another back-to-back truck adjacent to it. Four trucks were used as the loading condition. The internal girder 2A and 2B were closer to the loading path 7. This was the maximum loading condition among all load combination. The maximum displacement was obtained to be 3.68 mm. The girder 2B which is located adjacent to girder 2A was also displaced similarly. Path8 was away from the girders producing small displacement values. The two girders showed similar behavior for the loading. There was small amount of positive displacement noticed when the loading was on path 8. The loading started from the UHPC span which caused the beam to move upwards when the load was on stage 2 of the test. The maximum value of displacement was obtained when the load was at stop 7. The numeric value for the test was summarized in Figure 51 and Table 27.

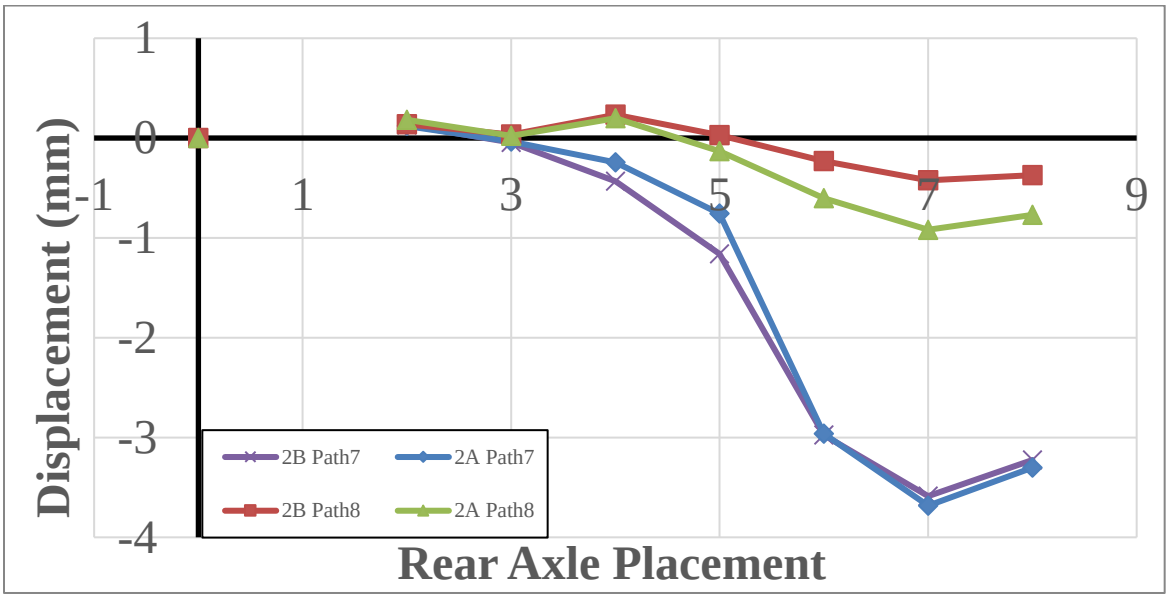

Figure 51. Displacement data for double truck loading on path7 and path8 of HPC span

Table 27. Numerical value of displacement (mm) data of double truck loading of path 7 and 8 in Figure 51

Stage (Stop)	***2B Path7***	***2A Path7***	***2B Path8***	***2A Path8***
0	0	0	0	0
1				
2	0.131724	0.120132	0.138351	0.183674
3	-0.04414	-0.03618	0.035128	0.023665
4	-0.4323	-0.24345	0.23344	0.198752
5	-1.16188	-0.75588	0.029345	-0.13018
6	-2.97415	-2.96361	-0.23055	-0.603
7	-3.58761	-3.6831	-0.4234	-0.91873
8	-3.22479	-3.30138	-0.37165	-0.77002

6.2.4 Displacement of internal girder under triple truck loading

The triple truck loading was conducted with three trucks parallel to each other placed at an equal distance from opposite guard rails. The displacement on stage 1 was not calculated as the image for the loading was not obtained. The maximum displacement was obtained on stop 7 where maximum axle load was placed. The maximum displacement value for the stop was 2.52 mm. The value was less compared to double truck load as the load was more distributed along the bridge compared to the loading condition of two trucks where the loading was considered on one side of the bridge. The two beams adjacent to each other demonstrated similar behavior and the maximum displacement value was 2.35 mm. There was some upward displacement on stage 2 as the loading started from UHPC span. The value of upward displacement was small compared to the negative displacement which amounted to 0.0377 mm. The numerical value for the

displacement is summarized in Figure 52 and Table 28.

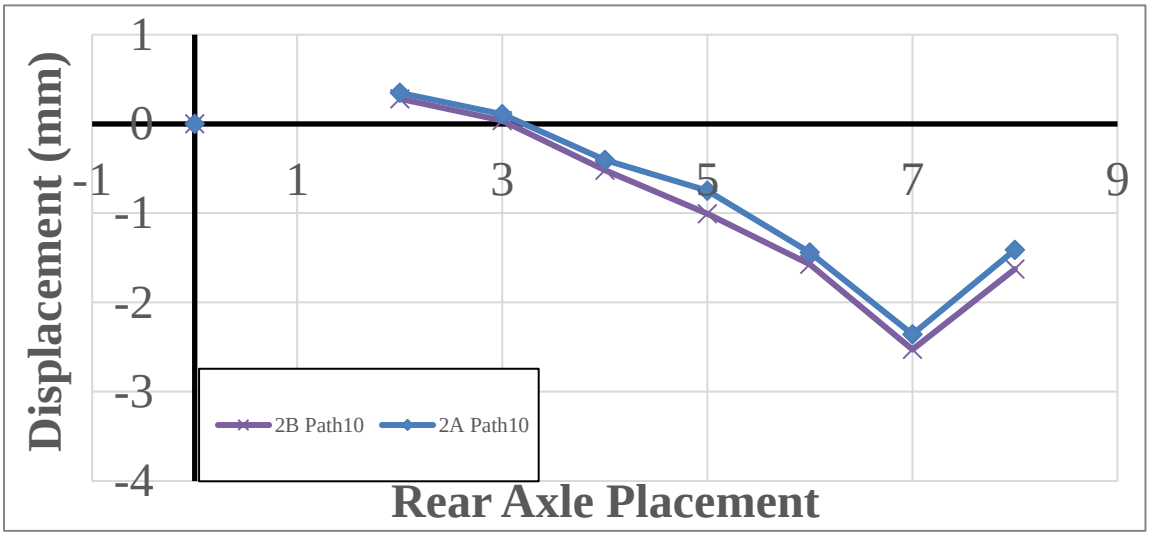

Figure 52. Displacement data for triple truck loading on path 10 of HPC span

Table 28. Numerical value of displacement data of triple truck loading on path 10 in Figure 52

Stage (Stop)	***2B Path10 (mm)***	***2A Path10 (mm)***
0	0	0
1		
2	0.282535	0.348152
3	0.037754	0.108797
4	-0.51763	-0.40414
5	-1.00609	-0.74585
6	-1.57146	-1.43756
7	-2.52683	-2.35645
8	-1.62691	-1.40878

b) Go Pro Hero +

The Go Pro Hero + was monitoring internal girder 4A and 4B. A negative displacement indicates downward deflection while a positive displacement would mean the element moved upward. The loading started from the UHPC span from stop 0 to stop 8. The axle of the truck made three stops at first quarter, mid-span and second quarter of UHPC beam and also made similar stop on the HPC beam. The Go Pro Hero + camera was successful in capturing displacement for HPC beam. The camera was swapped for the test on day 2 and UHPC span was monitored for other loading conditions.

6.2.5 Displacement of internal girder under single truck loading from path1-6

When the front axle is on the UHPC span the HPC span moved upwards from stop 0 to 3 but when the truck moved towards the HPC span the deflection of the beam started to go downwards. There was a total of 9 stops which started from the UHPC span. The girders 4A and 4B are closest to path3. The girder 4A comes down the most with the maximum displacement value of 1.06mm. The beam 4B comes down with a displacement value of 0.9713mm. The maximum negative displacement was on path 7 for all paths. The displacement decreases gradually when the single truck loading moves away from girder 4A and 4B. Minimum positive displacement is noticed when loading is on path6 on stop 2. The displacement profile is similar to the displacement of girder 2A and 2B. The displacement value decreases gradually when the loading moves farther from girder 4A and 4B. The upward movement of the girder suggests that there was continuity between spans. The positive deflection on the beam is noticed when the truck loading is on the UHPC span of the bridge which is summarized in Figure 53 and Table

29.

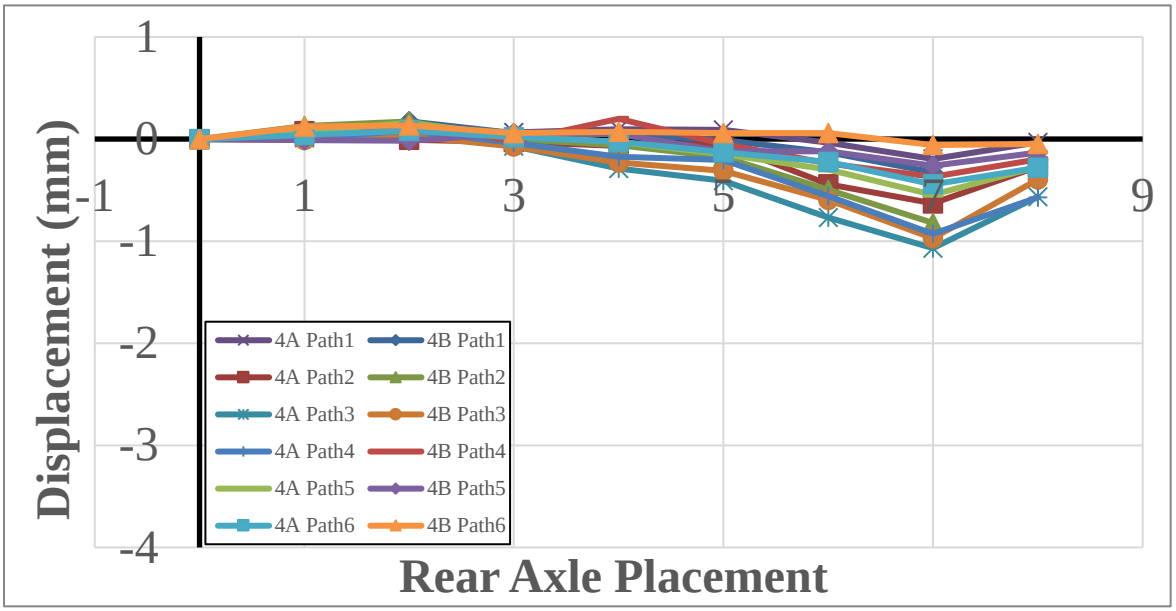

Figure 53. Displacement data for single truck loading on path1 to path6 for HPC span

Table 29. Numerical value of displacement (mm) for single truck loading from path 1 to 3 in Figure 53

Stage (Stop)	***4A Path1***	***4B Path1***	***4A Path2***	***4B Path2***	***4A Path3***	***4B Path3***
0	0	0	0	0	0	0
1	0.020894	0.061561	0.076595	0.126923	0.010469	-0.012
2	0.099217	0.173033	-0.00649	0.172085	0.063563	0.030365
3	0.063277	0.057472	-0.02975	-0.00173	-0.07118	-0.07197
4	0.095797	0.044904	-0.06585	-0.06022	-0.28872	-0.22945
5	0.089873	-0.01006	-0.0477	-0.17566	-0.40921	-0.31159
6	-0.03713	-0.13006	-0.44172	-0.49658	-0.76999	-0.5977
7	-0.19559	-0.32607	-0.62986	-0.82232	-1.06896	-0.97173
8	-0.03205		-0.27095		-0.56519	-0.39573

Table 29. Numerical value of displacement (mm) for single truck loading from path 3 to 6 in figure 53

Stage	***4A***	***4B***	***4A***	***4B***	***4A***	***4B***
(Stop)	***Path4***	***Path4***	***Path5***	***Path5***	***Path6***	***Path6***
0	0	0	0	0	0	0
1	0.000193	0.008673	0.077956	-0.00965	0.040625	0.121795
2	0.084113	0.156235	0.156722	-0.01677	0.081104	0.133647
3	-0.03988	-0.02184	0.031789	0.053586	0.016971	0.059126
4	-0.17425	0.198053	-0.02836	0.048189	-0.02578	0.071803
5	-0.20376	-0.04903	-0.14899	-0.12027	-0.13028	0.058042
6	-0.56053	-0.23788	-0.30019	-0.12034	-0.22418	0.058653
7	-0.92864	-0.36972	-0.54595	-0.2614	-0.44421	-0.05883
8	-0.5705	-0.19946	-0.26931	-0.13392	-0.27897	-0.04662

6.2.6 Displacement of internal girder under double trucks back-to-back loading

For the double back-to-back truck loading there were only 5 stops. When the truck transition to the HPC span the beam starts to move down. The upward movement of the HPC beam does not occur in this test as the loading starts from the UHPC span. The maximum displacement occurs when the two axles reach the mid-span of the HPC beam. This the maximum loading condition as the girders 4A and 4B are closest to path 1. The girder 4B has the maximum displacement value of 2.11 mm. The girder adjacent to 4A comes down. The displacement value decreases when the loading moves further away from girder 4A and 4B. Loading on Path 6D had the least displacement value on girder 4A and 4B. The least value of displacement was 0.04767 mm when the truck was moving

on path 6D. The numeric displacement value is summarized in Figures 54 and Table 31 and 32.

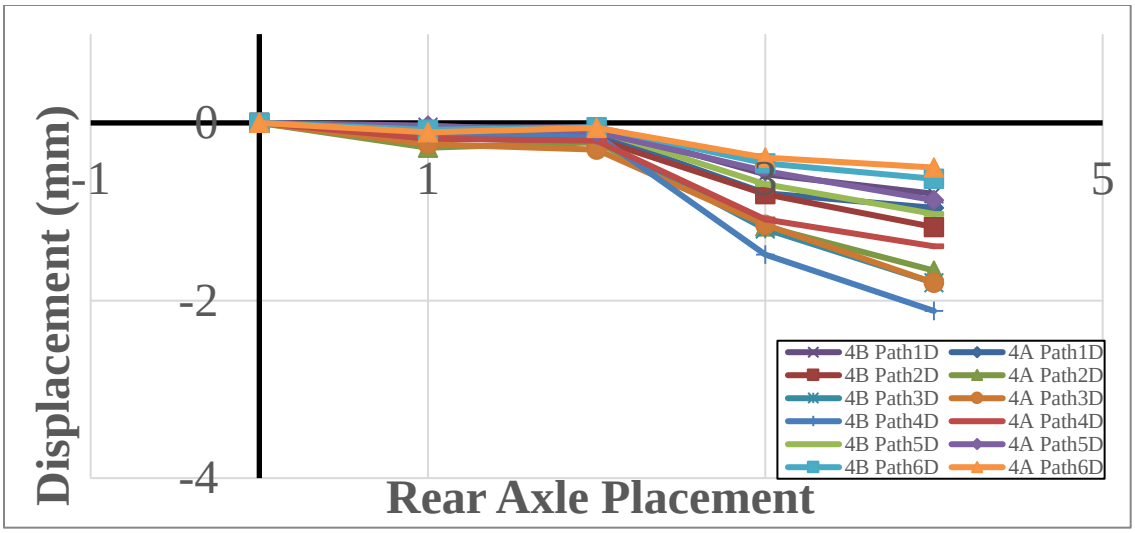

Figure 54. Displacement data for back-to-back loading from path 1 to 6

Table 31. Numerical value of displacement (mm) data for double truck loading from path 1D to 3D in Figure 54

Stage (Stop)	***4B Path1D***	***4A Path1D***	***4B Path2D***	***4A Path2D***	***4B Path3D***	***4A Path3D***
0	0	0	0	0	0	0
1	-0.04827	-0.05815	-0.12774	-0.27882	-0.12903	-0.23889
2	-0.04887	-0.12359	-0.18105	-0.21788	-0.18574	-0.3015
3	-0.58013	-0.79011	-0.80034	-1.16742	-1.1945	-1.14682
4	-0.79789	-0.95714	-1.17312	-1.66293	-1.80067	-1.80066

Table 32. Numerical value of displacement (mm) data for double truck loading from path 4D to 6D in Figure 54

Stage (Stop)	***4B Path4D***	***4A Path4D***	***4B Path5D***	***4A Path5D***	***4B Path6D***	***4A Path6D***
0	0	0	0	0	0	0
1	-0.12529	-0.1784	-0.06427	-0.02941	-0.07779	-0.10778
2	-0.1391	-0.2001	-0.08615	-0.10315	-0.04767	-0.05695
3	-1.48252	-1.08622	-0.68921	-0.54284	-0.45657	-0.39234
4	-2.11766	-1.38982	-1.02568	-0.8709	-0.6296	-0.50256

6.2.7 Displacement of internal girder under two double truck loading

The displacement on stage 1 was not calculated as the image for the loading was not obtained. The two trucks were placed back-to-back and there was another back-to-back truck adjacent to it. Four trucks were used as the loading condition. The internal girder 4A and 4B were equally away from path 7 and path8. This was the maximum loading condition among all load combination. The maximum displacement was obtained to be 2.82 mm. The girder 4B which is located adjacent to girder 4A was also displaced similarly. Path8 also resulted in similar displacement values. The load was distributed almost equally when the loading was on path 7 and 8. The two girders showed similar behavior for the loading. There was small amount of positive displacement noticed when the loading was on path 8. The loading started from the UHPC span which caused the beam to move upwards when the load was on stage 2 of the test. The maximum value of displacement was obtained when the load was at stop 7. The numeric value for the test was summarized in Figure 55 and Table 33.

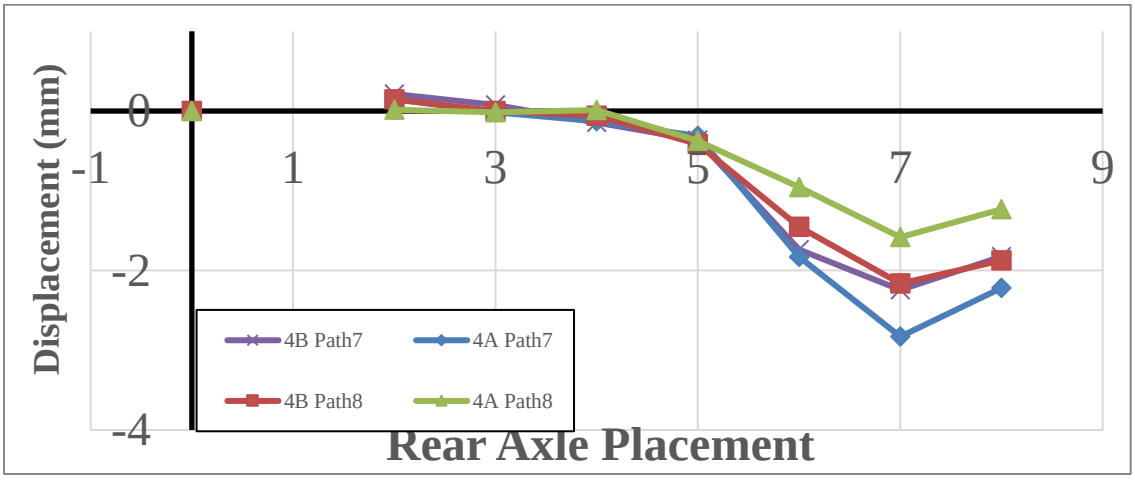

Figure 55. Displacement value for double truck back-to-back loading for path7 and 8 for HPC span

Table 33. Numerical value of displacement (mm) data of double truck loading of path 7 and 8 in Figure 55.

Stage (Stop)	***4B Path7***	***4A Path7***	***4B Path8***	***4A Path8***
0	0	0	0	0
1				
2	0.213296	0.148785	0.145555	0.015832
3	0.077488	-0.01477	-0.00099	-0.01747
4	-0.14408	-0.13052	-0.05916	0.012693
5	-0.3644	-0.3145	-0.41281	-0.37488
6	-1.73827	-1.83124	-1.45131	-0.95568
7	-2.24293	-2.82897	-2.16408	-1.5827
8	-1.82754	-2.21938	-1.87581	-1.23352

6.2.8 Displacement of internal girder under triple truck loading

The triple truck loading was conducted with three trucks parallel to each other placed at an equal distance from opposite guard rails. The displacement on stage 1 was not calculated as the image for the loading was not obtained. The maximum displacement was obtained on stop 7 where maximum axle load was placed. The maximum displacement value for the stop was 2.34 mm. The value was less compared to double truck load as the load was more distributed along the bridge compared to the loading condition of two trucks where the loading was considered on one side of the bridge. The two beams adjacent to each other demonstrated similar behavior and the maximum displacement value was 2.29 mm. There was some upward displacement on stage 2 as the loading started from UHPC span. The value of upward displacement was small compared to the negative displacement which amounted to 0.0209 mm. The displacement value is also similar to the displacements for girder 2A and 2B. The numerical value for the

displacement is summarized in Figure 56 and Table 34.

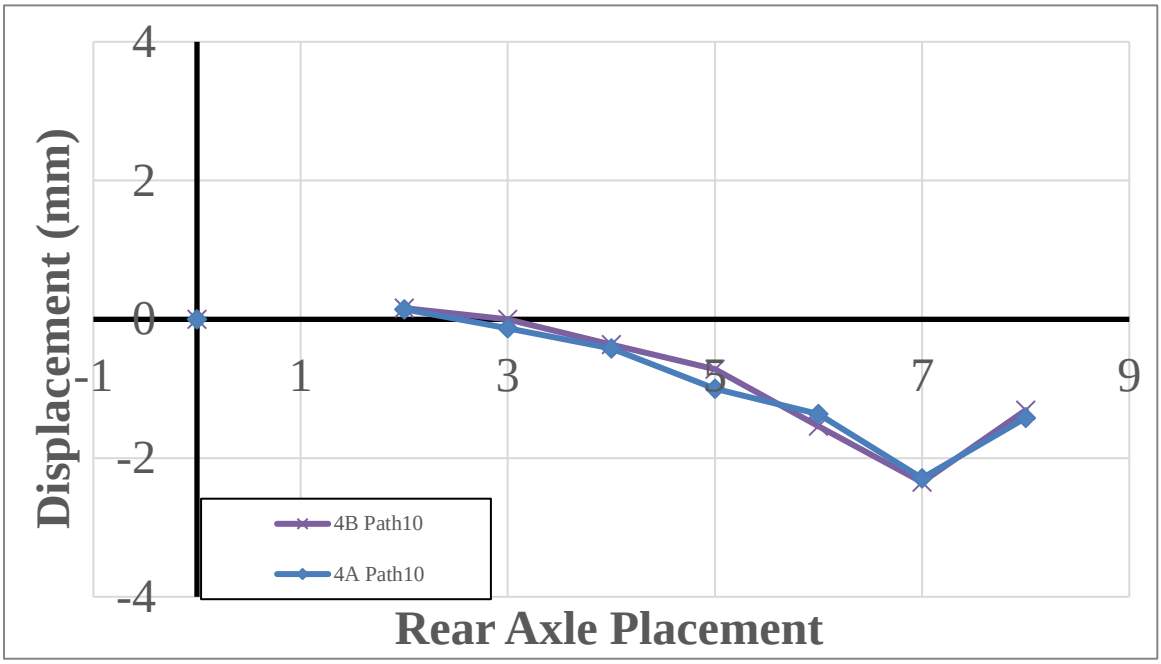

Figure 56. Displacement data for triple truck loading on path 10 on HPC span

Table 34. Numerical value of displacement (mm) data of triple truck loading on path 10 in Figure 56

Stage (Stop)	***4B Path10***	***4A Path10***
0	0	0
1		
2	0.161097	0.144491
3	-0.00209	-0.13022
4	-0.36503	-0.42218
5	-0.7193	-0.999
6	-1.54193	-1.36401
7	-2.34778	-2.29067
8	-1.30783	-1.42176

c) DMK 1

The DMK 1 was monitoring internal girder 6A and 5B of the HPC span of the bridge. A negative displacement indicates downward deflection while a positive displacement would mean the element moved upward. The loading started from the UHPC span from stop 0 to stop 8.

6.2.9 Displacement of internal girder under single truck loading from path1-6

When the front axle is on the UHPC span the HPC span moved upwards from stop 0 to 3 but when the truck moved towards the HPC span the deflection of the beam started to go downwards. The girders 6A and 5B are closest to path4 and path5. The girder 5B comes down the most with the maximum displacement value of 1.603 mm. The beam 6A comes down with a displacement value of 1.55 mm. The displacement decreases gradually when the single truck loading moves away from girder 6A and 5B. Girder 6A and 5B undergo similar displacement under loading along path 5. Minimum positive displacement is noticed when loading is on path1. There is an upward movement observed at the end of the test on path 1 when the truck had reached the last stop. The value for upward movement was 0.28 mm. The maximum negative displacement occurred at stop 7 for loading on all paths. The upward movement of the girder suggests that there was continuity among the spans. The numerical value of displacement is summarized in Figure 57 and Table 35 and

36.

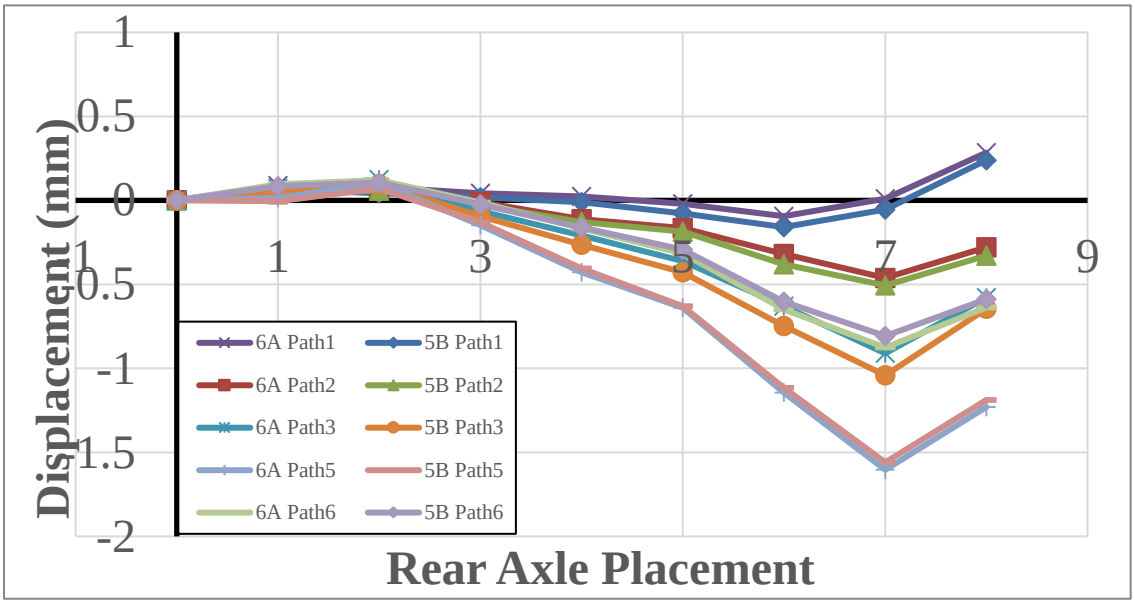

Figure 57. Displacement of back-to-back loading for path1 to path 6 for HPC span

Table 35. Numerical value of displacement (mm) for single truck loading from path 1 to 3 in figure 57

Stage (Stop)	***6A Path1***	***5B Path1***	***6A Path2***	***5B Path2***	***6A Path3***	***5B Path3***
0	0	0	0	0	0	0
1	0.087679	0.064476	0.039011	0.036657	0.071936	0.05205
2	0.078451	0.042753	0.069201	0.057832	0.124903	0.096142
3	0.04165	0.017121	-0.01034	-0.02757	-0.06459	-0.09416
4	0.023303	-0.01171	-0.11262	-0.12802	-0.20803	-0.26335
5	-0.02059	-0.07842	-0.16431	-0.18583	-0.36125	-0.42827
6	-0.09412	-0.15904	-0.31862	-0.37955	-0.62963	-0.74701
7	0.009721	-0.05411	-0.46162	-0.50629	-0.91049	-1.0414
8	0.284491	0.239294	-0.27923	-0.32878	-0.57771	-0.64573

Table 36. Numerical value of displacement (mm) for single truck loading from path 5 and 6 in figure 58

Stage (Stop)	***5B Path5***	***6A Path5***	***5B Path6***	***6A Path6***
0	0	0	0	0
1	0.01399	-0.00561	0.096186	0.084554
2	0.10417	0.070385	0.120223	0.106101
3	-0.14738	-0.13056	-0.01281	-0.02468
4	-0.42780	-0.40417	-0.16662	-0.16224
5	-0.64014	-0.62989	-0.31518	-0.29348
6	-1.14499	-1.1146	-0.64841	-0.60346
7	-1.60354	-1.55926	-0.87573	-0.80744
8	-1.22918	-1.18807	-0.63687	-0.58795

6.2.10 Displacement of internal girder under two double truck loading

The displacement on stage 1 was not calculated as the image for the loading was not obtained. The two trucks were placed back-to-back and there was another back-to-back truck adjacent to it. Four trucks were used as the loading condition. The internal girder 6A and 5B were monitored when the truck moved on path 7 and 8. This was the maximum loading condition among all load combination. The maximum displacement was obtained to be 4.05 mm. The trucks were moving on path8 where the maximum negative displacement was obtained. The girder 5B which is located adjacent to girder 6A was also displaced similarly. Path7 was away from the girders producing small displacement values. The two girders showed similar behavior for the loading. There was small amount of positive displacement noticed when the loading was on path 8. The loading started from the UHPC span which caused the beam to move upwards when the load was on stage 2 of the test. The maximum value of displacement was obtained when

the load was at stop 7. The numeric value for the test was summarized in Figure 58 and Table 37.

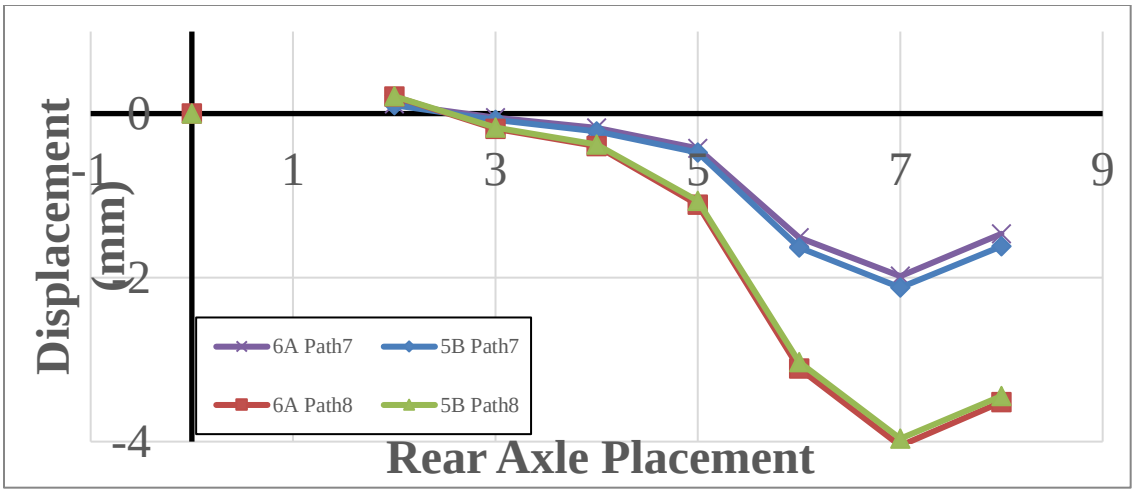

Figure 58. Displacement data of double back-to-back loading for path 7 and path8 on HPC span

Table 37. Numerical value of displacement (mm) data of double truck loading of path 7 and 8 in Figure 59.

Stage (Stop)	***6A Path7***	***5B Path7***	***6A Path8***	***5B Path8***
0	0	0	0	0
1				
2	0.118347	0.101907	0.209392	0.210816
3	-0.0481	-0.07621	-0.18657	-0.17155
4	-0.17631	-0.21817	-0.39643	-0.37746
5	-0.42502	-0.47593	-1.11143	-1.06516
6	-1.51127	-1.6333	-3.10793	-3.02987
7	-1.98286	-2.12122	-4.05076	-3.96391
8	-1.4672	-1.61834	-3.51718	-3.44511

6.2.11 Displacement of internal girder under triple truck loading

The triple truck loading was conducted with three trucks next to each other and parallel. The displacement on stage 1 was not calculated as the image for the loading was not obtained. The maximum displacement was obtained on stop 7 where maximum axle load was placed. The maximum displacement value for the stop was 3.24 mm. The value was less compared to double truck load as the load was more distributed along the bridge compared to the loading condition of two trucks where the loading was considered on one side of the bridge. The two beams adjacent to each other demonstrated similar behavior and the maximum displacement value was 3.24 mm. There was significant upward displacement on stage 2 as the loading started from UHPC span suggesting continuity between spans. The value of upward displacement was small compared to the negative displacement which amounted to 0.629 mm. The numerical value for the displacement is summarized in Figure 59 and Table 38.

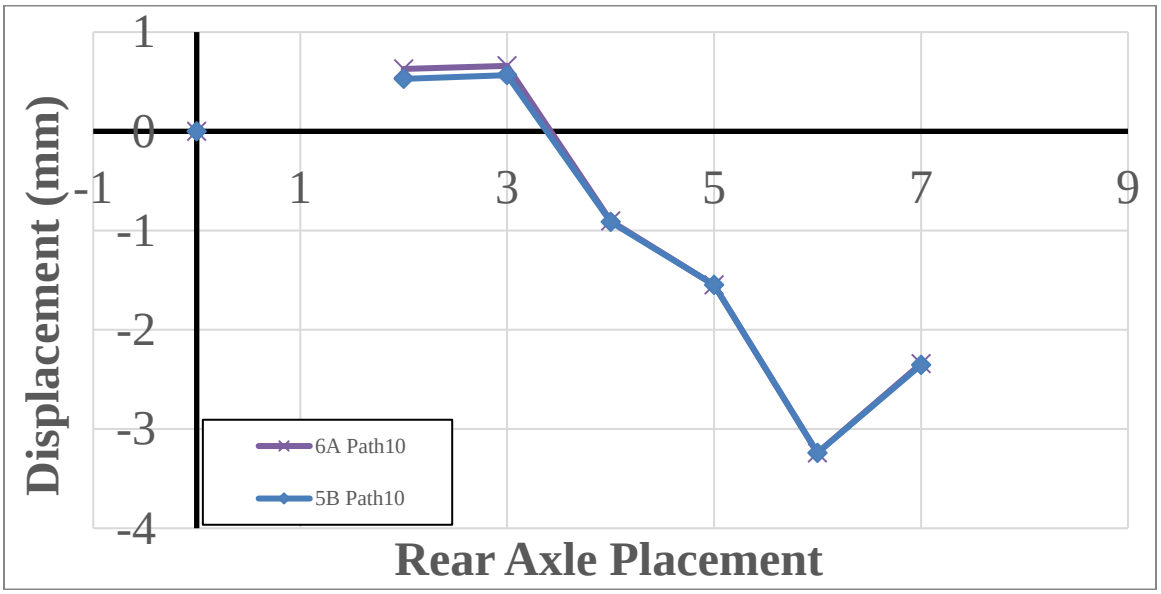

Figure 59. Displacement data for triple truck loading on path 10 for HPC span

Table 38. Numerical value of displacement (mm) data of triple truck loading on path 10 in Figure 59

Stage (Stop)	***6A Path10***	***5B Path10***
0	0	0
1		
2	0.62908	0.52703
3	0.659581	0.566005
4	-0.9038	-0.91311
5	-1.54989	-1.54893
6	-3.24005	-3.24124
7	-2.34123	-2.35373

d) Ampscope 1

The Go Pro Hero 3 1 was monitoring internal girder 8A and 7B. A negative displacement indicates downward deflection while a positive displacement would mean the element moved upward. The loading started from the UHPC span from stop 0 to stop 8.

6.2.12 Displacement of internal girder under single truck loading from path1-6

When the front axle is on path 1 of the UHPC span the UHPC span moved downwards from stop 0 to 5 but when the truck moved towards the HPC span the deflection of the beam started to go upwards. The girders 8A and 7B are closest to path6. The girder 8A comes down the most with the maximum displacement value of 1.65mm. The beam 7B comes down with a displacement value of 1.61 mm. The displacement decreases gradually when the single truck loading moves away from girder 8A and 7B. Minimum positive displacement is noticed when loading is on HPC side of the bridge. The upward movement

of the girder suggests that there was continuity in the beam. Figure 60 and Table 39 show displacement on stem 7B and 8A of UHPC span.

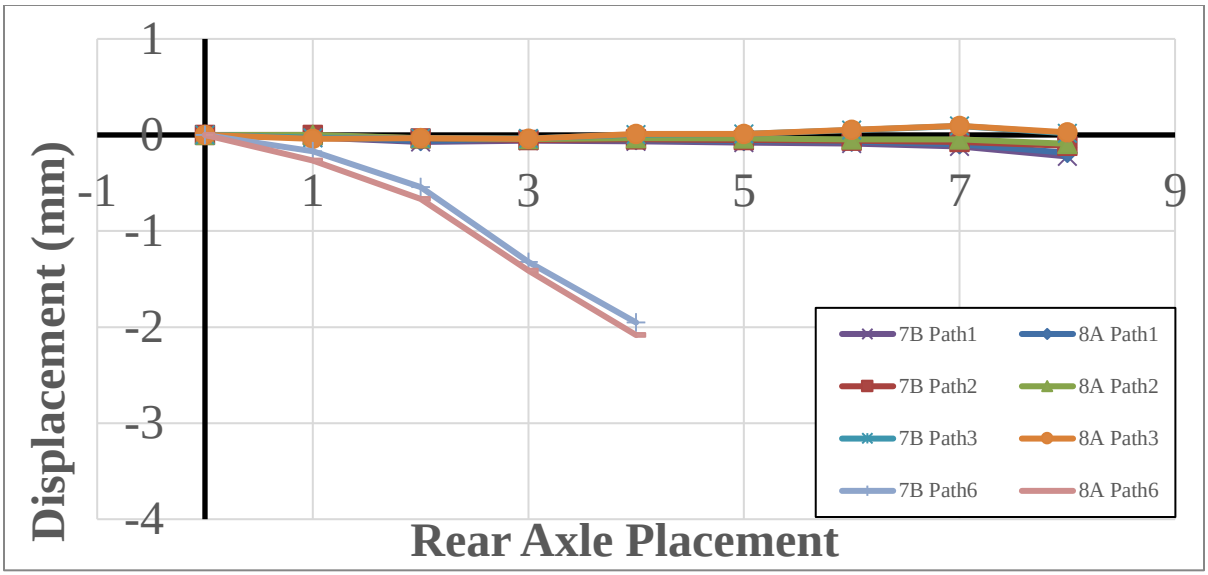

Figure 60. Displacement data for single truck loading on path 1,2,3 and 6 on UHPC span

Table 39. Numerical value of displacement (mm) data for single truck loading in Figure 60

Stage (Stop)	*7B Path1*	*8A Path1*	*7B Path2*	*8A Path2*	*7B Path3*	*8A Path3*	*7B Path6*	*8A Path6*
0	0	0	0	0	0	0	0	0
1	-0.02606	-0.02058	-0.00084	-0.0008	-0.0288	-0.04056	-0.16891	-0.26699
2	-0.07335	-0.0617	-0.03502	-0.03343	-0.0337	-0.03301	-0.54163	-0.66471
3	-0.05787	-0.04251	-0.05327	-0.04174	-0.03626	-0.03778	-1.32042	-1.41141
4	-0.06746	-0.0529	-0.04679	-0.03252	0.003842	0.011708	-1.95241	-2.08309
5	-0.07916	-0.06176	-0.05303	-0.03559	0.009999	0.010725		
6	-0.08908	-0.06998	-0.06014	-0.04671	0.052	0.052614		
7	-0.11929	-0.09649	-0.07157	-0.04513	0.093449	0.094982		
8	-0.22332	-0.18528	-0.11235	-0.0915	0.018592	0.026289		

6.2.13 Displacement of internal girder under two double truck loading

The displacement on stage 1 was not calculated as the images for the loading was not obtained. The two trucks were placed back-to-back and there was another back-to-back truck adjacent to it. Four trucks were used as the loading condition. The internal girder 8A and 7B were closer to the loading path 8. The displacement profile for this particular loading condition looked arbitrary. The reason for the random displacement pattern can be a missing image in the sequence. The missing image can be a reason for a shift in the displacement which can shift the graph and make the profile appear random. The numeric value for the test was summarized in Figure 61 and Table 40.

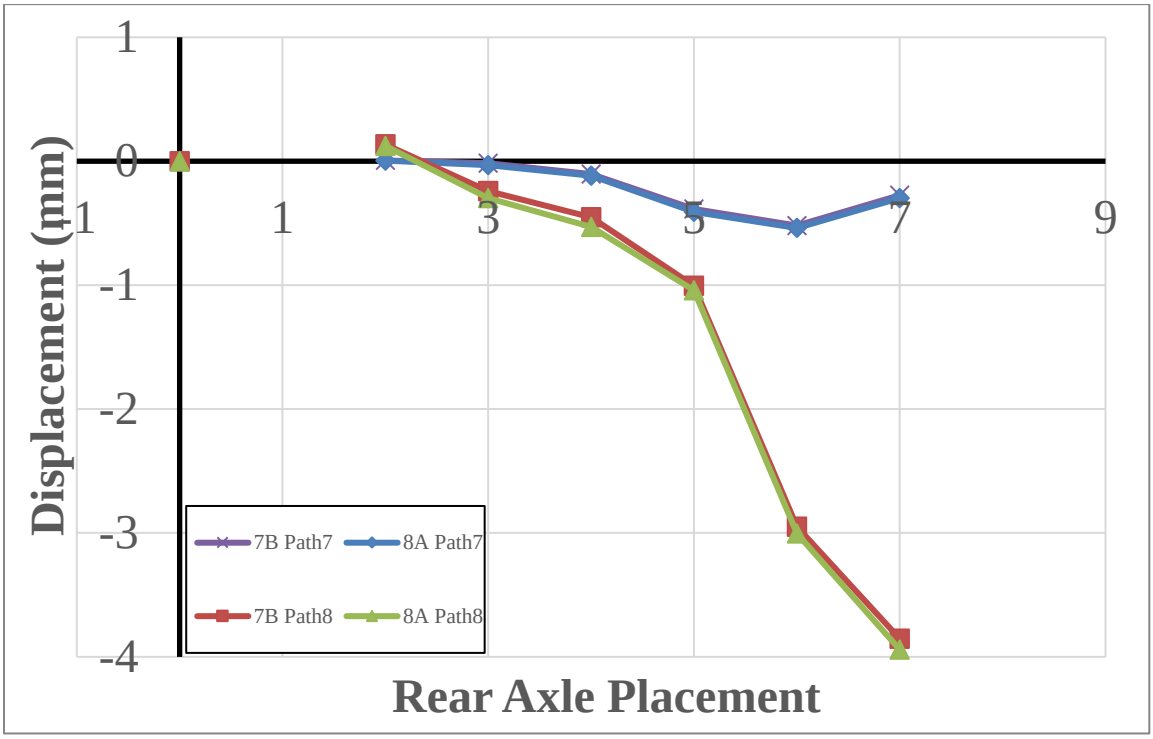

Figure 61. Displacement profile for double back-to-back for path 7 and 8 on HPC span

Table 40. Numerical value of displacement (mm) data of double truck loading of path 7 and 8 in Figure 62

Stage	***7B***	***8A***	***7B***	***8A***
(Stop)	***Path7***	***Path7***	***Path8***	***Path8***
0				
1				
2	0.006127	0.004615	0.134722	0.123993
3	-0.01693	-0.03073	-0.24209	-0.29763
4	-0.10301	-0.11772	-0.45194	-0.52908
5	-0.38606	-0.40815	-1.00644	-1.04203
6	-0.51947	-0.53929	-2.94911	-3.00389
7	-0.27577	-0.29669	-3.85368	-3.94157

6.2.14 Displacement of internal girder under triple truck loading

The triple truck loading was conducted with three trucks parallel to each other placed at an equal distance from opposite guard rails. The displacement on stage 1 was not calculated as the image for the loading was not obtained. The maximum displacement was obtained on stop 7 where maximum axle load was placed. The maximum displacement value for the stop was 2.64 mm. The value was less compared to triple truck load as the load was more distributed along the bridge compared to the loading condition of two trucks where the loading was more concentrated to one side of the bridge. The two beams adjacent to each other demonstrated similar behavior and the maximum displacement value was 2.63 mm. There was some upward displacement on

stage 2 as the loading started from UHPC span. The value of upward displacement was small compared to the negative displacement which amounted to 0.08 mm. The numerical value for the displacement is summarized in Figure 62 and Table 41.

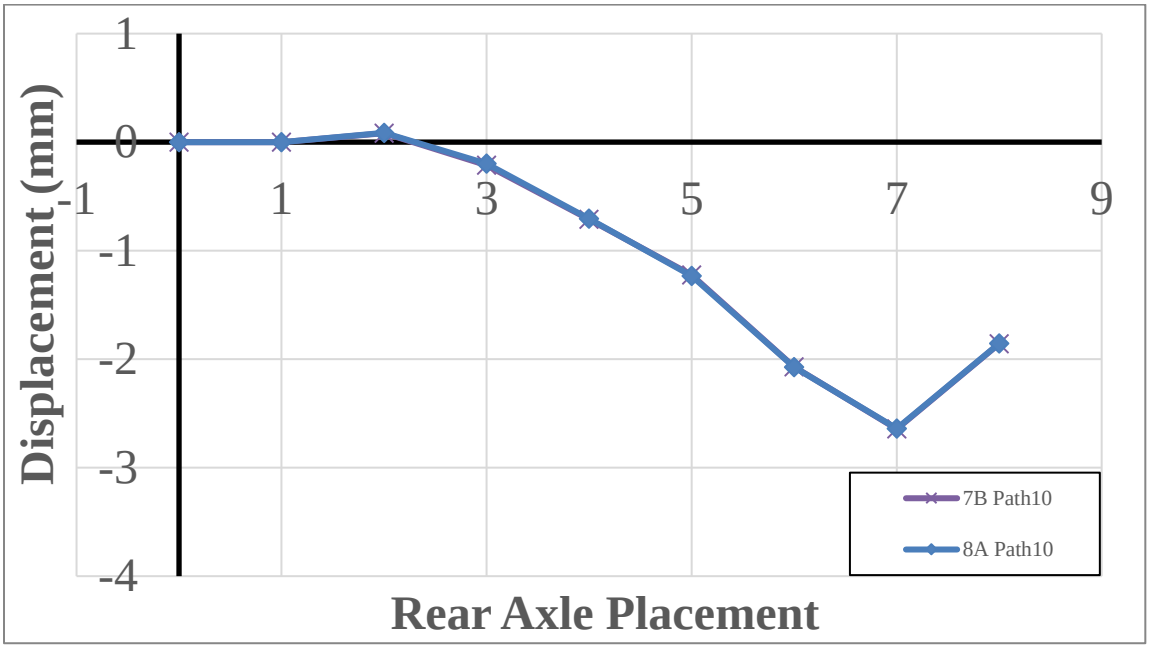

Figure 62. Displacement data for triple truck loading on Path 10 of HPC span

Table 41. Displacement data (mm) for triple truck loading on path 10 for Figure 62

Stage (Stop)	***7B Path10***	***8A Path10***
0	0	0
1	0	0
2	0.082462	0.085731
3	-0.21273	-0.19954
4	-0.71023	-0.70613
5	-1.22546	-1.23302
6	-2.07166	-2.07477
7	-2.64404	-2.63942
8	-1.85991	-1.8554

e) Go Pro Hero3 2

The Go Pro Hero 3 2 was monitoring internal girder 2A and 2B of the UHPC span. A similar camera Go Pro Hero 3 1 was monitoring the opposite side of the UHPC span. A negative displacement indicates downward deflection while a positive displacement would mean the element moved upward. The loading started from the UHPC span from stop 0 to stop 8.

6.2.15 Displacement of internal girder under double trucks back-to-back loading

There was only 5 stops for the double back-to-back truck loading. When the truck start on the UHPC span the beam starts to move down. The upward movement of the UHPC beam does not occur in this test as the loading transitions from the UHPC span to the HPC span. The maximum displacement occurs when the two axles reach the mid-span of the UHPC beam. This is the maximum loading condition as the girders 2A and 2B are closest to path 2. The girder 2A has the maximum displacement value of 2.16mm. The girder adjacent to 2A comes down. The displacement value decreases when the loading moves further away from girder 2A and 2B. Loading on Path 6 had the least displacement value on girder 2A and 2B. The numeric displacement value is summarized in Figure 62 and Table 42 and Table 43.

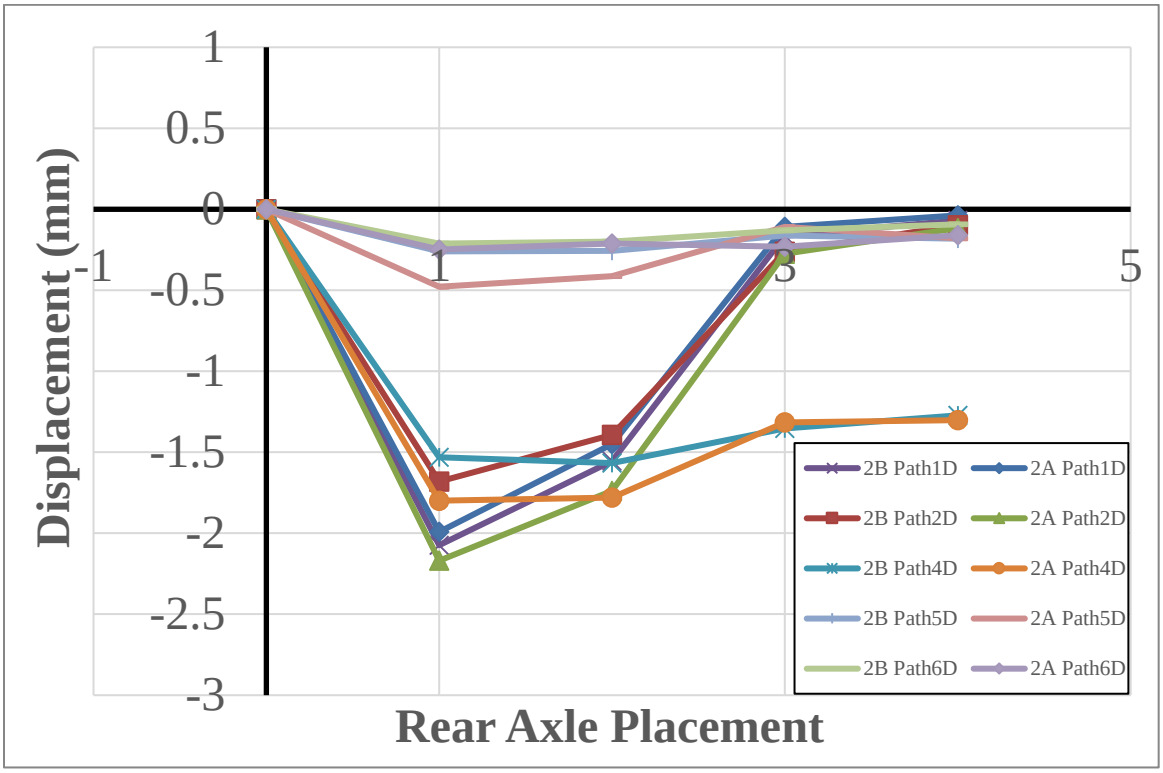

Figure 62. Displacement data for back-to-back loading for path 1,2,4,5 and 6 for UHPC span

Table 42. Displacement data (mm) for back-to-back loading on path 1,2 and 4 for Figure 62

Stage (Stop)	***2B Path1D***	***2A Path1D***	***2B Path2D***	***2A Path2D***	***2B Path4D***	***2A Path4D***
0	0	0	0	0	0	0
1	-2.07394	-1.99171	-1.68095	-2.16969	-1.5319	-1.79905
2	-1.55555	-1.44998	-1.39289	-1.73839	-1.56687	-1.77942
3	-0.16313	-0.10819	-0.26378	-0.27444	-1.3529	-1.31494
4	-0.06884	-0.03691	-0.09836	-0.11659	-1.27317	-1.30163

Table 43. Numerical displacement data for back-to-back loading on path 5 and 6 for Figure 62

Stage (Stop)	***2B Path5D***	***2A Path5D***	***2B Path6D***	***2A Path6D***
0	0	0	0	0
1	-0.26	-0.47834	-0.21173	-0.24815
2	-0.2569	-0.41199	-0.19958	-0.21093
3	-0.16115	-0.10944	-0.13143	-0.23072
4	-0.18092	-0.1796	-0.09302	-0.16103

6.2.16 Displacement of internal girder under two double truck loading

The displacement on stage 1 was not calculated as the image for the loading was not obtained. The two trucks were placed back-to-back and there was another back-to-back truck adjacent to it. Four trucks were used as the loading condition. The internal girder 2A and 2B were closer to the loading path 7. This was the maximum loading condition among all load combination. The maximum displacement was obtained to be 3.47 mm. The girder 2B which is located adjacent to girder 2A was also displaced similarly. Path8 was away from the girders producing small displacement values. The two girders showed similar behavior for the loading. There was small amount of positive displacement noticed when the loading was on path 8. The loading started from the UHPC span which caused the beam to move upwards when the load was on stage 2 of the test. The numeric value for the test was summarized in Figure 63 and Table 44.

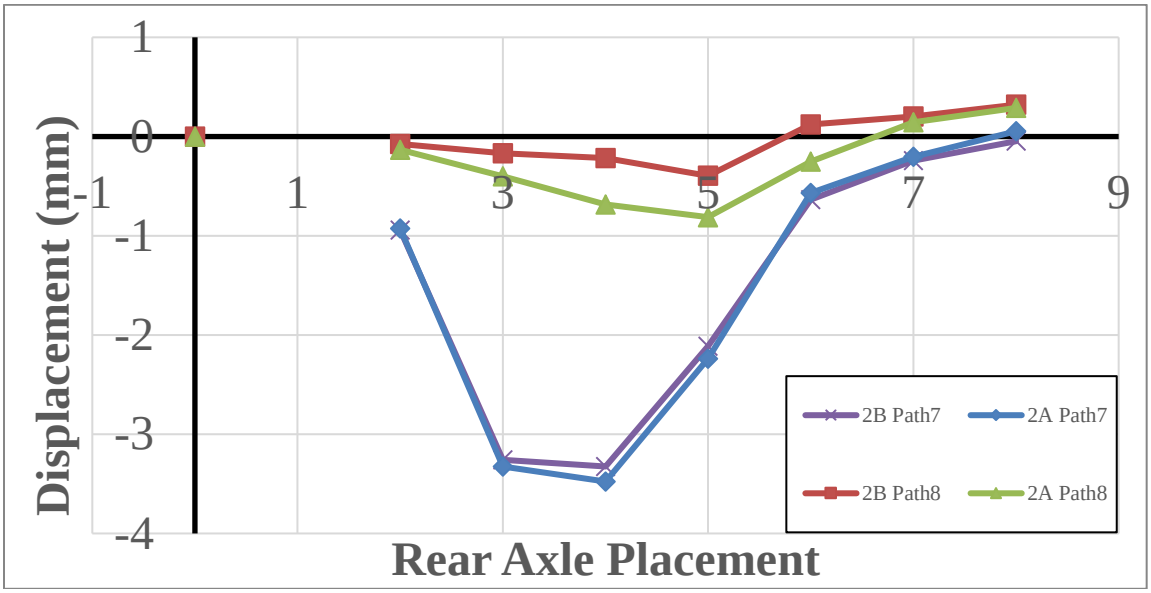

Figure 63. Displacement data for double back-to-back loading for path 7 and 8 for UHPC span

Table 44. Numerical value of displacement (mm) data of double truck loading of path 7 and 8 for Figure 63

Stage (Stop)	***2B Path7***	***2A Path7***	***2B Path8***	***2A Path8***
0	0	0	0	0
1				
2	-0.94226	-0.92572	-0.07585	-0.13277
3	-3.25648	-3.32491	-0.16867	-0.40182
4	-3.32531	-3.47684	-0.21659	-0.68295
5	-2.11398	-2.23881	-0.39576	-0.81207
6	-0.63674	-0.56878	0.121103	-0.25274
7	-0.24216	-0.20463	0.202452	0.144861
8	-0.0469	0.053066	0.321206	0.288461

6.2.17 Displacement of internal girder under triple truck loading

The triple truck loading was conducted with three trucks parallel to each other placed at an equal distance from opposite guard rails. The displacement on stage 1 was not calculated as the image for the loading was not obtained. The maximum displacement was obtained on stop 4 where maximum axle load was placed. The maximum displacement value for the stop was 1.87 mm. The value was less compared to triple truck load as the load was more distributed along the bridge compared to the loading condition of two trucks where the loading was considered on one side of the bridge. The two beams adjacent to each other demonstrated similar behavior and the maximum displacement value was 1.76 mm. There was some upward displacement on stage 7 as the loading started from UHPC span. The value of upward displacement was small compared to the negative displacement which amounted to 0.28 mm. The numerical value for the displacement is summarized in Figure 64 and Table 45.

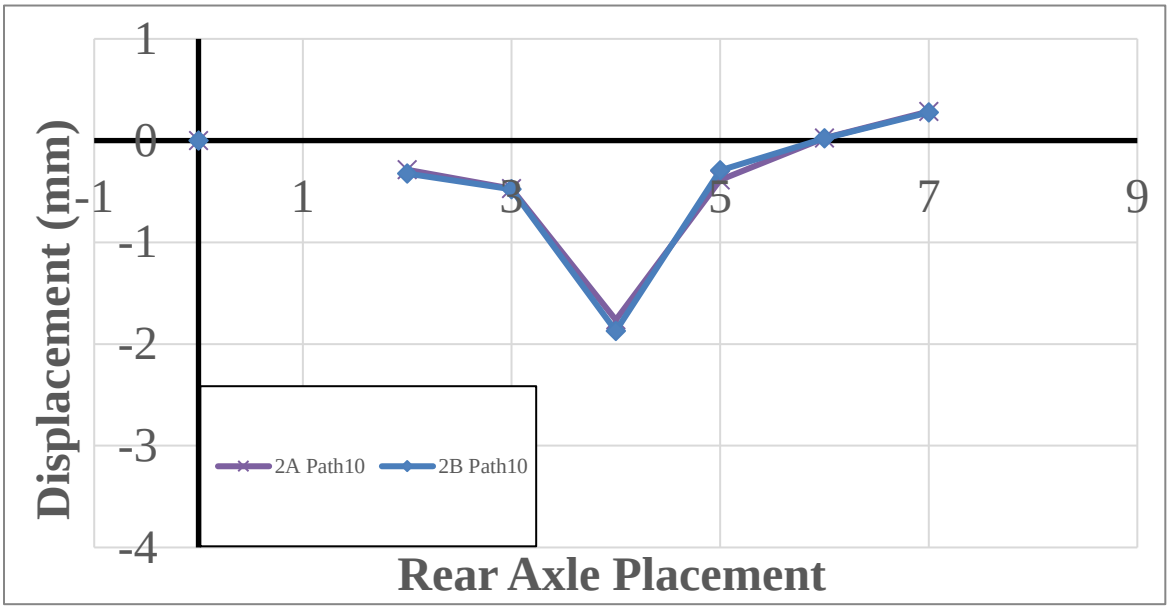

Figure 64. Displacement data for triple truck loading on path 10 for UHPC span

Table 44. Numerical value of displacement (mm) data of triple truck loading on path 10 for Figure 64

Stage (Stop)	***2A Path10***	***2B Path10***
0	0	0
1		
2	-0.28645	-0.32438
3	-0.47294	-0.47884
4	-1.7632	-1.87195
5	-0.38834	-0.29442
6	0.0234	0.0226
7	0.286334	0.2763

f) Go Pro Hero+

The Go Pro Hero + was monitoring internal girder 4A and 4B of the UHPC span. A negative displacement indicates downward deflection while a positive displacement would mean the element moved upward. The loading started from the UHPC span from stop 0 to stop 8. Another Go Pro Hero + was monitoring the HPC span on the other side of the UHPC span for the same loading condition. The UHPC beam began to deform as the loading started. The beam deflected upwards when the loading reached the HPC span. The upward displacement was less compared to the negative displacement.

6.2.18 Displacement of internal girder under single truck loading from path1-6

When the front axle is on path 1 of the UHPC span the UHPC span moved downwards from stop 0 to 6 but when the truck moved towards the HPC span the deflection of the beam started to go upwards. The girders 4A and 4B are closest to path2. The girder 4B comes down the most with the maximum displacement value of 1.92 mm. The beam

4A comes down with a displacement value of 1.69 mm. The displacement decreases gradually when the single truck loading moves away from girder 4A and 4B. Minimum displacement effect was observed when the loading was on path 6 of the bridge. The upward movement of the girder suggests that there was continuity among the spans. Figure 65 and Table 46 and 47 summarize those findings.

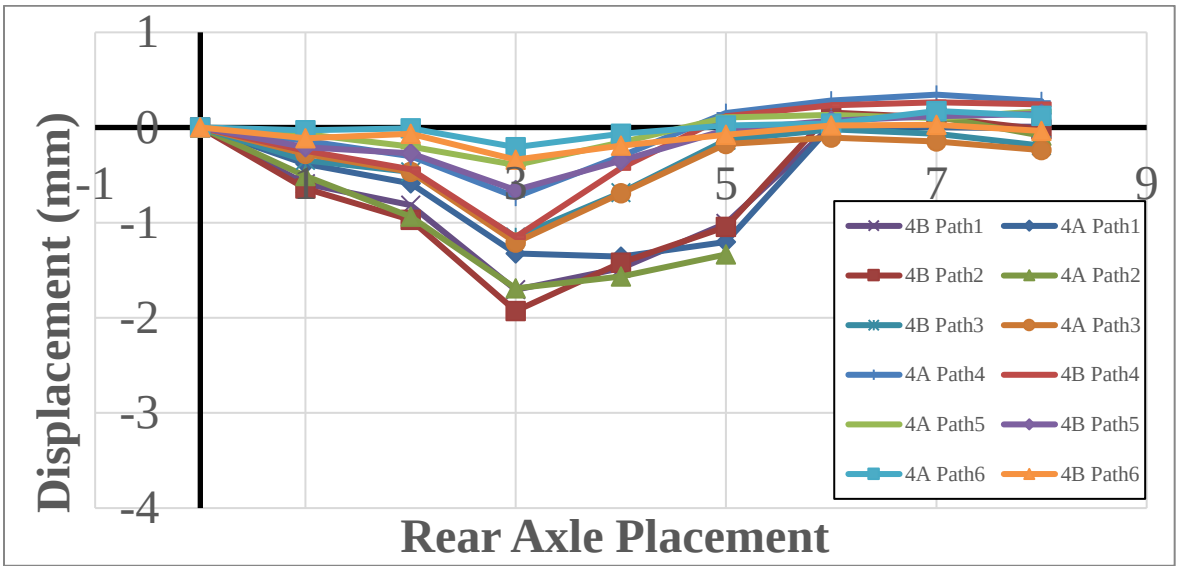

Figure 65. Displacement data for single truck loading of path 1 to 6 on UHPC span

Table 46. Numerical value of displacement (mm) for single truck loading from path 1 to 3 in Figure 65

Stage (Stop)	***4B Path1***	***4A Path1***	***4B Path2***	***4A Path2***	***4B Path3***	***4A Path3***
0	0	0	0.000000	0	0	0
1	-0.58939	-0.38145	-0.642307	-0.51081	-0.34392	-0.27873
2	-0.81613	-0.588	-0.971592	-0.93661	-0.46483	-0.46668
3	-1.70564	-1.32407	-1.928393	-1.69066	-1.15144	-1.20814
4	-1.47966	-1.35698	-1.421806	-1.56748	-0.68401	-0.69054
5	-1.00671	-1.20458	-1.046424	-1.33297	-0.13414	-0.17409
6	0.016653	0.016477	0.156980		-0.01765	-0.10545
7	0.015716	0.00498	0.106676	0.114119	-0.06528	-0.14741
8	0.009332	-0.01224	-0.020374	-0.08514	-0.19167	-0.23667

Table 47. Numerical value of displacement (mm) for single truck loading from path 4 to 6 in Figure 65

Stage (Stop)	***4A Path4***	***4B Path4***	***4A Path5***	***4B Path5***	***4A Path6***	***4B Path6***
0	0	0	0	0	0	0
1	-0.13935	-0.2439	-0.06875	-0.20686	-0.02893	-0.11428
2	-0.30087	-0.43894	-0.20023	-0.2714	-0.0076	-0.06726
3	-0.72996	-1.15106	-0.3939	-0.65751	-0.20664	-0.33784
4	-0.30302	-0.42457	-0.15639	-0.3499	-0.06766	-0.19045
5	0.151732	0.120354	0.105104	-0.02475	0.022228	-0.07732
6	0.282039	0.231669	0.133397	0.072703	0.042457	0.020314
7	0.345153	0.264816	0.098765	0.120134	0.173279	0.028574
8	0.278221	0.242284	0.170502	0.142618	0.12345	-0.03585

6.2.19 Displacement of internal girder under double trucks back-to-back loading

Only 5 stops were used for a double back-to-back truck loading. When the truck start on the UHPC span the beam starts to move down immediately. The upward movement of the HPC beam does not occur in this test as the loading starts from the UHPC span. The maximum displacement occurs when the two axles reach the first quarter of the UHPC beam. The maximum displacement occurs on girder 4B of path 4 with a value of 1.65 mm. The beam adjacent to beam 4B is displaced significantly less compared to beam 4A. This was similar case for all other loading paths. The minimum displacement occurred when the loading was on path6. The numeric displacement value is summarized in Figure 66 and Table 48 and 49.

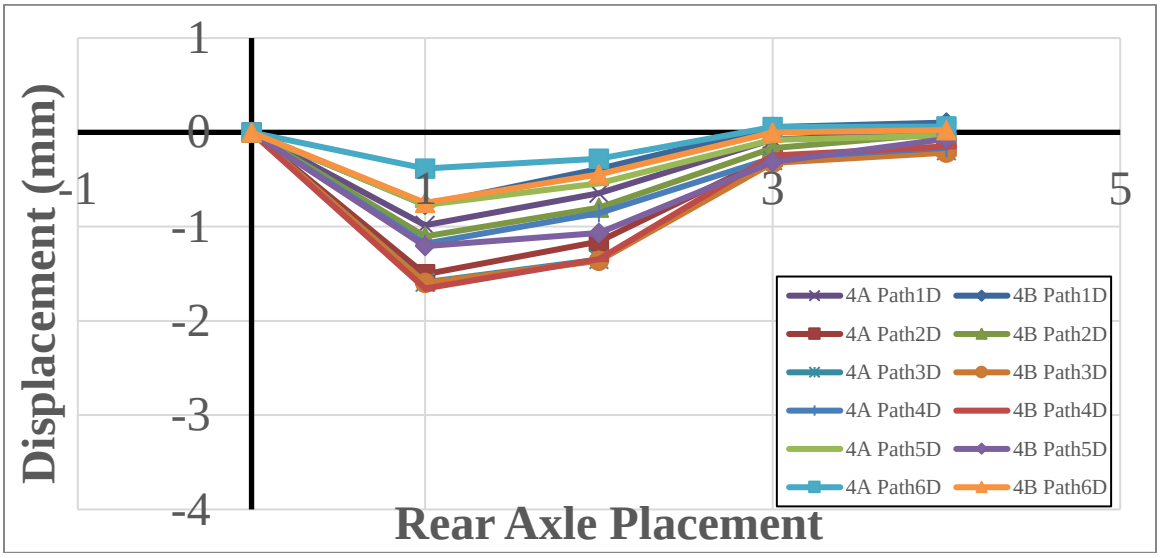

Figure 66. Displacement data for back-to-back loading from path 1 to 6 on UHPC span

Table 47. Numerical value of displacement (mm) data for double truck loading from path 1D to 3D in Figure 66

Stage (Stop)	***4A Path1D***	***4B Path1D***	***4A Path2D***	***4B Path2D***	***4A Path3D***	***4B Path3D***
0	0	0	0	0	0	0
1	-0.98502	-0.77003	-1.5052	-1.10338	-1.58977	-1.59696
2	-0.64727	-0.38937	-1.15913	-0.80011	-1.34968	-1.36254
3	-0.07535	0.056742	-0.25979	-0.16818	-0.29849	-0.3225
4	-0.00204	0.103711	-0.15068	-0.00886	-0.19601	-0.21374

Table 48. Numerical value of displacement (mm) data for double truck loading from path 4D to 6D in Figure 66

Stage (Stop)	***4A Path4D***	***4B Path4D***	***4A Path5D***	***4B Path5D***	***4A Path6D***	***4B Path6D***
0	0	0	0	0	0	0
1	-1.18046	-1.6562	-0.77054	-1.20731	-0.38349	-0.74718
2	-0.85746	-1.34693	-0.54197	-1.06736	-0.27911	-0.44676
3	-0.27341	-0.24663	-0.07809	-0.31373	0.055364	-0.00189
4	-0.16444	-0.15171	-0.03450	-0.07003	0.061615	0.023985

6.2.20 Displacement of internal girder under two double truck loading

The displacement on stage 1 was not calculated as the image for the loading was not obtained. The two trucks were placed back-to-back and there was another back-to-back truck adjacent to it. Four trucks were used as the loading condition. The internal girder 4A and 4B were monitored when the loading was done on path 7 and path8. This was the maximum loading condition among all load combination. The maximum displacement was obtained to be 2.93 mm. The girder 4B which is located adjacent to girder 4A was also displaced similarly but with a value of 2.53. Path8 was away from the girders producing smaller displacement values. The two girders showed similar behavior for the loading. There was small amount of positive displacement noticed when the loading was on stop 8. The loading started from the UHPC span which caused the beam to move downwards immediately when the load was on stage 2 of the test. The loading condition is concentrated on path 7 unlike triple truck loading where the distributed along the bridge. During the maximum value of displacement was obtained when the load was at stop 7. The numeric value for the test was summarized in Figure 67 and Table 50.

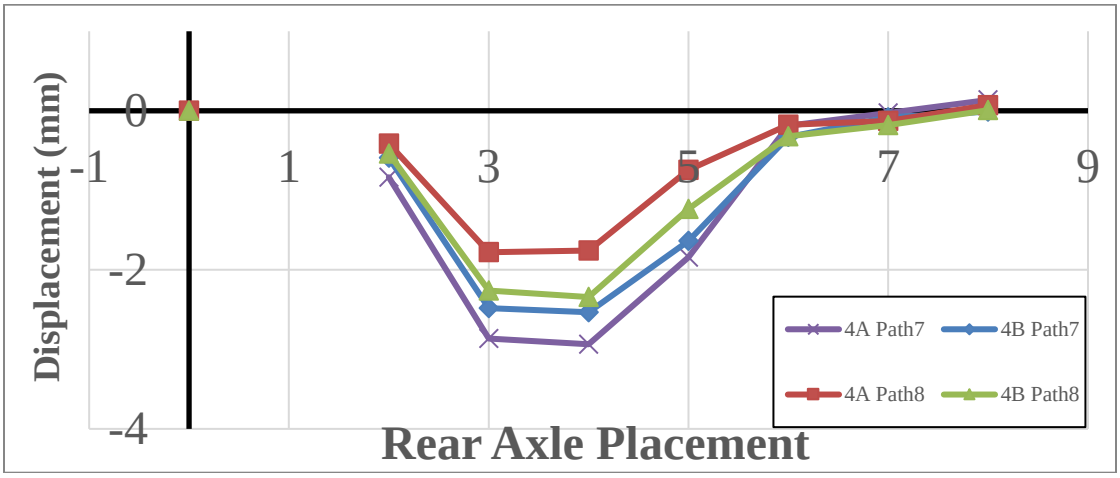

Figure 68. Displacement of double back-to-back loading from path 7 and 8 for UHPC span

Table 50. Numerical value of displacement (mm) data of double truck loading of path 7 and 8 for Figure 68

Stage (Stop)	***4A Path7***	***4B Path7***	***4A Path8***	***4B Path8***
0	0	0	0	0
1				
2	-0.83632	-0.59147	-0.41501	-0.53807
3	-2.86524	-2.48110	-1.77858	-2.25915
4	-2.93613	-2.53342	-1.75679	-2.34245
5	-1.84111	-1.63707	-0.74441	-1.23607
6	-0.18623	-0.32964	-0.17663	-0.31980
7	-0.02547	-0.08148	-0.12656	-0.18020
8	0.13625	-0.01033	0.07143	0.00733

`

6.2.21 Displacement of internal girder under triple truck loading

The triple truck loading was conducted with three trucks parallel to each other placed at an equal distance from opposite guard rails. The displacement on stage 1 was not calculated as the image for the loading was not obtained. The maximum displacement was obtained on stop 3 where maximum axle load was placed. The maximum displacement value for the stop was 2.78 mm. The value was less compared to triple truck load as the load was more distributed along the bridge compared to the loading condition of two trucks where the loading was considered on one side of the bridge. The two beams adjacent to each other demonstrated similar behavior and the maximum displacement value was 2.64 mm. There was some upward displacement on stage 7 as the loading moved towards the HPC span. The value of upward displacement was

significantly small compared to the negative displacement which amounted to 0.33 mm. The two girders 4A and 4B are displaced similarly. The displacement value obtained for the girder 4A and 4B. The numerical value for the displacement is summarized in Figure 68 and Table 51.

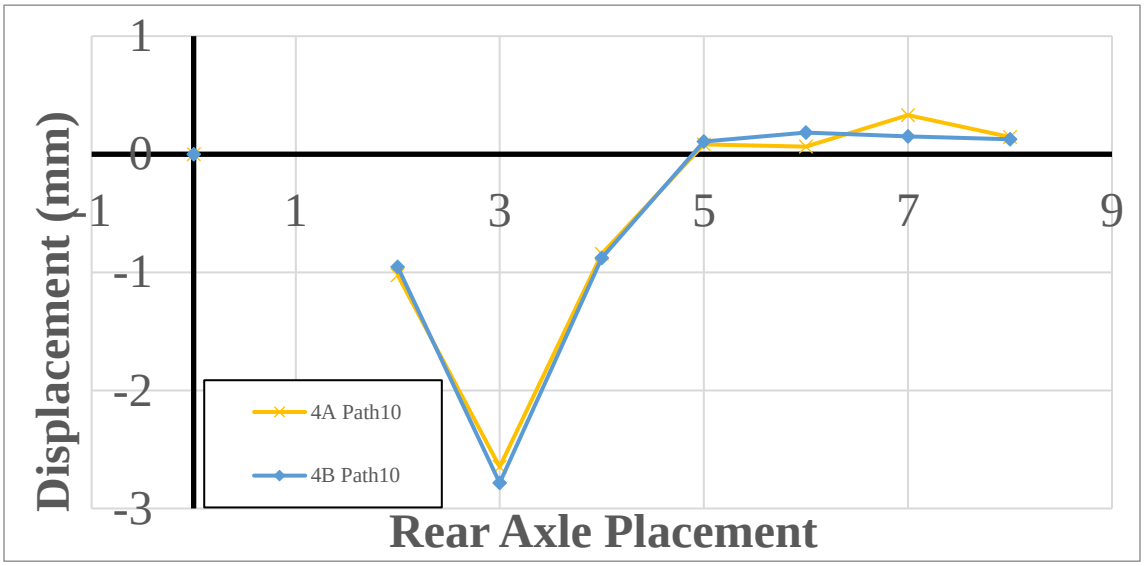

Figure 69. Displacement data for triple truck loading on path 10 for UHPC span

Table 50. Numerical value of displacement (mm) data of triple truck loading on path 10 in Figure 68

Stage (Stop)	***4A Path10***	***4B Path10***
0	0	0
1		
2	-1.024545	-0.954005
3	-2.647856	-2.784289
4	-0.844584	-0.878007
5	0.082667	0.108991
6	0.064651	0.183397
7	0.331249	0.151896
8	0.145936	0.125783

g) DMK 0

The DMK 0 was monitoring internal girder 6A and 5B. A negative displacement indicates downward deflection while a positive displacement would mean the element moved upward. The loading started from the UHPC span from stop 0 to stop 8. The loading started as single truck loading and later the loading was increased, and displacement profile was obtained respectively. The HPC span on the other side of the girder was monitored by DMK 1 camera system.

6.2.22 Displacement of internal girder under single truck loading from path1-6

When the front axle is on stop 3 for path 5 of the UHPC span the girder moved downwards from stop 0 to 5 but when the truck moved towards the HPC span the deflection of the beam started to go upwards. The girders 6A and 5B are adjacent to each other. The girder 6A comes down the most with the maximum displacement value of 1.48 mm. The beam 5B comes down with a displacement value of 1.41 mm for single truck loading on path 5. The displacement decreases gradually when the single truck loading moves away from girder 6A and 5B. Positive displacement was noticed when the loading was on HPC span. The magnitude of positive displacement is less compared to the negative displacement. The numerical data for displacements is summarized in Figure 69 and Table 52 and 53.

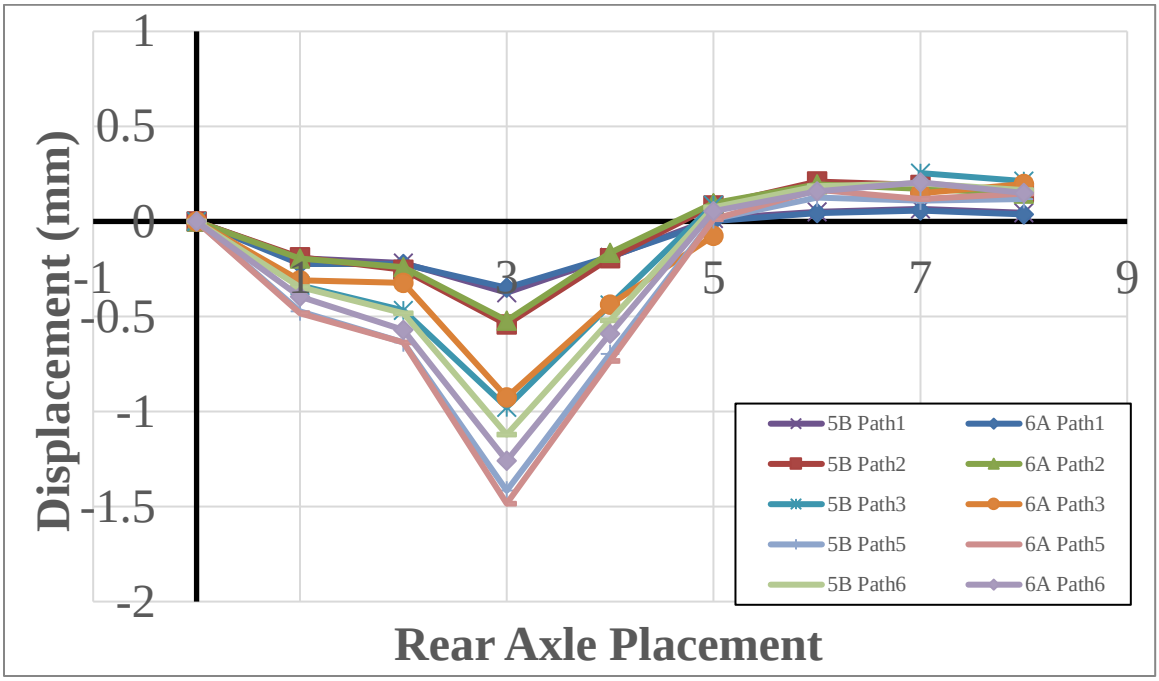

Figure 69. Displacement data for single truck loading from path 1 to 6 for UHPC span

Table 52. Numerical value of displacement (mm) for single truck loading from path 1 to 3 in Figure 69

Stage (Stop)	***5B Path1***	***6A Path1***	***5B Path2***	***6A Path2***	***5B Path3***	***6A Path3***
0	0	0	0	0	0	0
1	-0.19346	-0.22339	-0.18828	-0.19474	-0.33634	-0.3094
2	-0.21905	-0.22364	-0.25467	-0.24025	-0.46795	-0.32291
3	-0.37489	-0.34919	-0.54193	-0.5213	-0.97789	-0.92524
4	-0.18779	-0.18569	-0.19361	-0.1642	-0.43984	-0.43722
5	0.015067	0.001245	0.084548	0.095558	0.085376	-0.07624
6	0.050253	0.043872	0.209866	0.194736		
7	0.066015	0.057091	0.191475	0.172143	0.254407	0.147536
8	0.046068	0.036695	0.152637	0.145853	0.212103	0.196808

Table 53. Numerical value of displacement (mm) for single truck loading from path 5 and 6 in Figure 69

Stage (Stop)	***5B Path5***	***6A Path5***	***5B Path6***	***6A Path6***
0	0	0	0	0
1	-0.47304	-0.48363	-0.34546	-0.39557
2	-0.63679	-0.63704	-0.48382	-0.57139
3	-1.41621	-1.48429	-1.12141	-1.25891
4	-0.69677	-0.73324	-0.52069	-0.59129
5	0.012488	0.012141	0.074291	0.054671
6	0.12554	0.166524	0.185897	0.157634
7	0.108666	0.118056	0.200201	0.205777
8	0.118538	0.145944	0.165027	0.149312

6.2.23 Displacement of internal girder under double trucks back-to-back loading

Only 5 stops were used for a double back-to-back truck loading. When the truck start on the UHPC span the beam starts to move down. The upward movement of the HPC beam does not occur in this test as the loading starts from the UHPC span. The maximum displacement occurs when the two axles reach the first quarter of the UHPC span. The girder 6A has the maximum displacement value of 2.11 mm. The displacement value decreases when the loading moves further away from girder 6A and 5B. The maximum displacement occurred when the Loading was on path 5. Path 1 had the least displacement value on girder 6A and 5B. The least value of displacement was 0.023 mm when the truck was moving on path 6. The numeric displacement value is summarized in Figure 70 and Table 54 and 55.

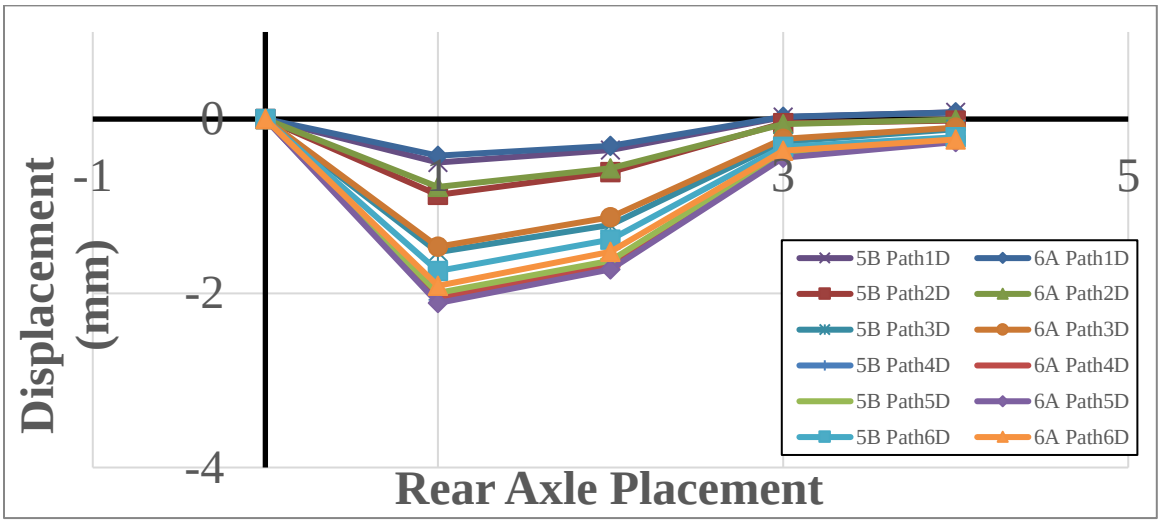

Figure 70. Displacement data for back-to-back loading from path 1 to 6 for UHPC span

Table 54. Numerical value of displacement (mm) data for double truck loading from path 1D to 3D for Figure 70

Stage (Stop)	***5B Path1D***	***6A Path1D***	***5B Path2D***	***6A Path2D***	***5B Path3D***	***6A Path3D***
0	0	0	0	0	0	0
1	-0.49839	-0.42017	-0.87004	-0.77874	-1.5277	-1.46561
2	-0.35592	-0.30914	-0.60999	-0.56331	-1.21544	-1.12728
3	0.023934	0.026137	-0.04833	-0.05742	-0.25935	-0.22508
4	0.078452	0.076468	-0.01895	-0.00788	-0.11585	-0.09669

Table 55. Numerical value of displacement (mm) data for double truck loading from path 4D to 6D for Figure 70

Stage (Stop)	***5B Path4D***	***6A Path4D***	***5B Path5D***	***6A Path5D***	***5B Path6D***	***6A Path6D***
0	0	0	0	0	0	0
1	-2.07566	-2.05686	-1.99577	-2.11215	-1.74411	-1.91401
2	-1.6835	-1.67486	-1.62775	-1.72617	-1.38479	-1.52412
3	-0.35372	-0.32816	-0.38539	-0.44455	-0.31855	-0.36149
4	-0.22335	-0.22238	-0.21723	-0.26231	-0.20891	-0.23451

6.2.24 Displacement of internal girder under two double truck loading

The displacement on stage 1 was not calculated as the image for the loading was not obtained. The two trucks were placed back-to-back and there was another back-to-back truck adjacent to it. Four trucks were used as the loading condition. The internal girder 6A and 5B were monitored for loading on path7 and path8. This was the maximum loading condition among all load combination. The maximum displacement was obtained to be 3.34 mm on path8 for girder 6A. The girder 5B which is located adjacent to girder 6A was also displaced similarly. Path7 was away from the girders producing small displacement values. The two girders showed similar behavior for the loading. There was small amount of positive displacement noticed when the loading was on path 8. The loading started from the UHPC span which caused the beam to move upwards when the load was on stop 8. The maximum value of displacement was obtained when the load was at stop 4. The numerical value for the test was summarized in Figure 71 and Table 56.

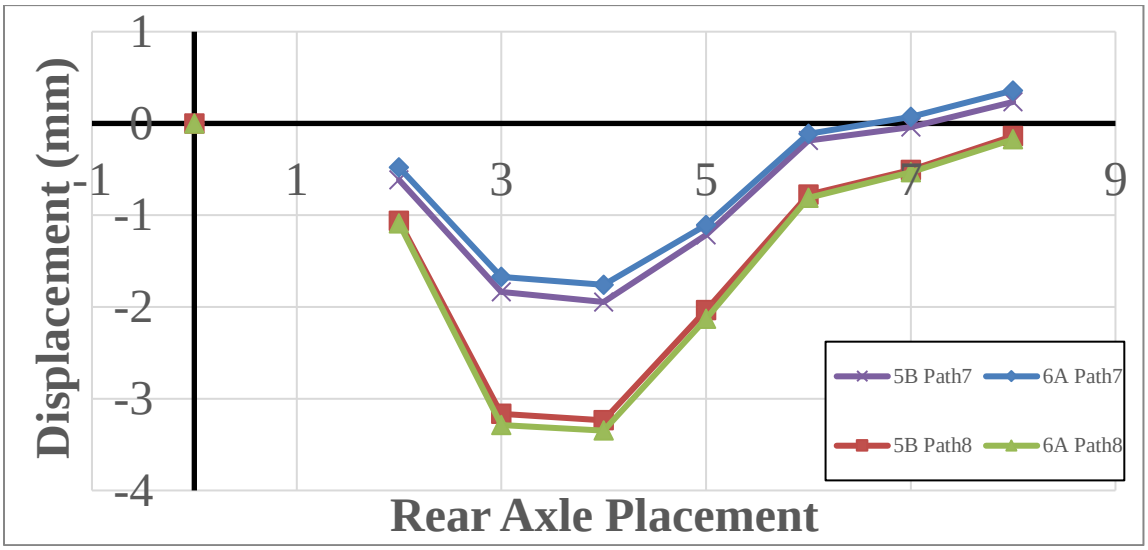

Figure 71. Displacement for double back-to-back loading for path7 and 8 for UHPC span

Table 56. Numerical value of displacement (mm) data of double truck loading of path 7 and 8 for Figure 71

Stage (Stop)	***5B Path7***	***6A Path7***	***5B Path8***	***6A Path8***
0	0	0	0	0
1				
2	-0.61589	-0.47992	-1.06325	-1.09077
3	-1.83468	-1.67234	-3.16508	-3.28566
4	-1.94622	-1.75894	-3.2361	-3.34812
5	-1.21558	-1.1081	-2.03518	-2.13011
6	-0.18699	-0.11463	-0.77465	-0.81142
7	-0.04018	0.070039	-0.50867	-0.53164
8	0.234713	0.358829	-0.13756	-0.17372

6.2.25 Displacement of internal girder under triple truck loading

The triple truck loading was conducted with three trucks parallel to each other placed at an equal distance from opposite guard rails. The displacement on stage 1 was not calculated as the image for the loading was not obtained. The maximum displacement was obtained on stop 4 where maximum axle load was placed. The maximum downward displacement value for the stop was 1.01 mm. The value was less compared to triple truck load as the load was more distributed along the bridge compared to the loading condition of two trucks where the loading was considered on one side of the bridge. The two beams adjacent to each other demonstrated similar behavior and the maximum upward displacement value was 0.52 mm. There was some upward displacement after stage 4 as the loading started from HPC span. The girder experienced less displacement when the loading was spread along the bridge compared to the double truck loading

where the loading was concentrated on one side of the bridge. The numerical data for the displacement is summarized in Figure 72 and Table 57.

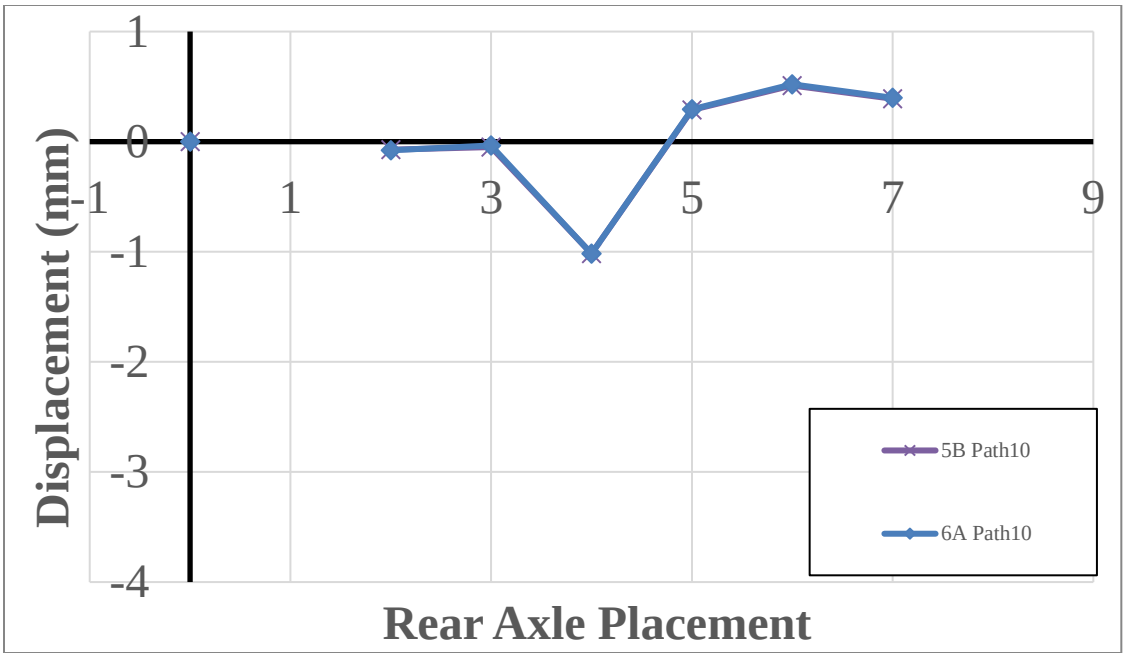

Figure 72. Displacement data for triple truck loading on path 10 of UHPC span

Table 57. Numerical value of displacement (mm) data of triple truck loading on path 10 in Figure 72

Stage (Stop)	***5B Path10***	***6A Path10***
0	0	0
1		
2	-0.07198	-0.07786
3	-0.04815	-0.03329
4	-1.01707	-1.01721
5	0.288744	0.294416
6	0.510313	0.521324
7	0.389813	0.398893

h) Ampscope 2

The Ampscope 2 was monitoring internal girder 7B and 8A. A negative displacement indicates downward deflection while a positive displacement would mean the element moved upward. The loading started from the UHPC span from stop 0 to stop 8.

6.2.25 Displacement of internal girder under single truck loading from path 1-6

When the front axle is on path 1 of the UHPC span the UHPC span moved downwards from stop 0 to 5 but when the truck moved towards the HPC span the deflection of the beam started to go upwards. The girders 8A and 7B are closest to path6. The girder 8A comes down the most with the maximum displacement value of 1.65mm. The beam 7B comes down with a displacement value of 1.61 mm. The displacement decreases gradually when the single truck loading moves away from girder 8A and 7B. Minimum positive displacement is noticed when loading is on HPC side of the bridge.

The findings are shown in Figure 73 and Table 58.

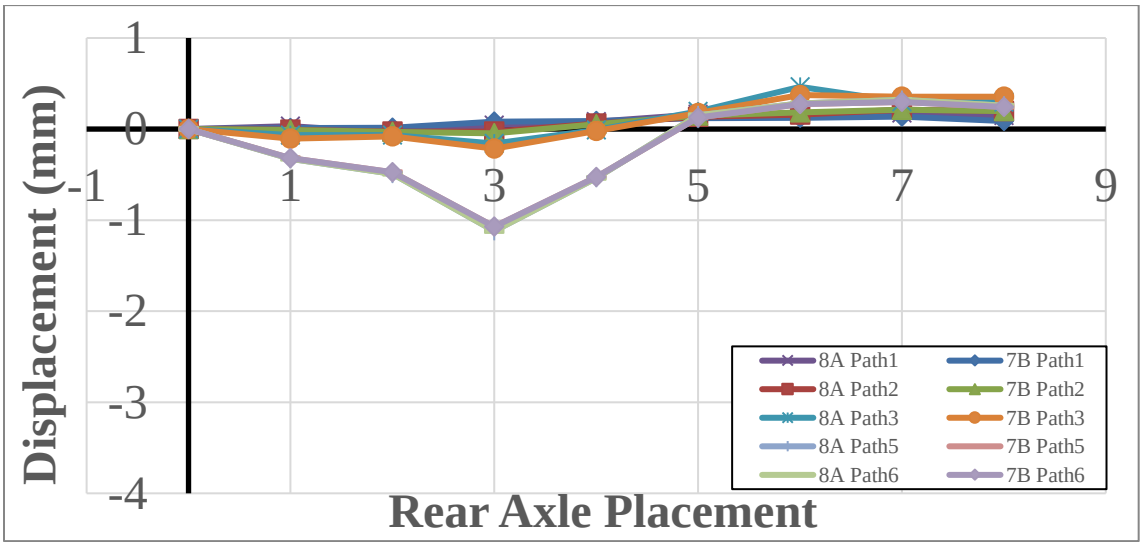

Figure73. Displacement profile under single truck loading from path 1 to 6 for UHPC span

Table 57. Displacement (mm) value of single truck loading from path 1 to 3 in Fig 73

Stage (Stop)	8A Path1	7B Path1	8A Path2	7B Path2	8A Path3	7B Path3	8A Path5	7B Path5	8A Path6	7B Path6
0	0	0	0	0	0	0	0	0	0	0
1	0.030541	0.010524	-0.00507	-0.01026	-0.06799	-0.10632	-0.32602	-0.32075	-0.32602	-0.32075
2	-0.03858	0.012896	-0.0285	-0.03112	-0.0677	-0.07918	-0.49095	-0.47517	-0.49095	-0.47517
3	0.041149	0.080801	-0.02706	-0.04683	-0.15842	-0.2151	-1.11913	-1.07182	-1.11913	-1.07182
4	0.082181	0.088702	0.059207	0.053003	-0.00921	-0.01963	-0.53644	-0.52752	-0.53644	-0.52752
5	0.163227	0.120128	0.134115	0.146166	0.193172	0.174369	0.152071	0.126083	0.152071	0.126083
6	0.165811	0.122103	0.157915	0.183363	0.463518	0.373912	0.282113	0.274903	0.282113	0.274903
7	0.177363	0.136571	0.212854	0.212084	0.299899	0.35558	0.320833	0.297508	0.320833	0.297508
8	0.14872	0.088367	0.195822	0.195529	0.293794	0.35502	0.256767	0.241918	0.256767	0.241918

6.2.26 Displacement of internal girder under double trucks back-to-back loading

The double back-to-back truck for amp scope 1 monitored girder 8A and 7B of the UHPC span. The loading started on the UHPC side of the bridge and the bridge started to go down immediately after the loading started. Path 6 which was closest to the girder had the highest displacement value. The girder 8A and 7B went down in similar fashion and had similar displacement value. The displacement gradually decreased once the vehicle started to move further away from path 6. Small values of positive displacement were observed but the magnitude was very small compared to the negative deflection. The results are summarized in Figure 74 and Table 59 and 60.

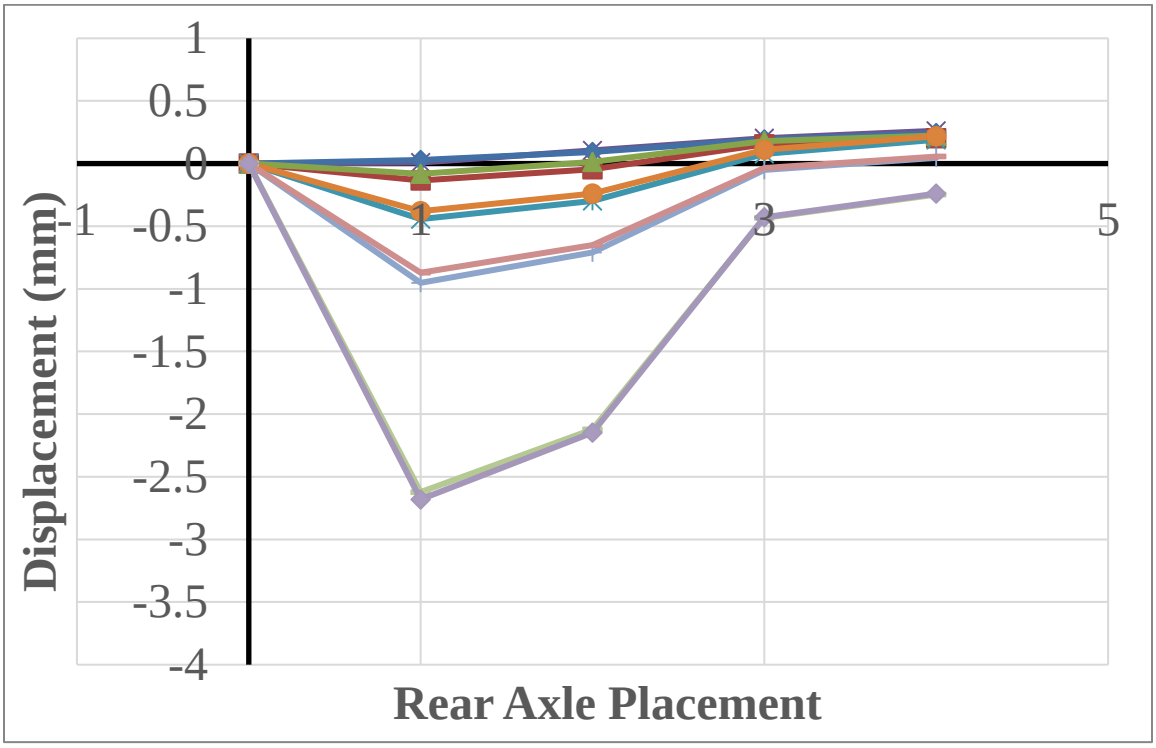

Figure 74. Displacement data for double truck loading path 1 to 6 for UHPC span

Table 59. Numerical displacement (mm) value of double truck loading from path 1 to 3 for Figure 74

Stage	***7B***	***8A***	***7B***	***8A***	***7B***	***8A***
(Stop)	***Path1D***	***Path1D***	***Path2D***	***Path2D***	***Path3D***	***Path3D***
0	0	0	0	0	0	0
1	0.008857	0.027526	-0.13494	-0.08185	-0.44331	-0.38021
2	0.104284	0.091361	-0.04566	0.013985	-0.29816	-0.24081
3	0.201532	0.191719	0.154252	0.18004	0.078111	0.110314
4	0.26199	0.242639	0.20282	0.223831	0.190289	0.218725

Table 60. Numerical displacement (mm) value of double truck loading from path 4 to 6 for figure 74

Stage (Stop)	***7B Path4D***	***8A Path4D***	***7B Path5D***	***8A Path5D***	***7B Path6D***	***8A Path6D***
0	0	0	0	0	0	0
1	-0.95174	-0.8711	-1.86688	-1.81852	-2.6223	-2.68037
2	-0.71015	-0.64956	-1.4973	-1.46349	-2.12254	-2.14704
3	-0.05087	-0.03612	-1.4939	-1.46133	-0.43256	-0.42827
4	0.045753	0.055851	-0.29216	-0.27388	-0.24663	-0.24051

6.2.27 Displacement of internal girder under two double truck loading

The two trucks were placed back-to-back and there was another back-to-back truck adjacent to it. Four trucks were used as the loading condition. The internal girder 8A and 7B were closer to the loading path 8. This was the maximum loading condition among all load combination. The maximum displacement was obtained to be 3.78 mm on stage 3. The girder 7B which is located adjacent to girder 8A was also displaced similarly. Path7 was away from the girders producing small displacement values. The two girders showed similar behavior for the loading. This was the maximum loading condition which produced maximum displacement value in the girder. The loading started from the UHPC span which caused the beam to move downwards. The maximum value of displacement was obtained when the load was at stop 3. The numeric value for the test was summarized in Figure 75 and Table 61.

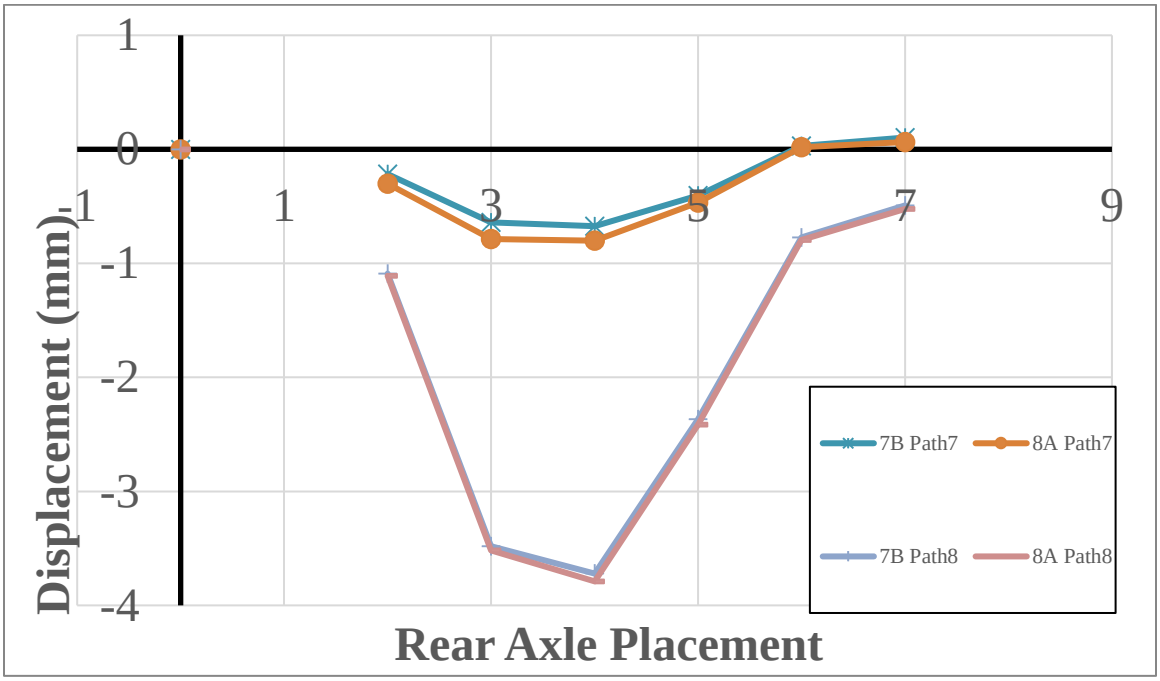

Figure 75. Displacement profile under double back-to-back loading for path 7 and 8 for UHPC span

Table 61. Numerical displacement (mm) value of double back-to-back truck loading from path 7 and 8 in Figure 75

Stage (Stop)	***7B Path7***	***8A Path7***	***7B Path8***	***8A Path8***
0	0	0	0	0
1				
2	-0.21738	-0.30223	-1.0902	-1.10954
3	-0.64226	-0.78605	-3.48148	-3.51805
4	-0.67419	-0.80137	-3.72111	-3.78941
5	-0.40467	-0.46679	-2.36619	-2.41341
6	0.030926	0.018048	-0.77188	-0.79664
7	0.103275	0.063898	-0.49221	-0.52338
8	0.219593	0.202438	-0.08293	-0.1151

6.2.28 Displacement of internal girder under triple truck loading

The triple truck loading was conducted with three trucks parallel to each other placed at an equal distance from opposite guard rails. The maximum displacement was obtained on stop 2 where maximum axle load was placed. The maximum displacement value for the stop was 2.59 mm. The value was less compared to triple truck load as the load was more distributed along the bridge compared to the loading condition of two trucks where the loading was considered on one side of the bridge. The two beams adjacent to each other demonstrated similar behavior and the maximum displacement value was 2.58 mm. There was some upward displacement after stage 4 as the loading started from UHPC span. The value of upward displacement was small compared to the negative displacement which amounted to 0.42 mm. The numerical value for the displacement is summarized in Figure 76 and Table 62.

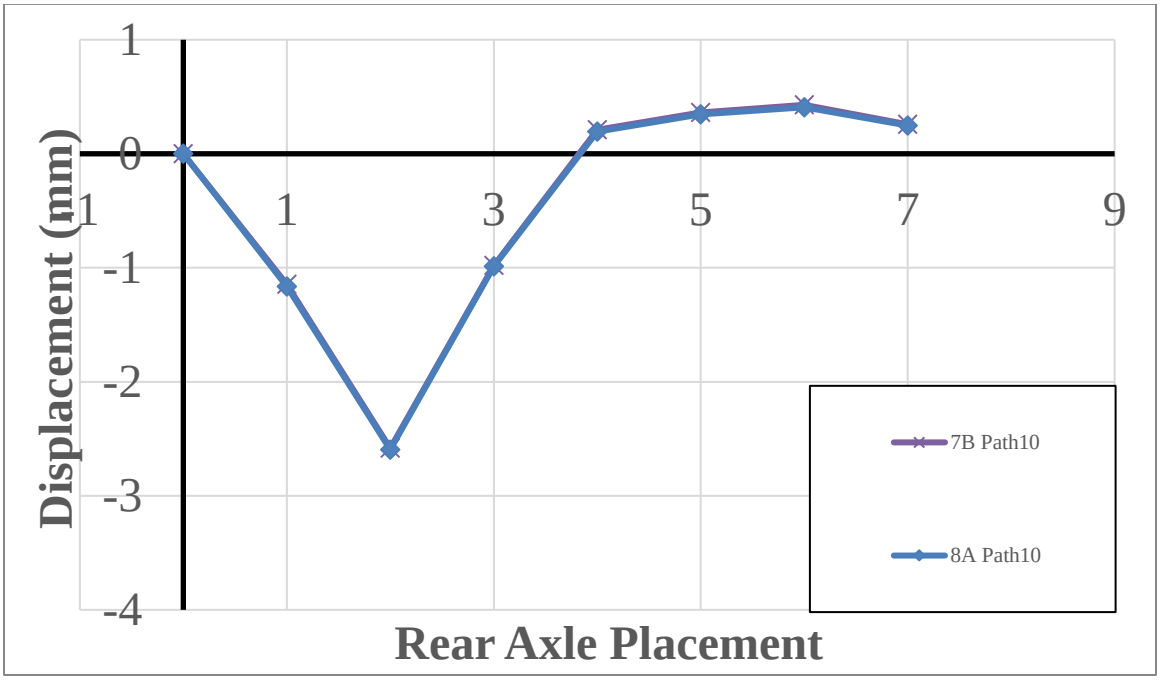

Figure 76. Displacement profile under triple truck loading on path 10 for UHPC beam

Table 62. Numerical displacement (mm) value for triple truck loading on path 10 in Figure 76

Stage	***7B***	***8A***
(Stop)	***Path10***	***Path10***
0	0	0
1	-1.14375	-1.16332
2	-2.58194	-2.59517
3	-0.97983	-0.9886
4	0.210604	0.194725
5	0.36324	0.343957
6	0.429165	0.407525
7	0.257081	0.247401

6.3 Out-of-plane displacement for pier of the bridge

The second test had a Hi-spec camera that observed the pier of the bridge. The HPC and UHPC span of the bridge were simply supported spans. The Z-displacement or out-of-plane displacement was captured. The double back-to-back truck was the loading combination which produced the highest displacement from the test. The z-displacement was checked for the same loading condition to account for maximum out-of-plane displacement. The z-displacement was small for single truck loading the value for z-displacement for single truck loading for path 1,2 and 3 and for the maximum loading on path7. The results are shown from Figure 77-80 and in Table 63-66.

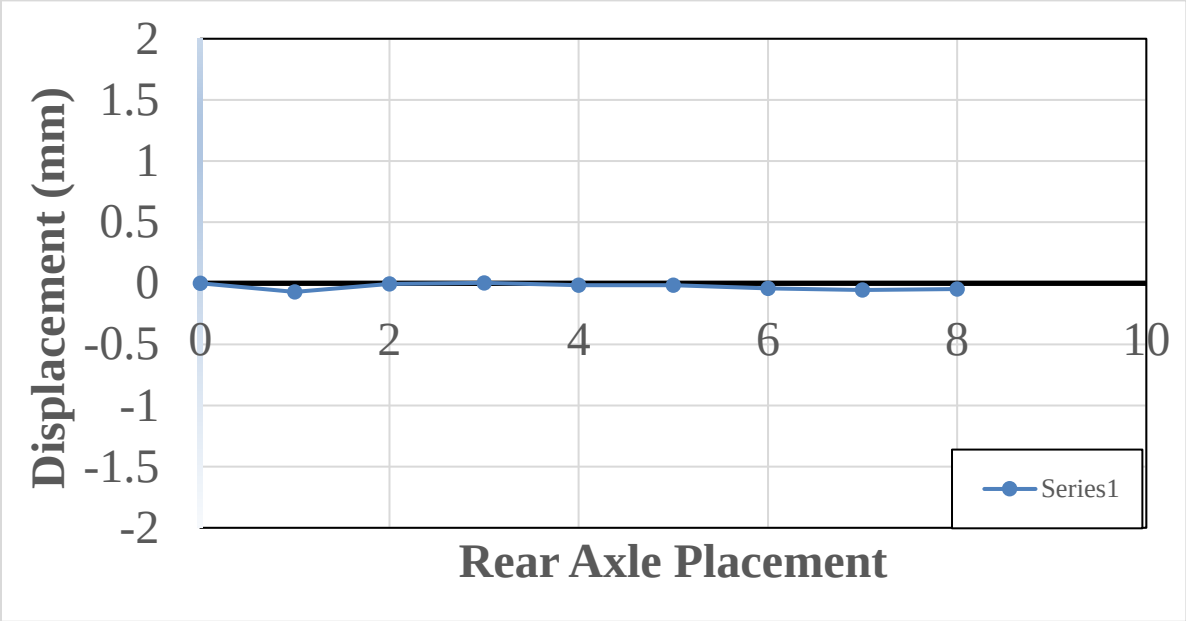

Figure 77. Out-of-plane displacement for single truck loading path1 from Hi-spec camera

Table 63. Numerical displacement (mm) value for z-displacement of pier for single truck loading on path 1

Stage	***Z-Displacement***
0	0
1	-0.070677314
2	-0.00431756
3	0.003562614
4	-0.016533767
5	-0.016232499
6	-0.041548514
7	-0.055957544
8	-0.04604118

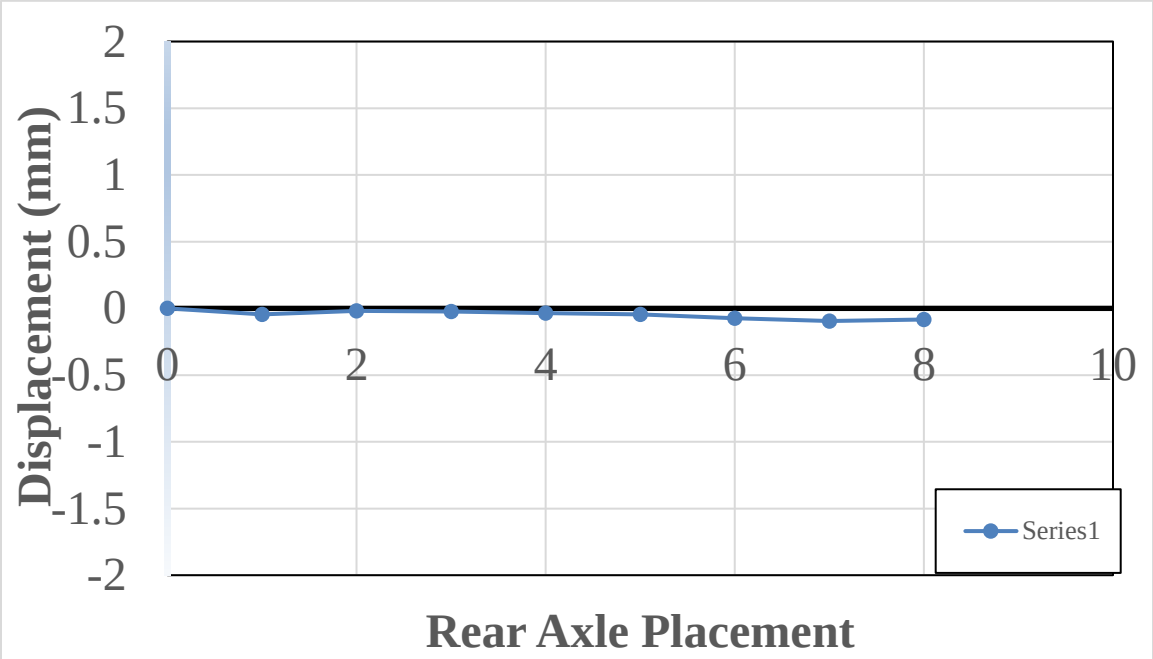

Figure 78. Out-of-plane displacement for single truck loading path2 from Hi-spec camera

Table 64. Numerical displacement (mm) value for z-displacement of pier for single truck loading on path 2

Stage	***Z-Displacement***
0	0
1	-0.044724071
2	-0.019412208
3	-0.024699118
4	-0.036576338
5	-0.044142375
6	-0.074344365
7	-0.094672779
8	-0.083952587

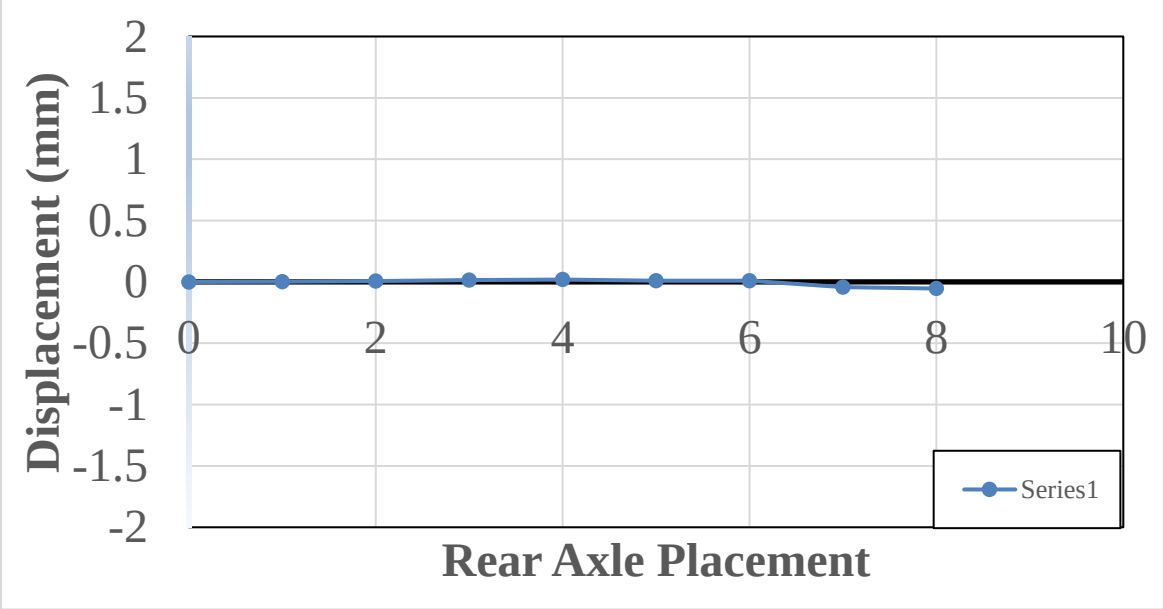

Figure 79. Out-of-plane displacement for single truck loading path3 from Hi-spec camera

Table 65. Numerical displacement (mm) value for z-displacement of pier for single truck loading on path 3

Stage	***Z-Displacement***
0	0
1	0.00208267
2	0.006393366
3	0.015736918
4	0.018788801
5	0.00991317
6	0.008782212
7	-0.041392949
8	-0.054075772

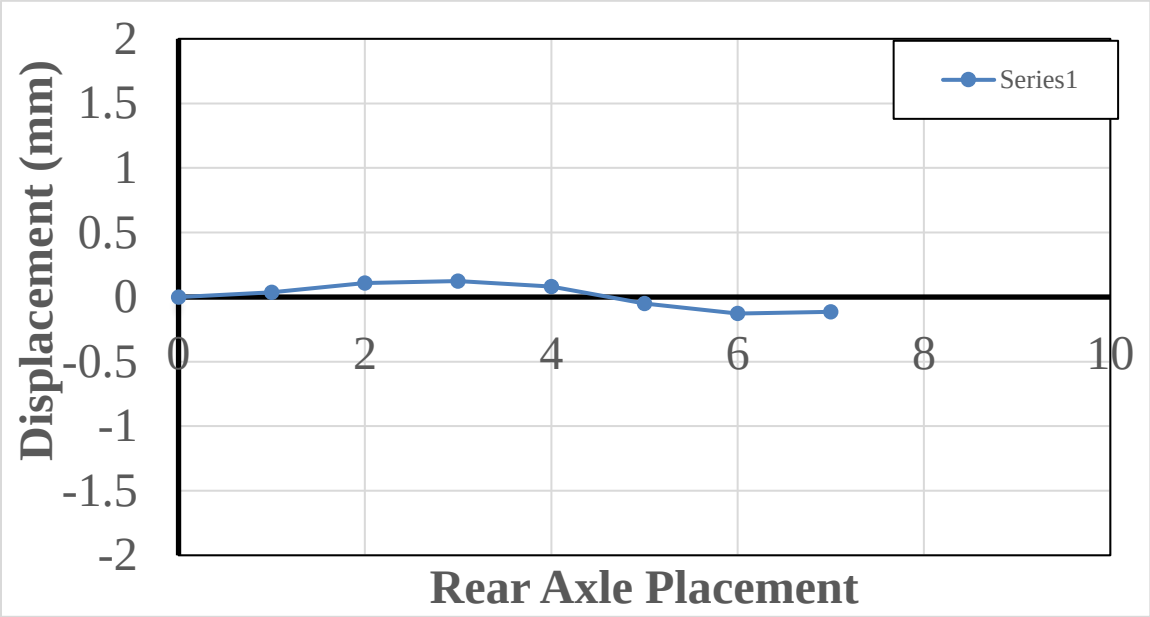

Figure 80. Out-of-plane displacement for single truck loading path3 from Hi-spec camera

Table 66. Numerical displacement (mm) value for z-displacement of pier for double truck loading on path 7

Stage	***Z-Displacement***
0	0
1	0.036729487
2	0.10782282
3	0.123955902
4	0.082219066
5	-0.049942586
6	-0.127700855
7	-0.115424829

6.4 Strain value measured for fascia girder Test 2019

The strain value for the test done in 2019 were computed similarly to the test done in 2018. A section was chosen one inch form the bottom of the beam and the strain value along the section was obtained from ARAMIS. The values were averaged for each

section and strain value for every loading stage was obtained and summarized in Table 67.

Table 67. Strain value measured for path1,2 and 3 for single truck loading measured by the 2M camera system

Stage	***Path1(με)***	***Path2(με)***	***Path3(με)***
0	0	0	0
1	-34.8697	104.3537	263.7668
2	-67.1364	55.23288	263.4691
3	-45.0611	79.78781	233.9504
4	145.8111	102.9427	298.3275
5	126.2731	138.7257	256.0396
6	206.5304	33.8249	99.12555
7	211.7528	69.51162	87.67319
8	167.4417	72.06975	126.8744

The camera system measured strain values for different path. The strain value ranged from -34.86 micrometers to 298.32 micrometers. The values were higher than the usual range. There were negative strain values for path 1. Path 3 which was away from the fascia girder had the highest strain values.

6.5 Displacement comparison for 2018 test results vs 2019 test results

The two tests were similar but different on one aspect. In the first test the displacement profile was plotted against span of the bridge in meters whereas the second test, the displacement was plotted against the stage. The stages were separated at a

distance of five feet. The comparison for displacement for fascia girder on HPC side of the bridge is shown in Figure 81-84.

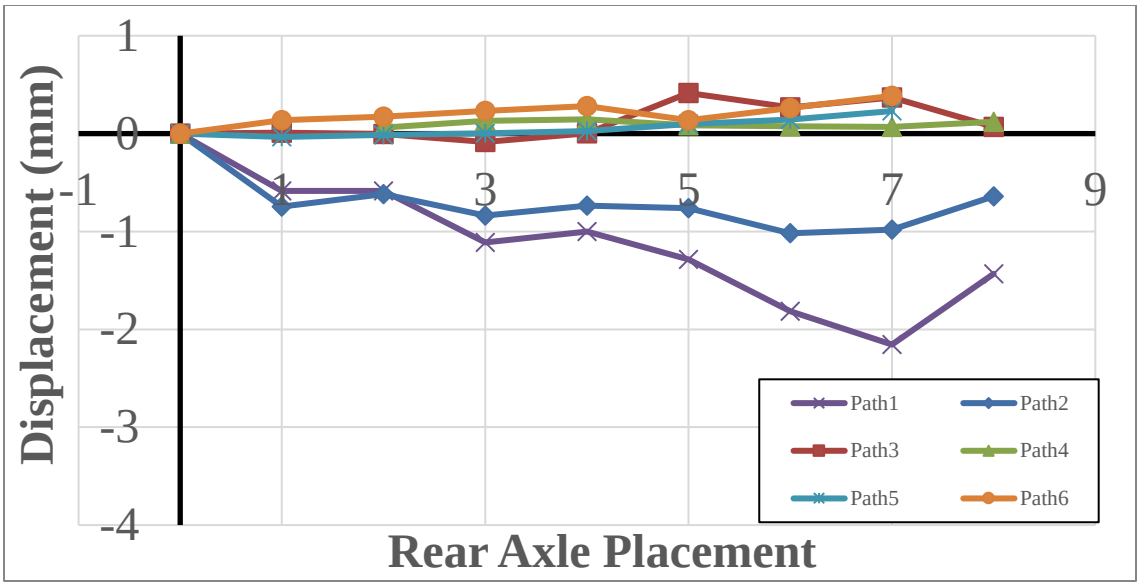

Figure 81. Displacement vs stage measured profile from 2M system for single truck loading for test on 2019

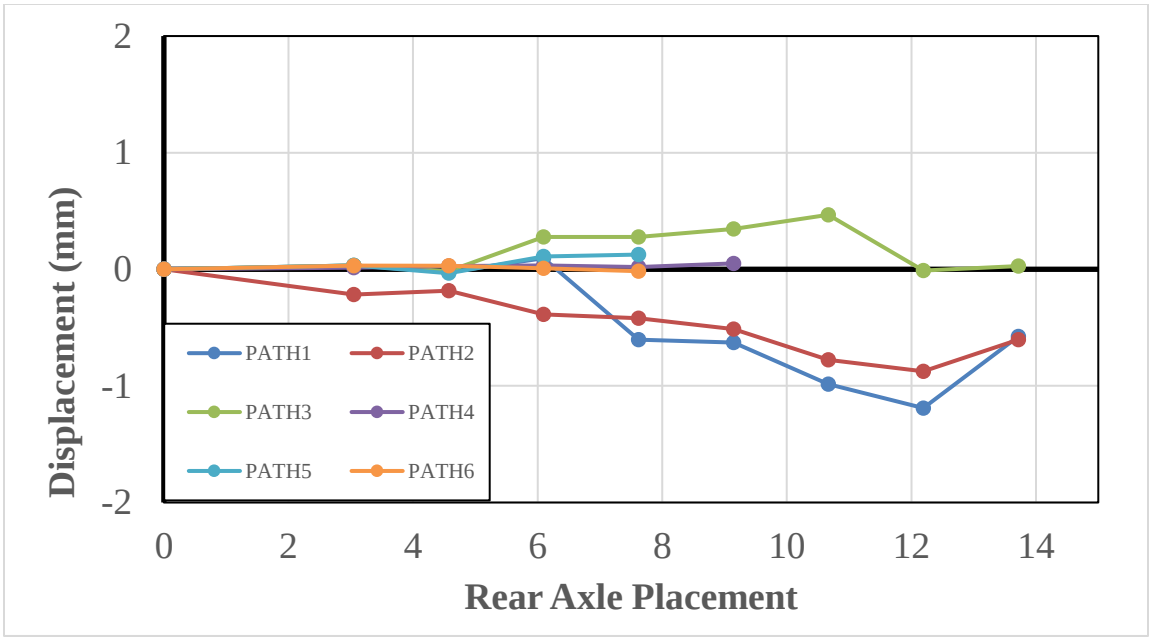

Figure 82. Displacement vs stage measured profile from Hispec1 system for single truck loading for test on 2018

The displacement profile for the two tests are similar the bridge moved down for path1 and path2 and started to move to move up for another path. The other path such as 3,4 and 5 moved away from the fascia girder which was being monitored by the 3D DIC system.

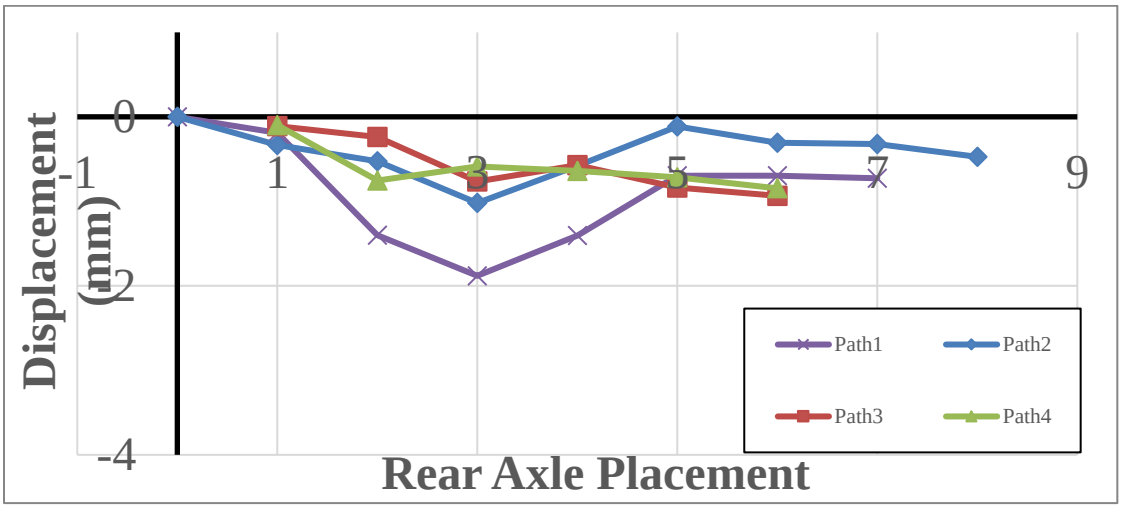

Figure 83. Displacement vs stage measured profile from Il5 system for single truck loading for test on 2019

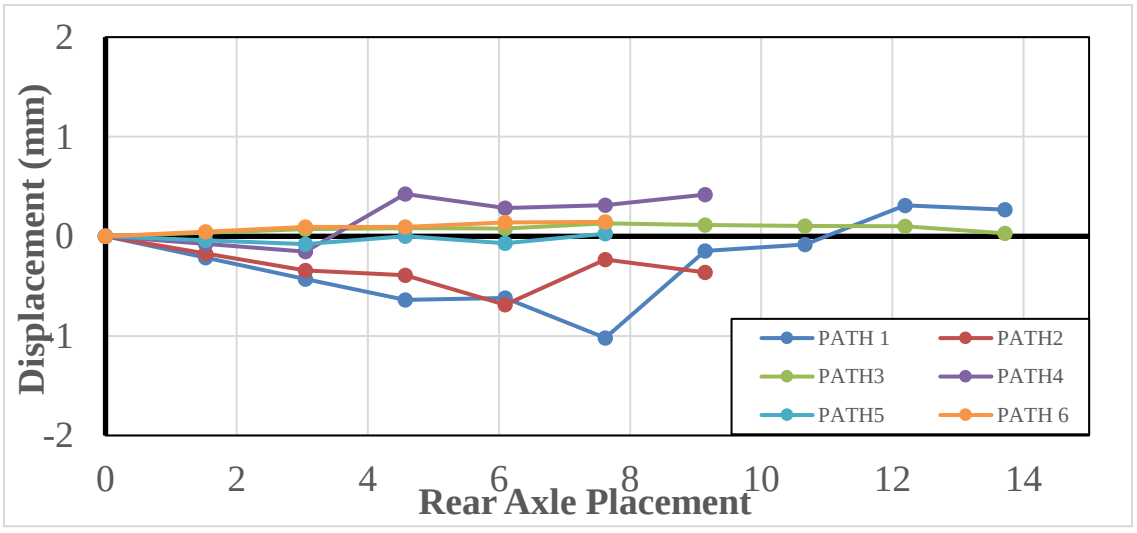

Figure 84. Displacement vs stage measured profile from IL5 system for single truck loading for test on 2018

The displacement profile for the two tests are similar the bridge moved down for path1 and path2 and started to move to move up for another path. This was not similar for the second test. One reason can be the truck made stops at a different place for both tests.

6.6 Dynamic test

Dynamic test was performed for both Test 1 and Test 2. The dynamic test was performed using the 3D camera system. The testing was done to assure if DIC is able to capture results for high speed run tests. The displacement and strain changes were captured using DIC. The change in color code on the beam shows displacement changes and strain changes. The results of displacements at the mid span of the north fascia HPC girder from the dynamic test are shown in Figure 85-92.

The first stage of the test where no loading is on the beam. Since this is the HPC beam the loading starts from the UHPC beam. The truck was not on the bridge at this instant. There is no displacement value observed on the beam which is represented by orange color code.

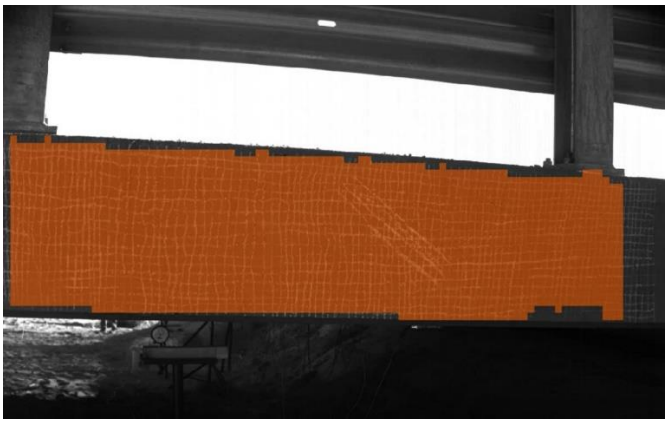

Figure 85. Dynamic test result for displacement on HPC span with no truck loading on the bridge

The loading had started from the UHPC side of the beam. The truck is already on the bridge. Small displacement occurred on the beam which was represented by Figure 86

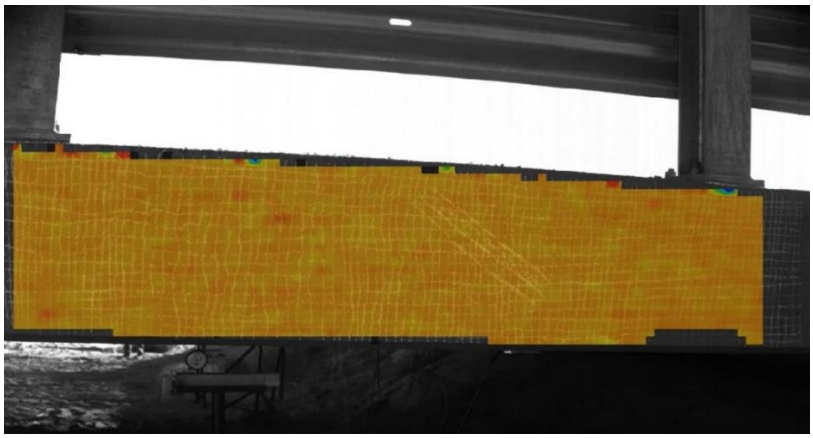

Figure 86. Dynamic test result for displacement on HPC span with truck loading starts on the bridge

This was the frame when front axle of the truck was on the HPC span of the bridge. The displacement value increased when front axle was on the bridge. The color code green represents displacement on the span.

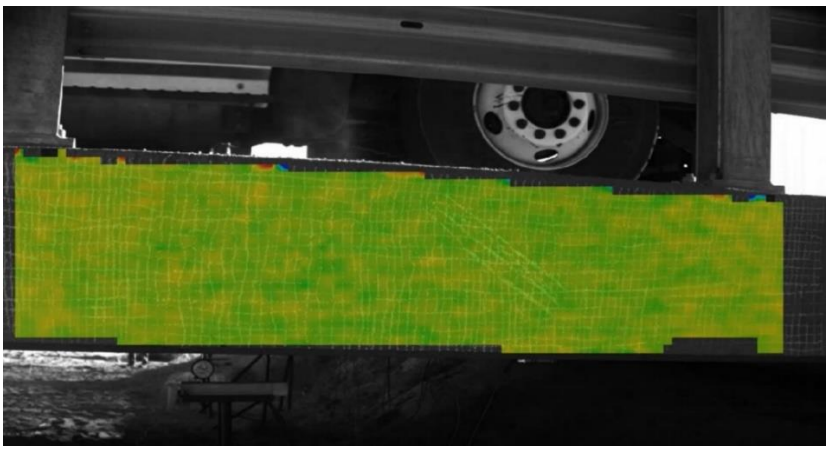

Figure 87. Dynamic test result for displacement on HPC span when front axle is on the midspan of the HPC beam

The truck was still on the HPC span. The displacement was still observed on the beam and the beam was still green. A puff of dust was also observed when the back axle approached the HPC beam. The color code green represented displacement on the span.

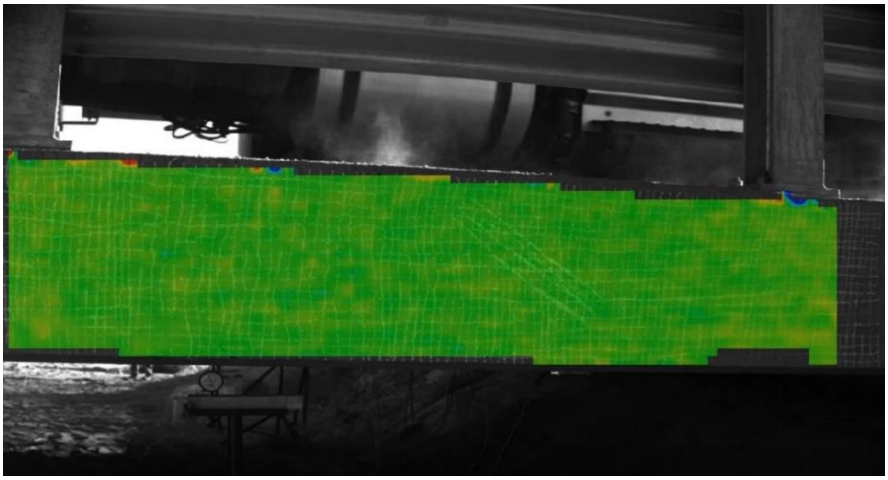

Figure 88. Dynamic test result for displacement on HPC span when the entire truck is on the HPC beam

When the rear axle of the truck which is the heavier axle reaches the HPC span of the bridge. The color code changed once the rear axle approached the mid span of the HPC beam.

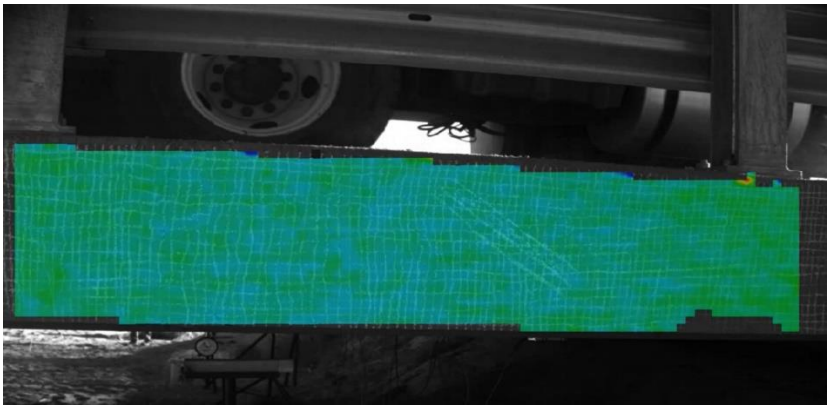

Figure 89. Dynamic test result for displacement on HPC span when rear axle is approaching on the midspan of the HPC beam

The rear axle reached the mid span of the HPC beam. This was the maximum loading condition. The color code changed to blue completely. This was the stage when the displacement obtained on HPC span was maximum.

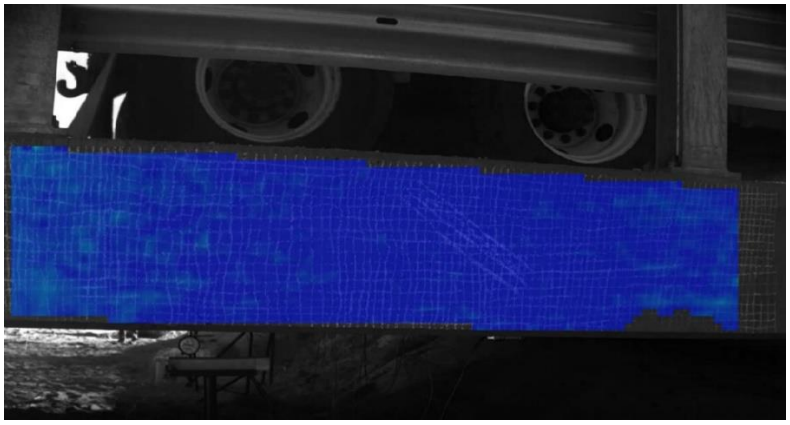

Figure 90. Dynamic test result for displacement on HPC span when rear axle is on the midspan of the HPC beam

Once the rear axle moved further on the bridge. The color code changed back to green. Small displacement values were represented. The truck at that instant was not off the bridge completely. Therefore, displacement was still observed on the span.

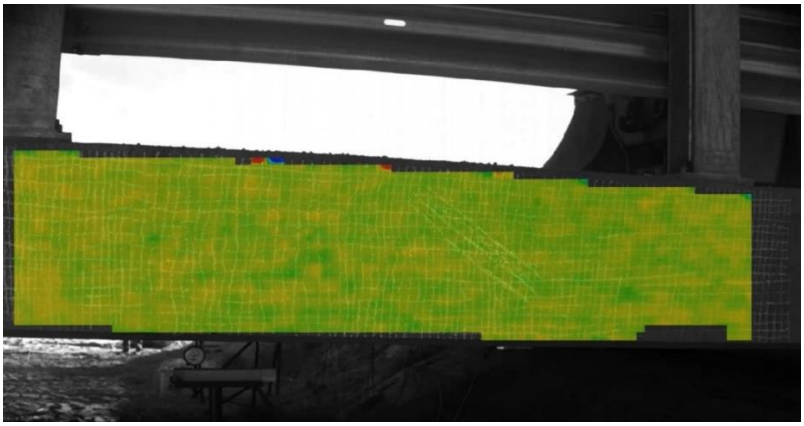

Figure 91. Dynamic test result for displacement on HPC span when the truck is leaving the bridge

The truck moved further and away from the HPC span. No displacement is observed on the bridge. The color code is similar to that of the no loading on the first stage where the truck was on the other side of the bridge. No displacement values are observed during this stage of test.

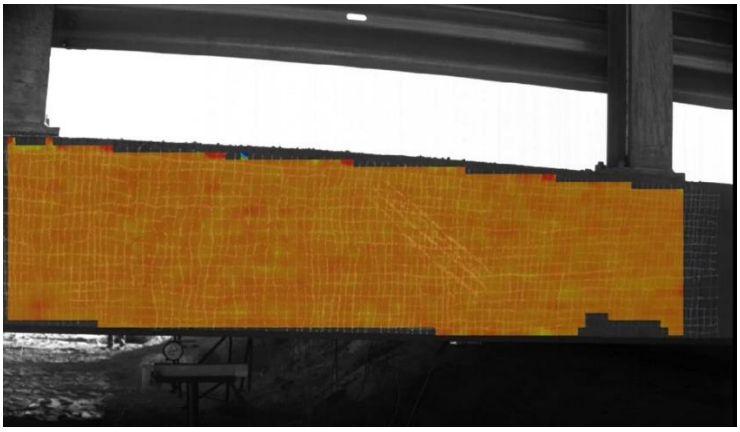

Figure 92. Dynamic test result for displacement on HPC span when the truck is completely off the bridge

Similarly, the major strain changes in the fascia beam of the HPC span are shown in the Figure 93-99 below. In Figure 93 no strain is observed as there was no loading on the bridge. The condition was when the truck was not on the bridge.

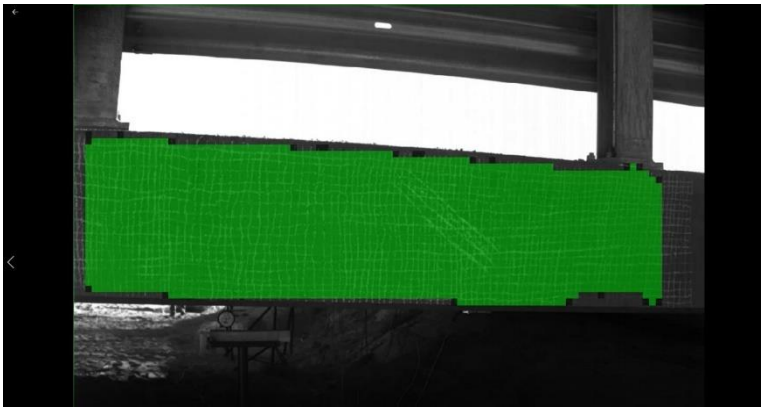

Figure 93. Dynamic test result for strain on HPC span when the truck is completely off the bridge

From Figure 94 the pattern starts to appear on the beam when the loading started on the UHPC span of the bridge. Small changes on the span of the bridge appeared representing strain produced when the loading started on the UHPC span of the bridge.

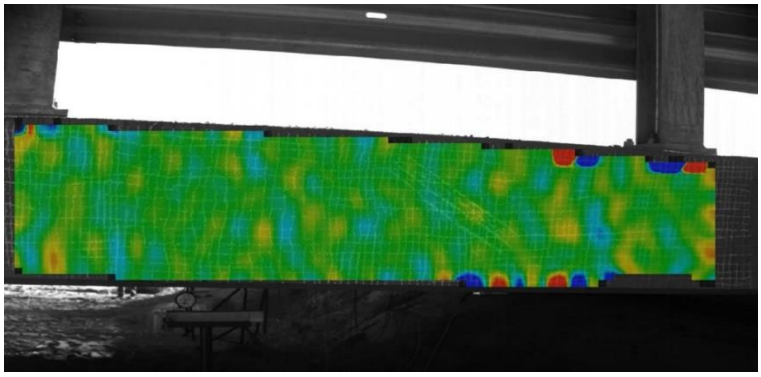

Figure 94. Dynamic test result for strain on HPC span when the truck is on the bridge

When the front axle of the truck was on the HPC span (Figure 95) the bridge started to show more strain which was represented by the patterns seen. The pattern started to become more distinct when the loading increased.

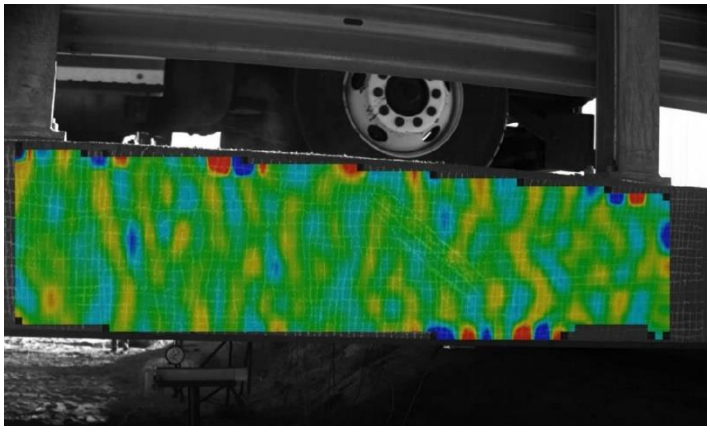

Figure 95. Dynamic test result for strain on HPC span when the front axle of the truck is on the bridge

When the axle load moved further the pattern started to dissipate slowly (Fig 96). A puff of dust was observed when the rear axle of the truck approached the HPC span.

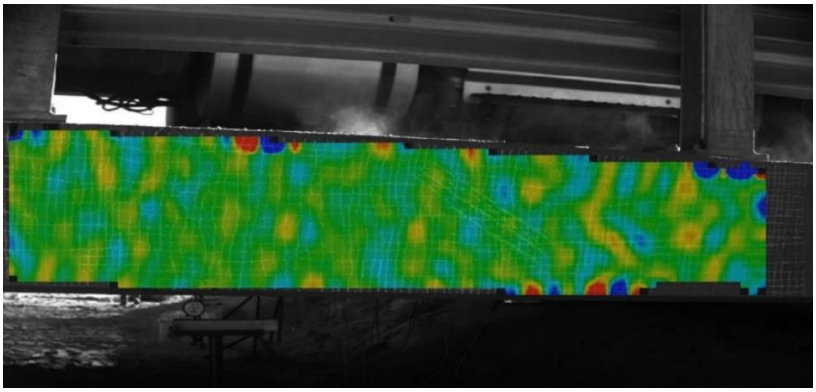

Figure 96. Dynamic test result for strain on HPC span when rear axle is approaching on the midspan of the HPC beam

The pattern started to reappear when the rear axle of the truck was on the HPC span (Figure 97). This was the maximum loading condition of the test.

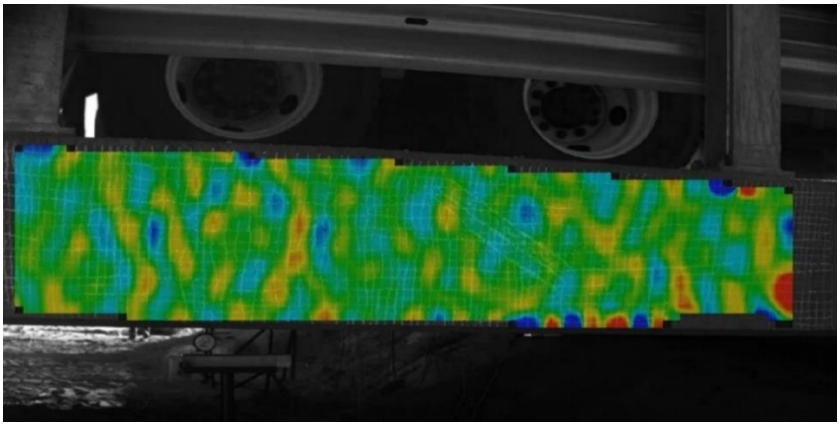

Figure 97. Dynamic test result for strain on HPC span when rear axle is on the midspan of the HPC beam

The truck then moved further, and no axle load was present on the bridge. The pattern started to dissipate, and the span was back at its original color (Figure 98).

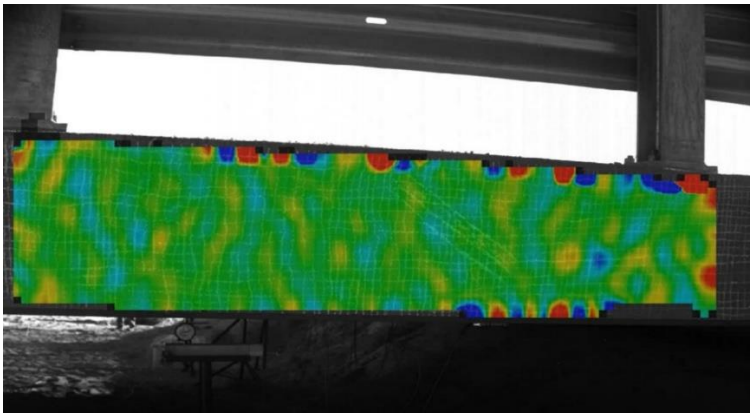

Figure 98. Dynamic test result for strain on HPC span when rear axle is off the midspan of the HPC beam

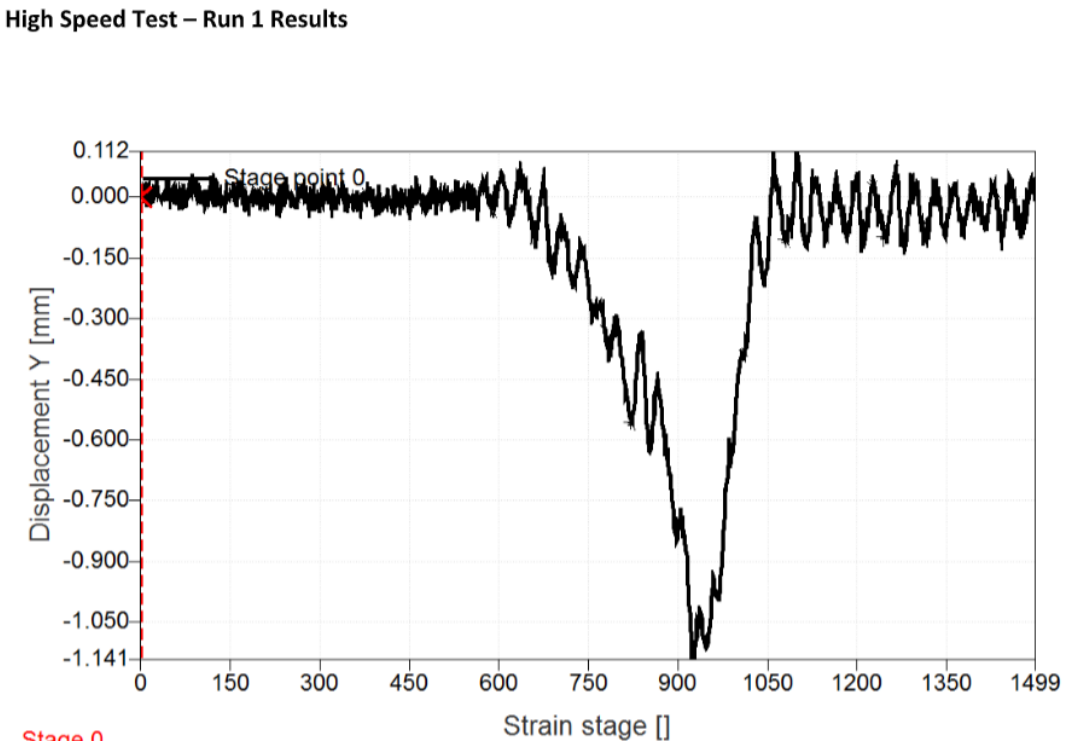

Figure 99. Displacement profile is captured for the High-Speed test run captured by the Hi-spec camera when loading was on the HPC span of the bridge.

The result obtained from the dynamic test was used to compute frequency of the bridge. Figure 99 shows the displacement versus stage of dynamic test at midspan of the HPC fascia girder. Free vibration of the span can be observed after stage 1050 where the truck was already out of the span. The bridge was in free vibration after the loading. The frequency of the span of the bridge was calculated by measuring the time between two successive peaks after the truck is completely off the bridge. The frequency can be used to compute stiffness of the bridge. The frequency for the bridge was 19.23 Hertz.

6.7 Comparison of Displacement data with dial gauges

The displacement data obtained from DIC was compared with the data obtained from dial gauges. The dial gauge data was calibrated, and the first reading was taken in the morning. The reference data was the first reading for every test throughout the day. This didn't account for temperature changes during the day. The test conducted using DIC used a new zero every time a test was done. The DIC data was compared with the dial gauges and following observation was made and was summarized from Table 68-71.

Table 68. Comparison between dial gauge vs DIC displacement data for single truck loading

Path 1 Single Truck Loading on UHPC beam Girder 6 Southern Stem

Axle Position	*DIC (mm)*	*Dial Gauge (mm)*
Q1	0.10	0.10
M	0.12	0.13

Table 69. Comparison between dial gauge vs DIC displacement data for single truck loading

Path 2 Single Truck Loading on HPC beam Girder 1 Southern Stem

Axle Position	*DIC (mm)*	*Dial Gauge(mm)*
Q1	-0.65	-0.55
M	-1.04	-0.85
Q2	-0.40	-0.39

Table 70. Comparison between dial gauge vs DIC displacement data for triple truck loading

Path 10 Triple Truck Loading on HPC beam Girder 6 Southern Stem

Axle Position	*DIC (mm)*	*Dial Gauge (mm)*
Q1	-1.55	-2.36
M	-3.24	-3.10
Q2	-2.34	-2.26

Table 71. Comparison between dial gauge vs DIC displacement data for triple truck loading

Path 10 Triple Truck Loading on HPC beam Girder 1 Southern Stem

Axle Position	*DIC (mm)*	*Dial Gauge (mm)*
Q1	-0.40	-0.55
M	-0.75	-0.85

The data presented in the table above are comparisons for the test done in the morning. The dial gauges compared well with the measurement obtained from DIC for many of the tests. As the day progressed the dial gauges were not able to account for temperature changes whereas the DIC was using a new zero every time a test was conducted. The Table 72-75 below represent the comparison of DIC data with dial gauge data for the test that were conducted on the later part of the day.

Table 72. Comparison between dial gauge vs DIC displacement data for double truck loading

Path 1D Double Truck Loading on HPC beam Girder 1 Southern Stem

Axle Position	*DIC (mm)*	*Dial Gauge (mm)*
M	-0.32	-0.87
Q2	-1.75	-1.33

Table 73. Comparison between dial gauge vs DIC displacement data for double truck loading

Path 3D Double Truck Loading on HPC beam Girder 1 Southern Stem

Axle Position	*DIC (mm)*	*Dial Gauge (mm)*
Q1	-0.12	0.67
M	-0.99	0.48

Table 74. Comparison between dial gauge vs DIC displacement data for double truck loading

Path 4D Double Truck Loading on HPC beam Girder 1 Southern Stem		
Axle Position	***DIC (mm)***	***Dial Gauge (mm)***
Q1	-0.75	1.01
M	-1.18	0.90

Table 75. Comparison between dial gauge vs DIC displacement data for double truck loading

Path 6D Double Truck Loading on HPC beam Girder 1 Southern Stem		
Axle Position	***DIC (mm)***	***Dial Gauge (mm)***
Q1	-0.08	1.36
M	-0.21	1.34

The data presented in the Tables 72-75 varied. The dial gauge was taking the same reference value throughout the test. The error due to temperature changes accumulated and erroneous results were obtained during the end of the testing period. The displacement given by dial gauge reading were positive when the trucks were on the mid span of the bridge which is not possible. The difference in displacement was large.

Chapter 7

Conclusions and Recommendation for Future Work

This thesis analyzes the ability of DIC to adequately measure strain and displacement in highway bridges. This was done by testing on two spans UHPC and HPC reinforced concrete bridge superstructure designed by New Mexico State University (NMSU) and constructed outside of Las Cruces, New Mexico. The testing was completed using Digital Image Technology. The conclusion of this study is specified as a) Test 1 and b) Test 2

Test 1

- One span of the structure was constructed using UHPC and the other HPC. During test 1 four 3D and four 2D DIC systems were deployed to monitor displacements at various locations of the structure under controlled prescribed loading. The loading was selected as to generate maximum flexural and shear responses within both spans. Images were captured at each static positioning of the loading on the bridge. These images were processed using the ARAMIS GOM DIC software package to generate displacement and strain measurements.
- The displacement data obtained from DIC were used to obtain deflection profile of the two spans of the bridge. The deflection profile was used to monitor the behavior and performance of UHPC and HPC beams. The maximum displacement was obtained higher for HPC beam than the UHPC beam for all types of load test. The loading conditions and load paths were similar for both tests and the results obtained showed UHPC beam deflected less than the HPC beam. The maximum

displacement data for single truck loading test for HPC beam was found to be 1.19mm whereas the maximum displacement data for the UHPC beam was found to be 1.02mm. The results appear to indicate that the UHPC span is stiffer than the HPC span. This can be seen from the smaller displacements of the exterior fascia girders monitored by the HiSpec1 and IL5 systems under identical loading conditions. It was noted in some tests that there was very small upward displacement of an exterior girder which suggests the possibility of the bridge twisting slightly. In any case, all displacement measurements were well below the maximum allowed by AASHTO Bridge Design Specifications.

- The strain data obtained from the DIC had very little accuracy when compared to the data obtained from strain gauges. Therefore, for the purpose of performance evaluation for UHPC and HPC beams strain data were used from the strain gauges. The data obtained from the strain gauges was more comprehensive and the behavior of the UHPC and HPC beam were characterized based on the data from strain gauges.
- Since this was the first time this team has deployed DIC in the field there was uncertainty as to the best method for calibrating the 3D DIC systems. The team elected to calibrate the systems in the structural engineering laboratory at NMSU then carefully transport the systems to the field for installation. Once in the field some systems became uncalibrated and needed to be recalibrated in the field using either a large GOM calibration cross or GOM calibration panel. This resulted in a delayed start in when data was able to be gathered and therefore some load tests

were not able to be monitored. The load testing occurred over a 3-day period. Each day, the GoPro, IL5 and HiSpec1 systems were taken down and the cameras left in their same position and orientation in relation to each other in attempts to reduce the need to calibrate the systems each night. The HiSpec1 system was able to say calibrated however the IL5 system needed to undergo recalibration each day. The 2M system was left out each night and kept in place. This system kept its calibration throughout the entire testing. There were also instances where the IL5 and HiSpec1 systems lost connection with the computer which required a restart of the system and some load testing data was not captured. The GoPro systems were used for 2D DIC analysis, so no calibration was needed. The GoPro systems were both operated using a remote control from the command station which was near the IL5 and HiSpec1 systems. It was noticed that occasionally some images were not actually taken by these cameras as the signal from the remote was not received. This again resulted in some data not being collected. The challenges faced were all overcome, and the team showed that DIC is a feasible method for measuring deformations during load testing of highway bridges.

- This being the research teams first deployment of DIC systems for in-situ structural evaluation of bridges there were challenges that needed to be overcome and were. To the knowledge of the research team this testing was the largest number of DIC systems deployed at one time for bridge load testing. This work shows the feasibility of using DIC to measure in-situ displacement measurements for experimental load testing of highway bridges.

Test 2

- The second test was conducted on February 2019. The second test included the use of eight 2D system and the internal girders were monitored during the test. The loading condition were similar to the one on the first test. The displacement was better explained for the second test and were a better interpretation to the loading conditions. The upward displacement was again observed on the second test and also was confirmed by dial gauges shows that there is presence of continuity in the bridge causing the bridge to move upwards when loading is on other half of the bridge.
- The test was also conducted with dial gauges. The readings obtained from the dial gauges were both positive and negative values. The values supported the upward movement of the bridge which was also observed from DIC. The displacement data from DIC was compared with the dial gauges and reasonable accuracy was observed. The displacement was accurate when the loading condition was increased during the test, i.e. when the loading condition increased from single truck loading to double truck loading. The magnitude of displacement can have a relation with the accuracy of the measurement.
- The behavior of the bridge was observed more precisely during the second test as 4 separate camera systems were able to produce similar result which was a big improvement over the first test. The displacement pattern was similar for all internal girders for similar loading conditions. A small upward displacement was observed when the loading was on the other span.

- This being the research teams second deployment of DIC systems for in-situ structural evaluation of bridges there were challenges that needed to be overcome and were. To the knowledge of the research team this testing was the largest number of DIC systems deployed at one time for bridge load testing. This work shows the feasibility of using DIC to measure in-situ displacement measurements for experimental load testing of highway bridges.
- Dynamic high-speed test was also conducted for both test and DIC was able to capture results for the test. The speed of the vehicle was obtained and dynamic displacement and strain results were also captured by the 3D DIC camera system.

Future Work

The work presented in the study contributes to health monitoring work done on bridge assessment from Digital Image Technology. The deflection profile for the span of the bridge was easily obtained and performance of the two different spans were analyzed. The strain data obtained were less accurate compared to the data obtained from strain gauges. Since the camera system were only capturing the images for fascia girders, further studies can install a camera system for every girder in the bridge. The results for displacement would also result in accurate data when there is separate camera system for every girder. During the processing of the images in ARAMIS, the deviation size had to be increased for the software to recognize the pattern. For the strain data the number of input images can be increased by taking the images in smaller intervals. This would provide a lot of input data and reduce the noise while micro-strains are being measured. After

obtaining the strain value across the girders in the bridge distribution factor for the bridge can be calculated and compared. A comparison of distribution of load along the bridge can be vital to characterize the performance of UHPC beam with HPC beam.

In this time, cameras and image technologies has been improving in leaps and bounds, the civil engineering community can significantly benefit from new applications and models for improved condition assessment. As is currently done in steel structures and mechanical engineering industries DIC is being used to quantify deformation, similar concept should be applied in civil engineering. While much work and additional testing similar to what was presented in this study, needs to be undertaken, there is no doubt that improvements can be made to an existing system which needs improvements.

References

AASHTO. (2010). Manual for Bridge Evaluation. Washington AASTHO ASCE. Retrieved from https://store.transportation.org/Common/DownloadContentFiles?id=1712

Aramis, G. (2019). GOM Aramis Website. (GOM) Retrieved January 19, 2019, from https://www.gom.com/metrology-systems.html

Aydilek, A. H. (2007). Digital Image Analysis in Geotechnical Engineering Education. Journal of Professional Issues in Engineering Education and Practice,133(1), 38-42. doi:10.1061/(asce)1052-3928(2007)133:1(38)

Bell, E, et al. (2010). Digital Imaging for Bridge Deflection Measurement of a Steel Girder Composite Bridge. University of New Hampshire, Durham. Retrieved from https://trid.trb.org/view/1092045

Brogan, P.A., et al. (2010). Digital Image Correlation application to structural health monitoring. Retrieved from http://engineering.tufts.edu/cee/shm/documents/TRB2011DigitalImageCorrelation.pdf

Bryne, E., (2017). Comparing 2D DIC data to Theory/strain gauges/other techniques. Correlated Solutions. Retrieved from https://www.correlatedsolutions.com/support/index.php?/Knowledgebase/Article/View/79/1/comparing-2d-dic-data-to-theorystrain-gaugesother-techniques

Hohmann, B., et al. (2012). Digital Image Correlation (DIC): An Advanced Nondestructive Testing Method for Life Extension of Nuclear Power Plants. Trilion Quality Systems. Retrieved from https://inis.iaea.org/search/search.aspx?orig_q=RN:43070906

Küntz, M., Jolin, M., Bastien, J., Perez, F., & Hild, F. (2006). Digital image correlation analysis of crack behavior in a reinforced concrete beam during a load test. Canadian Journal of Civil Engineering, 33(11), 1418-1425. doi:10.1139/l06-106

Malesa, M., Szczepanek, D., Kujawińska, M., Świercz, A., & Kołakowski, P. (2010). Monitoring of civil engineering structures using Digital Image Correlation technique. EPJ Web of Conferences, 6, 31014. doi:10.1051/epjconf/20100631014

Nonis, C., Niezrecki, C., Yu, T., Ahmed, S., Su, C., & Schmidt, T. (2013). Structural health monitoring of bridges using digital image correlation. Health Monitoring of Structural and Biological Systems 2013. doi:10.1117/12.2009647

Sas, G., Blanksvärd, T., Enochsson, O., Täljsten, B., & Elfgren, L. (2012). Photographic strain monitoring during full-scale failure testing of Örnsköldsvik bridge. Structural Health Monitoring: An International Journal, 11(4), 489-498. doi:10.1177/1475921712438568

Yoneyama, S., & Ueda, H. (2012). Bridge Deflection Measurement Using Digital Image Correlation with Camera Movement Correction. Materials Transactions, 53(2), 285-290. doi:10.2320/matertrans. i-m2011843